BMI-1 - A novel Epigenetic Regulator of $CD8^+$ T Cell Differentiation

Vibha Airbail Venkatesh Udupa

ORCID ID

0000-0003-2497-1664

From Koteshwara, India

Submitted in total fulfilment of the requirements of the joint degree of Doctor of Philosophy (PhD)

of

The Department of Microbiology and Immunology

The University of Melbourne

and

The Medical Faculty

The Rheinische Friedrich-Wilhelms-Universität Bonn

Bonn/Melbourne, 2025

Performed and approved by The Medical Faculty of The Rheinische Friedrich-Wilhelms-Universität Bonn and The University of Melbourne

1. Supervisor: Prof. Joachim Schultze

2. Supervisor: Prof. Christian Kurts

Month and year of the original thesis submission: 02/2023

Month and year of the oral examination: 10/2024

Institute in Bonn: DZNE/ LIMES Institute, University Bonn

Table of Contents

Abbreviations

^{o}C	Degrees Celsius
AF647	Alexa Fluor 647
APC	Antigen presenting cell
APL	Altered peptide ligand
AP-1	Activator protein-1
BAL	Bronchoalveolar Lavage
BATF	Basic leucine zipper ATF-like transcription factor
BCR	B Cell Receptor
BLIMP1	B-lymphocye-induced maturation protein 1
Bp	Base pairs
BMI-1	B lymphoma Mo-MLV insertion region 1
BSA	Bovine Serum Albumin
CBX	Chromobox Protein
CD	Cluster of differentiation
cDNA	Complementary DNA
ChIP	Chromatin Immunoprecipitation
CPM	Counts per million
CpG	CpG dinulceotide
cRPMI	Complete Roswell Park Memorial Institute Medium
Ct	Cycle threshold
CTL	Cytotoxic T Lymphocyte
CTV	Cell Trace Violet
D	days
DC	Dendritic cell
DEG	Differentially Expressed Gene
DNA	Deoxyribonucleic acid
dNTP	Deoxynucleotide triphosphate
DP	Double Positive (Thymocyte)
D-PBS	Dulbecco’s PBS
EOMES	Eomesodermin

EDTA	Ethylene diamine tetra acetic acid
EED	Extra embryonic development protein
EGTA	Ethylene glycol tetra acetic acid
EZH2	Enhancer of Zeste homologue 2
F	Forward primer
FACS	Fluorescence activated cell sorting
FCS	Featl Calf Serum
FDR	False Discovery Rate
FITC	Fluorescein isothiocyanate
FMO	Fluorescence minus one
G4	SIIGFEKL peptide
GZMA	Granzyme A
H3	Histone 3
H3K9AC	Acetylation of H3 lysine 9
H3K9me3	Trimethylation of H3 lysine 9
H3K4me3	Trimethylation of H3 lysine 4
H3K27ac	Acetylation of H3 lysine 27
H3K27me3	Trimethylation of H3 lysine 27
H2AK119ub	Monoubiquitination of H2A Lysine 119
HDAC	Histone deacetylase
Hrs	Hours
JARID	Jumonji And AT-Rich Interaction Domain Containing 2
KLF	Kruppel like factor
KLRG1	Killer cell lectin-like receptor subfamily G member 1
KO	Knock-out
LFA-1	Lymphocyte function associated antigen 1
LEF1	Lymphoid enhancer binding factor 1
LiCL	Lithium chloride
LCMV	Lymphocytic choriomeningitis Virus
µM	Micromolar
mM	Millimolar
µg	Microgram

MACS	Magnetic activated cell sorting
MDS	Multidimensional scaling analysis
MFI	Median Fluorescence Intensity
MHCI	Major histocompatibility Complex class I
MHCII	Major histocompatibility Complex class II
mRNA	Messenger ribonucleic acid
MPEC	Memory precursor effector cell
N4	SIINFEKL peptide
NFAT	Nuclear Factor of Activated T cells
NF-kB	Nuclear factor kappa-light-chain-enhancer of activated B cells
NK	Natural Killer cell
NKT	Natural Killer T cell
NP	Influenza A nucleoprotein
OVA	Ovalbumin
PA	Influenza A acid polymerase
PB	Pacific Blue
PBS	Phosphate buffered saline
PCR	Polymerase chain reaction
PE	Phycoerythrin
PerCP	Peridinin-chlorophyll-protein
PFU	Plaque forming units
p.i.	Post infection
PRR	Pattern recognition receptor
pMHC	Peptide+MHC
PR8	Influenza A/Puerto Rico/8/34 virus
qPCR	Real time polymerase chain reaction
Q4	SIIQFEKL
R	Reverse primer
RING1	Ring finger protein 1
RYBP	RING1 YY1 binding protein
RBC	Red blood cell(s)

RE	Relative Expression
rhIL-2	recombinant human IL-2
RNA	Ribonucleic acid
rpm	Revolutions per minute
RT-PCR	Reverse transcriptase polymerase chain reaction
SEM	Standard error of the mean
SLEC	Short Lived Effector Cell
SP	Single Positive (Thymocyte)
STAT	Signal transducer and activator of transcription
T-BET	T-box expressed in t cells
TCF-1	T cell factor 1
TCM	Central memory CD8+ T cell
TCR	T cell receptor
TE	Transcriptional Enhancer
TEM	Effector memory CD8+T cell
Th (1,2, 17)	T helper cell (type 1, 2 or 17)
TNF	Tumour necrosis factor
TF	Transcription Factor
TMEM	Memory $CD8^+$ T cell
TN	Naïve $CD8^+$ T cell
Treg	Regulatory T cell
TRM	Tissue Resident memory
TSS	Transcriptional Start Site
TVM	Virtual Memory T cell
U	Units
US	Unstimulated
WT	Wild type
X31	Influenza re-assortant between A/Aichi/2/68 (H3N2) and A/Puerto Rico/8/34 (HN1)
ZEB2	Zinc-finger E-box binding homeobox 2

List of Tables

List of Figures

Abstract

$CD8^+$ T cells are important for the elimination of intracellular pathogens and tumours. Activation of naive $CD8^+$ T cells triggers their differentiation and clonal expansion, resulting in the formation of effector cells which can eliminate the pathogens via direct killing of infected host cells. Importantly, once the infection is cleared, a long-lived pool of memory T cells remains, which can respond more rapidly to secondary infection without the need for further differentiation, often providing immunity. However, our understanding of gene regulatory mechanisms that control the process of differentiation are largely unknown. Posttranslational modification of histone proteins regulates gene transcription by directly affecting chromatin compaction, or by serving as substrates for binding of chromatin remodelling complexes that influence gene regulation by various mechanisms. Here we identify a well-known chromatin remodelling histone modifier, canonical Polycomb Repressive Complex 1 (cPRC1) as a major regulator of $CD8^+$ T cell differentiation. The core complex of cPRC1 in $CD8^+$ T cells contains RING1B – a ubiquitin ligase that catalyses ubiquitination of Lysine 119 on H2A, one of the Polycomb group Ring Finger (PCGF) proteins BMI-1 which regulates enzymatic activity, Chromobox proteins CBX4 and CBX7 which are responsible for targeting the complex to the chromatin and Polyhomeotic-like protein 3 (PHC3) which is believed to assist forming higher order chromatin structure. Our results identify that CBX7/4, and BMI-1 are differentially regulated between naïve and activated $CD8^+$ T cells. Their expression was found to be regulated in accordance with TCR signal strength and pMHC-TCR affinity. We found that the deletion of BMI-1 from T cells resulted in an exaggerated effector response and skewing to terminal differentiation during primary infection with Influenza A Virus. This was accompanied by a failure to establish CD8 T cell memory. Upon secondary infection, the number and frequency of effector cells were reduced along with reduced polyfunctionality and increased EOMES and PD1 expression. By using ChIP-qPCR and ATAC-seq we understood that deletion of BMI-1 leads to reduced H2AK119ub and increased chromatin accessibility around the promoters of transcription factors that regulate effector differentiation. Overall, we

demonstrate that BMI-1 cPRC1 restrains terminal differentiation by repressing key transcription factors that drives differentiation and enables memory formation. Hence, BMI-1 and cRPRC1 is a crucial regulator of viral induced $CD8^+$ T cell differentiation.

Declaration

This is to certify that,

(i) the thesis comprises only my original work towards the PhD except where indicated in the preface.

(ii) The work contained in this thesis was conducted by myself, unless otherwise specified, with due acknowledgement has been made in the text to all the material used and

(iii) the thesis is fewer than the maximum word limit in length, exclusive of tables, maps, bibliographies and appendices or that the thesis is less than 100,000 words as approved by the Research Higher Degrees Committee.

Vibha Airbail Venkatesh Udupa

Date: 03rd February 2023

Preface

My contribution to experiments in each of the chapters was as follows:
Chapter 3: 99%
Chapter 4: 99%
Chapter 5: 90% (details below)

I acknowledge the important contributions to Chapter 5 experiments here:

- ◊ Daniel Thiele was vital in experimental design and carrying out the ATAC-seq experiments. Dr. Brendan Russ gave expert advice on experimental design and data analysis for ATAC-Seq and RNA-Seq experiments.
- ◊ I acknowledge the important contributions to the bioinformatical data analysis here: Adele Barugahare carried out all bioinformatics analysis on RNA-seq, ATAC-seq.

Acknowledgements

Like everyone else's PhD, my experience as well revolved around laughter, frustration, tears, relief, and happiness. I am thankful for the Melbourne Research Scholarship and Bonn Melbourne research and Graduate school that provided an opportunity to pursue a PhD at the University of Melbourne. I have gained so much experience in personal and professional life during this journey. I must thank the following individuals who have contributed greatly during my PhD.

First and foremost, I am grateful for my supervisor Prof. Stephen J. Turner for giving me an opportunity to do PhD in your laboratory. I am beyond words for the encouragement you have given me all these years. Thank you for all the discussions we had, and the guidance you have given me personally and professionally. You opened your door for me every time, no matter how stupid my experimental designs or my questions were. You were always excited to see the new data which encouraged me to push harder. My heartfelt thank you for supporting me through difficult times in my personal life. Thank you for providing an amazing work environment in your lab urging the incorporation of precise and flawless research methodologies.

I would like to thank my Bonn Supervisor Prof. Joachim Schultze for his contributions during all the meetings we have had. COVID-19 prevented me to gaining an amazing experience in your laboratory. However, you have provided the assistance required despite the pandemic and the time zone difference we had.

I am indebted to have Dr. Brendan Russ as my co-supervisor. You are not just my mentor but a wonderful friend. You have constantly reminded me that PhD or life, in general, is a marathon, not a sprint. I will never forget this. I cannot imagine my PhD journey without your insights into my work, not to mention the life advice. Thank you for teaching me how to do proper molecular biology. I am thankful for the many coffee/ life advice sessions we have had. You tolerated all my annoying door-knocks to discuss the experiments. You made me forget that I came to a

new country, new culture when I joined the lab. You were there for me every time I had frustrations, pain, and loss I went through in my personal life. I would not have completed this thesis if it wasn't for you. Thank you.

I would like to thank my PhD advisory committee members in Melbourne, Prof. Sammy Bedoui, Prof. Thomas Gebhardt and Prof. Damian Purcell for their time and the insights they gave me during my annual presentations. I would also like to thank my Bonn thesis committee members, Prof. Christian Kurts and Prof. Natalio Garbi.

I would like to express my gratitude to Prof. Kim Good-Jacobson for providing us with *Bmi1* floxed mice which is the main resource for my project and for the valuable discussions. I would also like to thank Dr. Andrea Di Pietro for his help during my PhD. I would like to thank Prof. Mariapia Degli Esposti and her lab members for the inputs to my project during lab meetings and for sharing their cell counter.

It was fun working with the members of La Gruta Lab while sharing the lab space. Thank you Prof. Nicole La Gruta for your thoughtful contributions and critical analysis when I presented in the joint lab meetings over these years. I have learnt a lot from your, brave, no-nonsense attitude. In no particular order, I would like to thank Dr. Claerwen Jones for her guidance with ethics, Dr.Pirooz Zareie for all the inspiration I get from you, Dr. Angela Nguyen for your kindness and support, and Dr. Tabinda Hussain for showing what hard work means. I would also like to thank Justin Zhang and Daniel Thiele. Dan you are one of my best friends. Thank you for all the help during our experiments specifically planning and performing ATAC-Seq presented in this thesis. Thanks for cheerleading all the experimental success and just for being funny.

Members of Turner lab have played an impeccable role in my understanding of the subject. I have been fortunate enough to have the company and motivation from all of you. Thank you, Alison Morey, Jason Lee, and Thomas Bruer for being

great PhD buddies. Thank you, Jessie Ellemor, for managing the lab, for your patience, and your help during the early morning culls and tissue processing. I would also like to thank Dr. Jasmine Li. I am thankful for sharing your technical expertise and ATAC-seq protocol with us and thank you for encouraging me in every way. My dearest friend Taylah Bennett, my partner in crime, thank you for doing a PhD alongside me. You were home for me away from home. Thank you for chatting with me for hours and listening to my rants. I have always admired you in every way. Thank you for being there for me all the time.

I would like to thank the animal technicians in the Animal Research laboratory (ARL) Monash University for taking care of our mice colony. I also extend my gratitude to the staff at the Flowcore for assisting with my hundreds of sorting sessions.

I sincerely appreciate Sherrie Young and Lauren Perillo for helping me get official things in Monash done without hassle. My heartfelt thanks to Dr. Marie Greyer for everything. You were there when I started my application to the program and helped me through each and every administrative task. Thank you for being student-friendly coordinator for all of us in the Bonn-Melbourne program. My thanks also goes to my Bonn coordinators Lucie Delforge and Sandra Rathman for your timely help.

I would like to thank Prof. Balaji K.N at IISc Bangalore for giving me the opportunity to start my career in research. My friends Tanushree, Bhavna, and Meghana thank you for your friendship.

Finally, I am nothing without my dearest family. Shubha Udupa, my twin sister, you are my rock. Thank you so much for all the motivation, hyping, and cheerleading you have done all along. I love you very much. Now that you have started your PhD journey, I hope I can reciprocate. Thank you, Dr. Aravind Acharya, for being a wonderful husband, my best friend, and my everything. Thank you for tolerating me and motivating me during our good and bad times.

Many thanks to my In-laws, and my brother-in-law, Aravinda Udupa. Lastly, my heartfelt gratitude to my parents Susheela and Venkatesh Udupa. Amma, you are the best mother any child could ask for. Thank you for all the hard work you have put in to raise your girls. You told us we can do whatever we want without caring about the prejudice of society. Appa, you left us in the middle of everything. Not a single day goes by without remembering you. My entire thesis is dedicated to you, Appa. I am hoping you are seeing your little girl finish her PhD from heaven along with the child I unfortunately lost.

List of Publications:

1. Taylah J. Bennett*, **Vibha Udupa*** and Stephen J Turner. Running to stand still: Naïve CD8+ T cells actively maintain the quiescent program. ***Int J Mol Sci****,* 2020. doi: 10.3390/ijms21249773

2. Andrea Di Pietro, Jack Polmear, Lucy Cooper, Timon Damelang, Tabinda Hussain, Laurnen Hailes, Kristy O'Donnell, Vibha Udupa, Tian Mi, Simon Preston, Areen Shtewe, Uri Hershberg, Stephen J Turner, Nicole La Gruta, Ay W Chung, David M Tarlinton, Christopher D Scharer, Kim L Good-Jacobson. Targeting BMI-1 in B cells restores effective humoral immune responses and controls chronic viral infection. ***Nat Immunol*** 2022. doi: 10.1038/s41590-021-01077-y

CHAPTER 1
Introduction

1.1 An overview of the immune system.

The immune system has two arms - the innate arm, which provides a generalised defence against infection, and the adaptive arm, which provides a tailored defence. Innate defences form the first line of protection against infection, and include barrier tissues (Janeway and Medzhitov, 2002) (skin and respiratory and gastrointestinal tracts) and cells which directly eliminate infection, including macrophages, natural killer (NK) cells, and dendritic cells (DCs). Innate immune cells respond rapidly (within minutes) but briefly to infection, and innate responses are triggered by recognition of pathogen-derived molecular “patterns”, which include double stranded RNA, and peptidoglycans. Upon activation, phagocytes including macrophages engulf pathogens and destroy them via proteolysis (Hirayama et al., 2017), while NK cells kill infected host cells through secretion of cytotoxic molecules including granzymes and perforin (Vivier et al., 2008). Finally, DCs can present pathogen derived antigens to immunologically naïve T cells, creating a bridge between the innate and adaptive arms of immune system (Iwasaki and Medzhitov, 2015).

The adaptive immune system responds more slowly to infection, but adaptive responses are tailored to the type of infection, and importantly, provide immunity to reinfection (immunological memory). Activation of adaptive immune cells (B and T lymphocytes) occurs via clonal receptors with exquisite specificity, such that a single receptor recognises a single antigen. To be able to respond to the broad array of possible pathogen threats, cells expressing a given receptor must therefore be rare, while the diversity of receptors expressed is tremendous. Indeed, the rarity of adaptive cells recognising a single pathogen necessitates that pathogen-specific adaptive lymphocytes must undergo clonal expansion to enable immune clearance. This need for expansion distinguishes innate and adaptive immune cells, with innate cell recognition of generic pathogen features meaning many more individual cells can respond to a particular pathogen.

Adaptive immune cells are also distinct from innate cells in that expression of functions required for pathogen clearance (including secretion cytokines and cytolytic molecules, and antibodies) is only acquired upon differentiation of antigen-naïve cells to an effector state. Combined with the need to clonally expand to generate a pool of cells sufficient to mediate immune clearance, the need to acquire effector functions explains the delayed adaptive immune response. Finally, adaptive immune responses result in the formation of immunological memory, whereby a pool of the expanded pathogen-specific lymphocytes persists, often for the life of the host, following clearance of the infection. These memory cells are quiescent but re-acquire effector functions rapidly after re-infection (within hours, as opposed to days for naïve responses), often before disease manifests.

Adaptive immune responses are characterised by humoral and cell-mediated components. B cells drive the humoral immune response by secreting antibodies which bind pathogen expressed surface antigens, thereby targeting the pathogen for destruction by macrophages (Akkaya et al., 2020). Additionally, antibody binding inhibits the entry of pathogens, including viruses, to host cells (Guthmiller et al., 2021).

A limitation of humoral immunity is that where pathogens enter host cells, they are no longer accessible to antibodies. In these instances, pathogen clearance must be mediated by T cells and NK cells. Cell mediated adaptive immunity is mediated by $CD4^+$ and $CD8^+$ T cells, which recognise antigenic peptides presented by major histocompatibility complexes (MHC) on antigen presenting cells (APCs), including DCs, macrophages, and B cells via heterodimeric T cell receptors (TCRs). Activation of $CD4^+$ T cells, which is mediated specifically by MHCII complexes, results in their differentiation to effector cells which secrete cytokines that regulate and coordinate the responses of B cells and $CD8^+$ T cells (described further below below). In contrast, activation of $CD8^+$ T cells by MHC1-peptide complexes results in effector cells producing anti-viral cytokines and

cytotoxic molecules, enabling direct killing of infected host cells which express the same peptide: MHC1 complexes. Moreover, $CD8^+$ T cells play an important role in tumour surveillance, killing host cells expressing neoantigens.

1.2 T cell differentiation and acquisition of lineage function.

Activation of naïve $CD4^+$ and $CD8^+$ T cells triggers a program of clonal expansion and concurrent differentiation and acquisition of lineage specific effector functions that enable elimination of the infection. Upon activation, $CD4^+$ T cells differentiate into helper T cell lineages which include T helper 1 (Th1), T helper 2 (Th2), T helper 17 (Th17 cells) and T regulatory cells (Treg). Each of these differentiation states are characterised by the production of specific cytokines that play distinct roles in eliminating infection (Luckheeram et al., 2012). Importantly, the nature of the infection determines the outcome of differentiation, such that the immune response is tailored to be most efficient for clearance of the pathogen at hand. For instance, viral infections skew differentiation towards a Th1 fate, which is characterised by secretion of interferon gamma; Interferon gamma (IFN-γ), in turn, causes upregulation of MHC expression on infected host cells, and drives effector $CD8^+$ T cell differentiation by signalling upregulation of the transcription factor TBET (Castro et al., 2018). In contrast, infection by extracellular parasites such as helminth worms drives Th2 differentiation. Th2 cells secrete Interleukin 4 (IL-4) which stimulates maturation of B cell antibody responses (Allen and Maizels, 2011).

In contrast to the diversity of differentiation outcomes that can result from $CD4^+$ T cell activation, $CD8^+$ T cell differentiation predominantly results in effector cells that secrete proinflammatory cytokines such as Tumor Necrosis Factor (TNF) and IFN-γ, and cytotoxic molecules such as the pore forming protein perforin, and granzyme proteases (GZMs) including GZMA, B and K (Jenkins et al., 2008, La Gruta et al., 2004, Jenkins et al., 2007). Consistent with adaptive immune responses being tailored for efficient elimination of the particular pathogen at hand, effector $CD8^+$ T cell responses are promoted by Th1 mediated secretion of IFN-γ, and are inhibited by IL-4 secreted by Th2 cells.

1.3 $CD8^+$ T cell differentiation facilitates cytotoxic functions and memory formation.

T cell responses to infection occur in three phases: clonal expansion, contraction, and memory formation. As described above, pathogen-specific, naïve T cells are quiescent and present at low frequency in the immune repertoire (La Gruta et al., 2010). These cells have an immense capacity to proliferate and clonally expand into effector T cells upon their interaction with APCs via T cell receptor (TCR) in addition to receipt of co-stimulatory and inflammatory signals (Viola and Lanzavecchia, 1996, Zinkernagel and Doherty, 1974, Curtsinger et al., 2003b). Importantly, once the infection is cleared, while most of the expanded T cell pool will die via apoptosis, a long-lived pool of memory T cells remains, which are capable of responding rapidly to secondary infection without the need for further differentiation, often providing immunity to reinfection (Kaech et al., 2002a) (summarised in Figure 1.1). While TCR ligation with peptide: MHC is sufficient to activate T cells, optimal $CD8^+$ T cell expansion and memory formation and function requires the integration of 3 signals:

Signal 1 involves interaction of the alpha-beta T cell receptor (TCR) dimer with peptide-MHC1 complexes (pMHC1) on the surface of APCs, which provides the specificity of the response. This interaction initiates downstream signaling pathways mediated by early response transcription factors including Activator Protein 1 (AP-1), Nuclear Factor of Activated T cells (NFAT) and Nuclear Factor (NF)- κB, which activate transcription of genes that drive the initiate the effector transcription program (Hwang et al., 2020). For example, AP-1 factors bind and activate IRF4, which is, in-turn, required to enable the metabolic reprogramming needed to fuel clonal expansion. Importantly, the strength of TCR-pMHC1 ligation influences T cell activation outcomes - while strong and repetitive TCR signalling drives efficient terminal effector $CD8^+$ T cell differentiation as well as memory differentiation (Teixeiro et al., 2009), low affinity TCR signalling results in a reduced magnitude of effector responses, but does not compromise memory formation (Zehn et al., 2009).

Signal 2 is provided by a receptor-ligand interaction between the naïve T cell and the APC. For instance, via interaction of CD28 expressed by the T cell with CD80/CD86 expressed on the surface of the APC. This interaction reduces the threshold of TCR signal required for T cell activation (Kundig et al., 1996, Tuosto and Acuto, 1998, Viola and Lanzavecchia, 1996) and promotes production of IL-2 by the T cell. IL-2 then signals in an autocrine manner to promote T cell survival, and thus enables T cell differentiation (Sperling et al., 1996, Boise et al., 1995).

Signal 3 is provided by pro-inflammatory cytokines and is crucial to induce complete activation of T cells. Signal 3 is important for generating functional $CD8^+$ T cells in case of diminished antigen load or weak TCR stimulus thus reducing the activation threshold (Curtsinger et al., 2003a, Richer et al., 2013). Kolumam *et al*. demonstrated that clonal expansion of antigen specific $CD8^+$ T cells in response to viral infection is dependent on type I interferons (Kolumam et al., 2005). While IFNα signalling is required for the expansion of CTLs during LCMV infection by limiting apoptosis, IL-12 is required for development of anti-vaccinia virus mediated $CD8^+$ T cell effector and memory responses (Xiao et al., 2009). In contrast, Denton *et al*. has demonstrated that during influenza infection, IL-18 is required but not IL-12 for the development of effector or memory $CD8^+$ T cells (Denton et al., 2007).

Taken together, integration of signal 1, 2 and 3 is required for a program of proliferation and differentiation which results in the formation of large pool of effector cells that secretes effector molecules which includes cytokines and cytotoxic molecules and directly kill the pathogens (Russ et al., 2013) (Figure 1.1). Majority (90-95%) of these effector cells are terminally differentiated and undergo apoptosis when the infection is cleared. A small population (5-10%) of cells persist to become long lived memory cells. These cells have lower threshold for activation and hence can be activated rapidly upon secondary infection without the need for further differentiation (Russ et al., 2013).

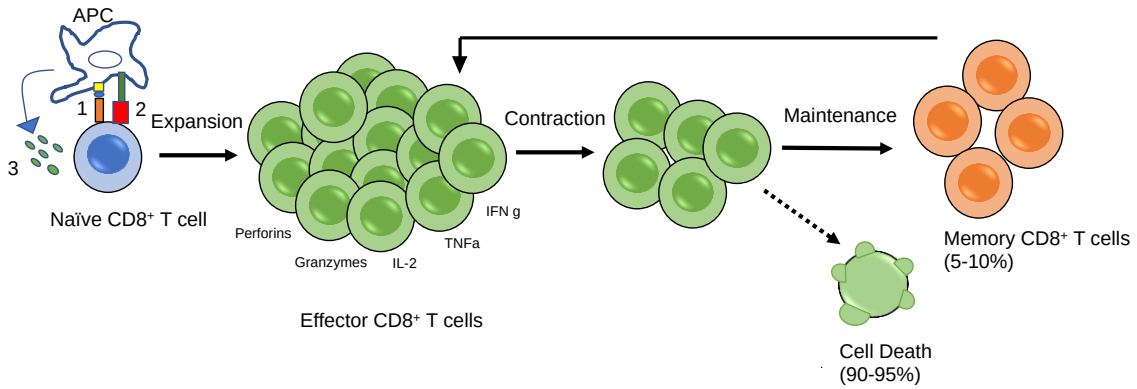

Figure 1.1: **Kinetics of CD8⁺ T cell differentiation**: Antigenic stimulation (signal1), costimulation (signal 2) and pro-inflammatory cytokines (signal 3) initiates clonal expansion and differentiation of naïve CD8⁺ T cells into a large pool of effector CD8⁺ T cells capable of secreting cytotoxic molecules such as perforins and granzymes and anti-viral cytokines such as Il-2, TNFα and IFN-γ. Once the infection is cleared, they undergo a contraction phase mediated by programmed cell death leaving behind a small pool of memory cells which rapidly responds to secondary infection. (Adapted from *Russ, B et al.* 2013 (Russ et al., 2013))

1.4 Transcriptional regulation during CD8⁺ T cell differentiation.

T cell activation results in the induction of transcriptional programs that drive differentiation to effector and memory states, and each differentiation state is characterised by expression of a unique set of transcription factors (TFs) that install and maintain the appropriate transcriptional program (reviewed in Kaech et al.(Kaech and Cui, 2012) and Russ et al. (Russ et al., 2012)). For instance, the regulatory activities of T-BET (T-box transcription factor TBX21), BLIMP-1 (B-lymphocyte-induced maturation protein-1), RUNX3 (Runt-related transcription factor 3), BATF (Basic leucine zipper transcription factor, ATF-like) and GATA3 drives effector differentiation (Cruz-Guilloty et al., 2009, Rutishauser et al., 2009, Kurachi et al., 2014, Tai et al., 2013), for instance by directly activating effector gene expression, while Eomesodermin (EOMES), T cell factor-1 (TCF-1), BCL6 and FOXO1 are involved in memory T cell differentiation and maintenance (Ichii et al., 2004, Jeannet et al., 2010, Hess Michelini et al., 2013), and the restraint of transcriptional networks driving effector differentiation. Thus, differentiation state

specific TFs are required establish differentiation state specific gene expression programs, while repressing transcriptional programs characteristic of alternative differentiation states.

1.4.1 TCF-1, BACH2 and LEF-1 enforce quiescence in naïve CD8⁺ T cells.

Naïve CD8⁺ T cells are characterised by a specific transcriptional profile that includes key markers of self-renewal and quiescence that maintain stemness, which interestingly, must be repressed during CD8⁺ T cell activation (Russ et al., 2012, Kaech and Cui, 2012) to enable effector differentiation. This includes expression of genes encoding Special AT-Rich Binding Protein (SATB1, encoded by *Satb1*), downstream effectors of the Wnt pathway such as T cell factor 1 (TCF-1, encoded by *Tcf7*), and Lymphoid Enhancer-Binding Factor 1 (LEF1 encoded by *Lef1*). SATB1 is a chromatin organizer capable of activating or repressing gene transcription (Yasui et al., 2002) and has been described to regulate the coordinated expression of cytokines in T-helper 2 (Th2) cells via remodelling of chromatin within the Th2 cytokine locus (Cai et al., 2006). Moreover, SATB1 represses PD-1 expression during CD8⁺ T cell activation by recruiting the Nucleosome Remodelling Deacetylase complex (NURD) to the *Pdcd1* enhancer region (*Pdcd1* encodes PD-1); in turn, histone deacetylation results in a transcriptionally repressed chromatin state (described in detail below) (Stephen et al., 2017). SATB1 is strongly expressed in naïve CD8⁺ T cells (in both mouse and human) and is repressed upon activation to enable expression of genes characteristic of effector and memory T cells (Russ et al., 2014, Nussing et al., 2019). For instance, in naïve but not effector T cells, SATB1 binds to and represses genes related to the immune lineage functions, such as cytokines and chemokines (Nussing et al., 2022).

Like SATB1, TCF-1 is strongly expressed by naïve CD8⁺ T cells and must be downregulated to permit effector T cell differentiation. Indeed, TCF-1 is crucial for maintaining naïvety through its repression of TFs such as BLIMP1 and TBET, which drive effector gene expression. TCF1 also promotes expression of TFs

such as BCL6, which, in-turn, represses genes favouring terminal effector differentiation (Danilo et al., 2018).

T cell activation results in the phosphorylation and translocation to the nucleus of AP-1 family TFs, which bind and activate genes encoding effector molecules including Interferon gamma, and chemokines CCL3 and CCL4 (Roychoudhuri et al., 2016). Thus, suppression of the activity of AP-1 TFs is also necessary for maintaining naïve T cell quiescence. This is achieved through binding of BACH2 to transcriptional regulatory regions that would otherwise be targeted by AP-1, thereby blocking AP-1 binding, and repressing TCR-responsive genes that drive effector differentiation (Scharer et al., 2017). Taken together, regulatory functions of TFs are crucial for maintaining the naïve state, and their removal upon activation is necessary for appropriate T cell activation.

1.4.2 IRF4, T-BET, and BLIMP-1 drive effector differentiation.

As described above, T cell activation results in dynamic changes in gene expression, whereby the naïve transcriptional program is repressed, and effector and memory transcriptomes are installed. However, these changes occur only if T cells overcome signalling thresholds that ensure appropriate activation. Interferon regulatory factor 4 (IRF4) is one factor that maintains this threshold, with transcriptional induction of *Irf4* only occurring when a sufficiently strong TCR signal having been received (Man et al., 2017). Indeed, IRF4 is an essential driver of effector differentiation, and in the absence of IRF4, activated cells fail to fully expand in response to infection (Man et al., 2013). Basic Leucine Zipper Transcriptional factor ATF-like (BATF) forms complexes with IRF4 which is necessary for expansion and effector differentiation, and this complex binds to the gene promoters of T-BET (encoded by *Tbx21*) and B lymphocyte-induced maturation protein 1 (BLIMP-1, encoded by *Prdm1*), which in turn, promotes the expression of effector/memory genes(Iwata et al., 2017). BATF-IRF4 complex along with its binding partners, c-Jun, JunB and JunD and targets the promoters of lineage specific factors like *Tbx21 and Prdm1* (Kurachi et al., 2014).

Like IRF4, T-BET is also crucial for the formation of effector responses, in part through its direct activation of effector molecules including IFN-γ, Granzyme B, and CCL5 (Sullivan et al., 2003). Prier *et al*. demonstrated that while T-BET is not required for early T cell activation (as IRF4 is), it is necessary for maintaining the expansion of effector T cells and subsequent acquisition of effector functions (Prier et al., 2019) IRF4 drives the metabolic changes needed to enable T cell differentiation (Man et al., 2017). Shan *et al*. showed that RUNX3 is essential for clonal expansion and activation of cytotoxic function of effector CTLs by binding to the promoter regions of *Ifng* and *Gzmb* (Cruz-Guilloty et al., 2009) (Shan et al., 2017). Indeed, as with BATF and IRF4, Cruz-Guilloty *et al*. showed that RUNX3 and T-BET act synergistically to regulate CTL differentiation and function (Cruz-Guilloty et al., 2009).

Finally, BLIMP-1 is crucial for effector differentiation in response to Influenza infection, and in the absence of *Prdm1*, effector and memory differentiation is diminished (Kallies et al., 2009) indicating that BLIMP-1 drives terminal differentiation (Rutishauser et al., 2009). This is likely because BLIMP1 represses expression of the inhibitory molecule PD-1, to thus enabling full T cell expansion (Lu et al., 2014).

Collectively, these TFs alone or with interaction with other TFs, are necessary for appropriate effector differentiation following viral infection because they repress the naïve program while activating genes necessary for effector differentiation.

1.4.3 EOMES, FOXO1, and TCF-1 are required for memory formation. Memory T cells are quiescent and maintain fate potential, and thus have shared attributes with naïve T cells. Therefore, it is not surprising that memory T cell formation and maintenance is regulated by a partly overlapping set of TFs to those required for the maintenance of naïvety. For instance, TCF-1 enables memory T cells to receive homeostatic IL-15 signals, through its direct promotion of EOMES expression, which, in-turn, upregulates CD122 (IL15RB) (Zhou et al., 2010). As such, EOMES, a TF which is a paralogue of T-BET, is required to

establish memory with T cells lacking EOMES undergoing clonal expansion but failing to survive long-term (Banerjee et al., 2010). As described above, TFs that drive terminal effector differentiation must be repressed to establish memory. While TBET deficient mice form excessive central memory cells, EOMES deficient mice contain fewer memory cells indicating the opposing roles of these TFs (Banerjee et al., 2010). Similarly, FOXO1, which maintains naïve T cell quiescence, also regulates memory formation by directly repressing T-BET, which would otherwise mediate terminal differentiation, thus favouring memory formation (Rao et al., 2012). Jeannet *et al*. demonstrated the role of TCF1 in memory formation by showing that T cells lacking *Tcf7* failed to establish memory precursor cells in response to viral infection (Jeannet et al., 2010).

While the strict temporal expression of differentiation state specific TFs is an important determinant of T cell differentiation, gene expression is regulated at a more fundamental level by the capacity of transcription factors to bind their targets. This, in-turn is influenced by the structure of the chromatin itself, which is also regulated to control T cell differentiation. The following sections summarise mechanisms that control chromatin structure.

1.5 Epigenetic regulation of $CD8^+$ T cell differentiation.

Epigenetic mechanisms are considered key regulators of cellular differentiation. Major epigenetic mechanisms include DNA methylation and post translational modifications (PTMs) of histone proteins positioned within regulatory genomic elements such as promoters and transcriptional enhancers (TEs). 147 bp of DNA is coiled around a complex of histone proteins H2A, H2B, H3, and H4 forming an octamer which forms the building units of chromatin (Figure 1.2 A and B). Histone proteins possess solvent-exposed N-terminal tails, and these histone tails can undergo several types of PTM, including methylation, acetylation, and ubiquitination (Kouzarides, 2007, Tessarz and Kouzarides, 2014). The pattern of nucleosome deposition and their associated PTMs serve to regulate the gene transcription by controlling access of TFs and the transcriptional machinery to genes. For example, a loose association or low nucleosome density at genomic

sites (a structure termed euchromatin) makes those site accessible to protein binding and is associated with increased gene transcription. Conversely, the intimate association of nucleosomes and DNA can block binding of the transcriptional machinery to prevent gene transcription. Thus, the positioning of nucleosomes must be tightly regulated to achieve appropriate gene expression (Knezetic and Luse, 1986, Morse, 2003) (Figure 1.2C).

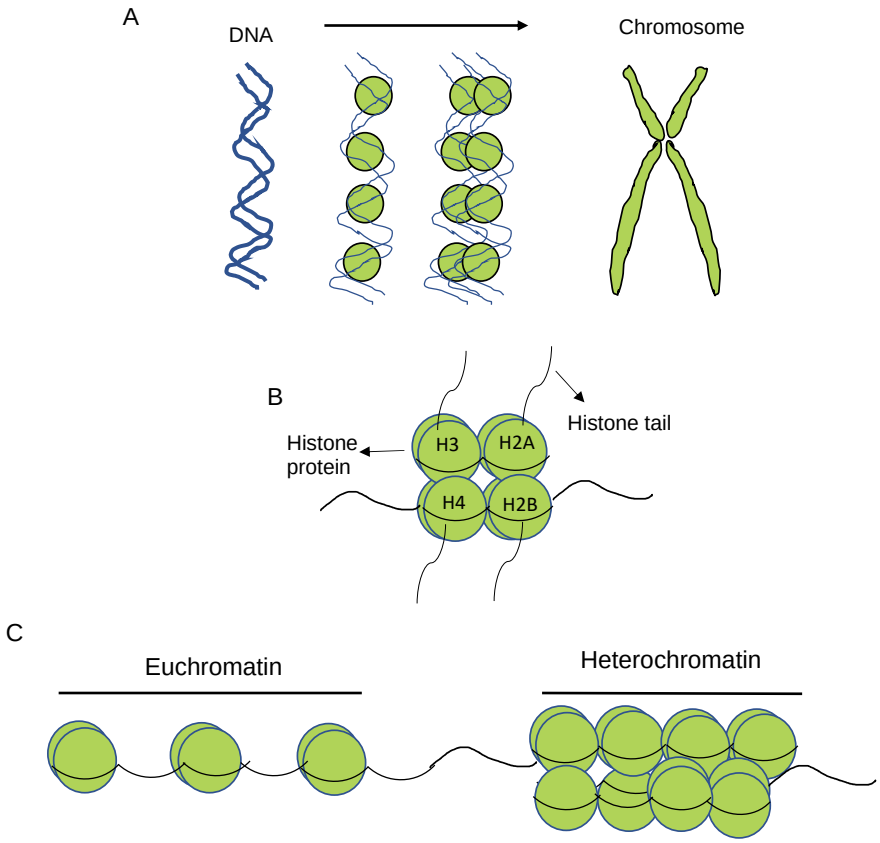

Figure 1.2 Chromatin is formed from DNA and histone proteins: A) 147bp of DNA is wrapped around histone proteins termed nucleosomes which is the fundamental unit of chromosome. B) Nucleosome consists of two copies of histone proteins termed H2A, H2B, H3 and H4 which is connected by linker histone H1 along with histone tails. C) Chromatin is categorised into two types: euchromatin which is less compacted and associated with active transcription and heterochromatin, associated with condensed chromatin which is inaccessible for transcription.

1.5.1 DNA methylation modulates gene transcription.

Methylation of DNA on cytosine residues within CpG dinucleotides is a stable modification that can be inherited across cell divisions. DNA methylation is

mediated by DNA methyltransferases such as DNA methyltransferase 3a (DNMT3a) (Okano et al., 1999), while active removal of methylation is mediated by Ten-Eleven Translocation (TET) enzymes (Ito et al., 2011). DNA methylation typically acts to repress transcription by sterically hindering binding of TFs to target regulatory elements. Indeed, transcriptional regulation by DNA methylation and histone PTMs often intersect. For example, maintenance of DNA methylation status relies on H3 lysine 9 (H3K9) methylation, which ensures stable binding of DNMT enzymes to target CpG islands (Rothbart et al., 2012). DNA methylation is well known to regulate $CD8^+$ T cell differentiation. Youngblood and collegues have investigated the global changes in methylation in naïve and effector CTLs to better understand the memory development (Youngblood et al., 2017). Remodelling of DNA methylation also dictates acquisition of effector phenotype and repression of naïve cells (Scharer et al., 2013).

1.5.2 Histone modifications regulate the gene expression.

Gene regulation occurs at multiple levels, with the most fundamental level of control being modulation of access of the transcriptional machinery to the gene regulatory regions including transcriptional enhancers and gene promoters. Histone PTMs serve as substrates for cellular machines that add, remove and shuffle nucleosomes to modulate access to gene regulatory regions, and ultimately to regulate gene transcription and cellular differentiation, including $CD8^+$ T cell differentiation (Russ et al., 2014). As mentioned previously, histone tails undergo several post-translational modifications (PTMs) including methylation, acetylation, phosphorylation, and ubiquitination. Moreover, it is the precise position and extent of deposition of each modification that determines the overall outcome on gene transcription (described in detail below). Finally, addition and removal of specific PTMs is carried out by a set of regulator proteins broadly termed as ‘erasers’ or ‘writers’, respectively, and these PTMs are then interpreted by ‘readers’ which enact changes in chromatin state to modulate transcription.

1.5.3 Histone acetylation is associated with active transcription.

Histone acetylation involves the addition of acetyl groups to lysine residues on the histone tail and is associated with accessible chromatin and active transcription. The means by which acetylation results in accessible chromatin is via charge repulsion of neighbouring acetylated nucleosomes, and a reduction in the affinity of the acetylated nucleosomes for the DNA itself, as acetylation reduces the overall positive charge of the histone proteins (Kouzarides, 2007, Bannister and Kouzarides, 2011). Histone acetylation is modulated by histone acetyl transferases (HATs) which catalyse the acetylation (Berndsen and Denu, 2008), whereas the removal is catalysed by histone deacetylases (HDACs) (Haberland et al., 2009). In $CD8^+$ T cells, expression of the lineage defining effector gene *IfnG* coincides with acetylation of histone H3 at lysine 9 (H3K9ac), with acetylation being maintained in memory T cells (Denton et al., 2011a). Acetylation is also maintained at the perforin and granzyme B encoding loci of memory T cells and coincides with the binding of RNA polymerase II (RNAPII), despite the cells being resting and not actively expressing effector molecules (Araki et al., 2008). Indeed, depletion of histone acetylation with the use of the histone acetyltransferase inhibitor curcumin largely abolishes the ability of memory T cells to upregulate these effector molecules following restimulation (Araki et al., 2008). Taken together, these data suggested that histone acetylation is required for effector gene expression in $CD8^+$ T cells, likely because it is required to enable RNAPII binding to effector gene promoters.

1.5.4 Histone methylation is found at active and repressed genes.

Histone methylation involves the addition of one, two or three methyl groups at lysine and arginine residues, and is catalysed by site-specific histone methyl transferases (HMTs) (Greer and Shi, 2012). Unlike histone acetylation, methylation can serve as a substrate for the recruitment of chromatin modifying complexes and transcriptional machinery. Additionally, unlike acetylation which is a hallmark of active transcription, methylation can be associated with both active and repressive chromatin structures. For instance, trimethylation of histone H3 lysine 27 and 9 (H3K27me3 and H3K9me3) are linked to transcriptional

repression, while H3K4me3 is deposited on actively transcribed genes (Greer and Shi, 2012).

H3K27me3 is a very well-studied histone modification in $CD8^+$ T cells and know to modulate the lineage specification (Russ et al., 2014, Gray et al., 2017). Enhancer of Zeste homologue 2, a part of the Polycomb Repressive Complex 2 (PRC2), catalyses H3K27 trimethylation, which is removed by the histone demethylases KDM6B and UTX (Cao et al., 2002) (Agger et al., 2007). H3K27me3 itself is then recognised by Polycomb Repressive Complex 1 (PRC1), the activity of which catalyses chromatin compaction (Detailed further in **section 1.6**) (Piunti and Shilatifard, 2021).

The repressive PTM H3K9me3, which is deposited by the histone methyl transferase SUV39h1, is associated with formation of heterochromatin and stable gene silencing (Rea et al., 2000). H3K9me3, through its interaction with Heterochromatin Protein 1 (HP1), initiates the formation of heterochromatin at lineage specific genes during development (Lachner et al., 2001, Jacobs and Khorasanizadeh, 2002), and in $CD8^+$ T cells, silences memory transcriptional programs following T cell activation to promote differentiation of terminal effector cells (Pace et al., 2018).

In contrast to H3K9mes and H3K27me3, H3K4 mono, di and trimethylation is associated with activated and transcriptionally poised genes. H3K4me1, a marker of transcriptional enhancers (TEs) can be found co-deposited with H3K27me3 at poised TEs and active or poised promoters, whereas H3K4me2 is generally associated with active TEs and genes and is often co-deposited with H3K27Ac (Bernstein et al., 2005). H3K4me3 is associated with the promoters of active genes (Santos-Rosa et al., 2002). Finally, H3K4me3 is preferentially deposited at gene promoters of actively transcribed genes, where it is often associated with H3K27ac and RNAPII, but also in combination with H3K27me3 at “bivalent” loci (Pokholok et al., 2005, Ng et al., 2003). This bivalent signature has been shown to mark genes that drive fate decisions in ESCs, but also in less primitive cell

types including $CD8^+$ T cells, where it poises genes for rapid activation or repression depending on the fate the cell adopts (Russ et al., 2014, Bernstein et al., 2006a, Araki et al., 2009).

1.5.5 Histone ubiquitination is associated with transcriptional repression.

Ubiquitination of histones occurs at lysine residues and can be associated with activate or repressive chromatin, depending on the position of the modification. While H2A ubiquitination is catalysed by the E3 ubiquitin ligase RING1B, and results in transcriptional repression, RNF20-catalysed ubiquitination of H2B which leads to the target gene activation (Cao and Yan, 2012, Zhang, 2003). Furthermore, ubiquitination is reversible and is mediated by deubiquitinating enzymes (DUBs) (Komander, 2010). Finally, of relevance to this thesis, the role of histone ubiquitination has not been studied in $CD8^+$ T cells.

***1.5.6 Coordination of multiple histone modifications defines transcriptional outcomes*.**

It is evident that the transcriptional outcome is dependent on the combination and degree of enrichment of histone modifications (Wang et al., 2008). Thus, it is crucial to analyse multiple histone modification to understand the role of histone modifications in regulating the gene expression. For instance, Denton *et al*. have shown that epigenetic signatures at the promoter of *ifnG* switches from repressed state to active state during effector differentiation (Denton et al., 2011a). Comparison of the incorporation of H3K9ac, H3K4me3, and H3K27me3 at the promoters between naïve and effector $CD8^+$ T cells showed that that there was an increased enrichment of permissive H3K4me3 and H3K9ac in effectors compared to naïve cells and concomitant decrease in the repressive chromatin modification H3K27me3. Moreover, there was a transcriptional poising of promoters with RNAPolII at the *TnfA* and *IfnG* loci in memory $CD8^+$ T cells providing a likely mechanistic basis for rapid secretion upon secondary infection (Denton et al., 2011a). Araki *et al*. have shown through a global analysis of H3K4me3 and H3K27me3 deposition in human, polyclonal, naïve and memory $CD8^+$ T cells that local deposition correlates with subset specific gene expression (Araki et al., 2009). Similarly, Russ *et al*. have demonstrated that the promoters

of T cell lineage commitment genes are enriched for both H3K27me3 and H3K4me3 termed bivalent loci, indicating the combination of histone modifications resulting in regulation of cellular differentiation (Russ et al., 2014). More Importantly, it was the addition and removal of H3K27me3 that was the most prominent change associated with the expression of genes. As mentioned previously, at those gene loci that were expressed, there was co-deposition of active/repressive marks at the same genomic location, and it was removal of the repressive mark that was associated with rapid transcriptional activation (Russ et al., 2014). In this regard, recent work published by Li et al. showed that a histone demethylase, KDM6B was critical in this early K27me3 removal, with removal of H3K27me3 occurring prior to first cell division, with early removal required to ensure appropriate staging of the differentiation program (Li et al., 2021). These histone modifications, not only alter the chromatin architecture, thus regulating the transcriptional outcome, but also recruit chromatin modifying enzymes that alter chromatin compaction and decompaction, thus inhibiting or favouring gene transcription, respectively.

1.6 Polycomb Repressive Complexes and transcriptional repression.

Polycomb repressive complexes (PRCs) are a highly conserved and well-studied group of chromatin-modifying machines that were initially identified in *Drosophila melanogaster* for their role in silencing of *Hox* gene cluster and which have since been shown to have broad roles gene silencing (Lewis, 1978). PRCs can be grouped into two major multiprotein complexes: PRC1 (Wang et al., 2004) and PRC2 (Margueron et al., 2008, Shen et al., 2008). PRC2 has histone methyl transferase activity (H3K27) and establishes repressive chromatin states, while PRC1 “reads” methylation signatures deposited by PRC2, and alters higher order chromatin organisation, contributing to stable transcriptional repression through ubiquitination of histone H2A at Lysine 119 (Aloia et al., 2013, Aranda et al., 2015).

1.6.1 Polycomb repressive complex is a diverse, multiprotein complex.

Both PRC1 and PRC2 are comprised of core and accessory components, with the accessory component determining specificity. The core PRC2 complex comprises of Suppressor of Zeste 12 (SUZ12) and Extra Embryonic Development (EED), which are required for the methyltransferase activity conferred by SET domain containing EZH1/2 (Figure 2A) (van Mierlo et al., 2019). This core complex is associated with several cofactors such as JARID2, PCL1-3, AEBP2 whose main functions are regulation of enzymatic activity and complex recruitment (van Mierlo et al., 2019).

PRC1 is not a single complex, but rather a core that can associate with a range of accessory proteins. The core complex of PRC1 contains RING1B – an E3 ubiquitin ligase that catalyses Lysine 119 on H2A – and one of the Polycomb group Ring Finger (PCGF) proteins (PCGF1-6). Further, based on their association with either the Chromodomain containing CBX proteins (2, 4, 6, and 8), or RING1 and YY1 binding proteins (RYBP), they are classified into canonical PRC1 or non-canonical PRC1 complexes, respectively (Figure 2B). Further, canonical PRCs always contain either PCGF2 (MEL18) or PCGF4 (BMI1), and one of the three Polyhomeotic-like proteins (PHC1, PHC2, and PHC3), while-non canonical PRC1 have one of the PCGF, PCGF1, 3, 5 and 6, with the PCGF component being necessary for the enzymatic activity of Ring1B (Gao et al., 2012, Di Croce and Helin, 2013).

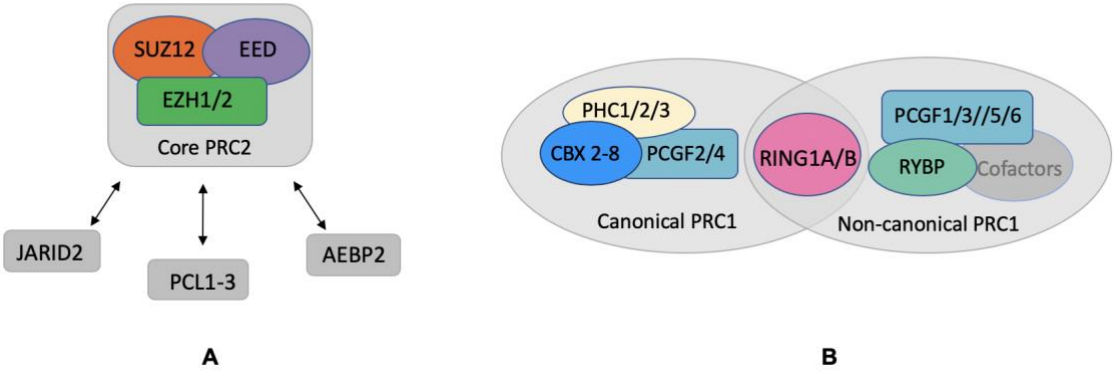

Figure 1.3: Classification of PRCs: PRCs can be divided into two PRC1 and PRC2, based on function and composition, while PRC1 complexes are further divided into canonical and non-canonical complexes. The PRC2 core components confer enzymatic activity (EZH1/2), or scaffold functions (SUZ12 and EED), and associate with a variety of cofactors (JARID2, PCL, AEBP2) (A). Canonical and non-canonical PRC1s have a common (RING1A/B) catalytic component, a PCGF component, and either a CBX or RYBP component.

1.6.2 Mechanism of Polycomb mediated gene silencing.

PRC2 and cPRC1 act together and sequentially to execute PRC mediated gene repression. PRC2 acts upstream of PRC1. PRC2 binds to chromatin and its catalytic subunit EZH2 trimethylates lysine 27 on H3 (Cao et al., 2002). This specific trimethylation is then read by the Chromodomain containing CBX component (mostly CBX4 and CBX7) of PRC1 (Fischle et al., 2003, Min et al., 2003). In turn, the E3 ubiquitin ligase RING1b monoubiquitinates lysine 119 on H2A, promoting the formation of heterochromatin and ultimately resulting in exclusion of transcriptional machinery to enact gene silencing (Figure 1.4) (Wang et al., 2004) via the formation of heterochromatin structures (Shao et al., 1999, Eskeland et al., 2010). Indeed, loss of PRC1 increases chromatin accessibility and subsequent transcription in Drosophila (Cheutin and Cavalli, 2018). Hence, H3K27me3 deposition is the initial step which marks chromatin for transcriptional repression. Subsequent recruitment of cPRC1 and deposition of H2AK119ub plays important role in transcriptional repression.

Importantly, H3K27me3 is not always required to recruit PRC1 to specific genomic regions as RYBP-PRC1 and the non-canonical PRC1 (ncPRC1) have

been shown to bind chromatin independently of PRC2 catalyzed trimethylation (Tavares et al., 2012). Morey *et al*. have shown that genes that are targeted by RYBP have lower levels of RING1B and H2AK119ub and more highly transcribed compared to CBX7 containing cPRC1 (Morey et al., 2013). Further, RYBP chiefly targets genes involved in metabolic processes and cell cycle progression, whereas cPRC1 regulates developmental genes that control lineage commitment, suggesting the importance of cPRC1 in regulating cellular fate decisions (Morey et al., 2013).

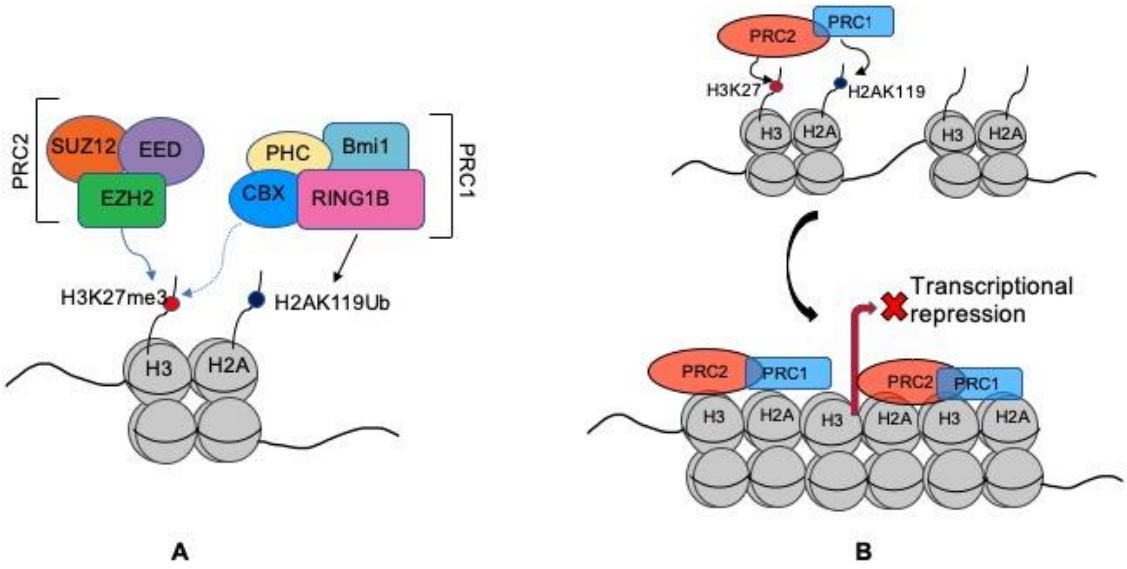

Figure 1.4: Canonical PRC 1 signaling: PRC2 binds to chromatin and trimethylates H3K27. The CBX components of PRC1 “read” the trimethylation, followed by RING1B mediated monoubiquitylation of Lysine 119 of H2A. This leads to the chromatin compaction and transcriptional repression.

1.7 The role of PRC components in regulating cellular fate decisions.

PRCs have key roles in regulating embryonic stem cell pluripotency, self-renewal and differentiation, and the role of various PRC components has been extensively studied in this context (Morey et al., 2012, Piunti and Shilatifard, 2021). Moreover, PRCs have key functions in mammalian embryogenesis with mutation of components within embryos typically resulting in gastrulation defects (reviewed in (Piunti and Shilatifard, 2021)). For instance, global deletion of EZH2, the catalytic component of PRC2, is embryonically lethal (O'Carroll et al., 2001).

Further knockout embryos for the PRC2 components such as EED and SUZ12 die during early post implantation stages, particularly during gastrulation (Schumacher et al., 1996, Pasini et al., 2004). RING1B knockout mice are embryonic lethal highlighting the importance of cPRC1 catalytic activity in regulating the very early stages of embryonic development (Voncken et al., 2003). Furthermore, RYBP KO mice also exhibit embryonic lethality highlighting the importance non-canonical PRC1 activity in embryogenesis (Pirity et al., 2005). The capacity to assemble distinct cPRC1 complexes with different components appears to be a mechanism that ensures appropriate cellular fate decisions (Morey et al., 2012, Blackledge and Klose, 2021). For instance, MEL-18, CBX7, CBX2, or BMI-1 mutant mice are born, but display distinct homeotic phenotypes. The gene targets of BMI-1 containing cPRC1 complexes in embryonic and hematopoietic stem cells include the *Hox* gene cluster (Cao et al., 2005). *Hox* genes are an evolutionarily conserved gene family which determine anterior-posterior body axis patterning, thereby influencing the development of bilateral organisms (Pearson et al., 2005). Indeed, the *Hox* gene cluster is a known target of cPRC1 and *Hox* gene expression is suppressed in embryonic stem cells (Kundu et al., 2018) (Cao et al., 2005). Upon receipt of differentiation signals, cPRC1 is downregulated, correlating with the upregulation of *Hox* genes and triggering cell lineage fate commitment of stem cells (Seifert et al., 2015). Therefore, the precise targeting of cPRC1 and associated components within the genome is a key regulatory mechanism that directs specific changes in chromatin structure and gene transcription that accompany embryonic stem cell differentiation.

Pluripotency and differentiation of mouse ESCs is regulated by different CBX-associated PRC1 complexes which have mutually exclusive functions, with maintenance of pluripotency depending on CBX7, and lineage commitment being driven by CBX2 and CBX4 (Morey et al., 2012). For instance, knocking-down CBX7 in ESCs induces premature differentiation by de-repressing lineage commitment markers which correlated with loss of H2AK119ub at these same gene loci, while overexpression of CBX7 inhibits differentiation (Cao et al., 2005,

O'Loghlen et al., 2012). Importantly, CBX7 occupancy of target gene loci is dependent on EZH2 mediated H3K27me3 deposition (Fischle et al., 2003). Upon ESC differentiation, CBX7 is downregulated and alternative CBX proteins, including CBX2 and CBX4 are incorporated into the cPRC1 leading to an altered genomic distribution of cPRC1 binding, and upregulation of pro-differentiation genes (Morey et al., 2012). However, it is not clear whether these findings extend beyond stem cell biology and represent a general mechanism by which cellular differentiation is regulated. Several studies in this regard have suggested the role of PRCs in neuronal differentiation (Desai et al., 2020), skeletal muscle differentiation (Caretti et al., 2004) and epidermal differentiation (Cohen et al., 2019). However, the role of PRCs in immune cell differentiation, and particularly T cells, has not been well studied in this context.

1.8 The role of PRCs in immune cell development and differentiation.

The role of polycomb proteins is well studied in haematopoiesis and maintaining the self-renewal capacity and multipotency of hematopoietic stem cells (HSCs). PRC2 components EED and EZH2 are known to regulate the development of HSCs in a developmental stage-specific manner. Loss of EED resulted in loss of adult HSCs leading to the expression of proliferation and differentiation genes in HSCs (Xie et al., 2014). Further, BMI-1 plays a crucial role in repressing the *Cdkn2a* locus which is critical for maintaining the self-renewal capacity of HSCs (Park et al., 2003, Oguro et al., 2006). The presence of different CBX components within HSCs specifies target selectivity and provides a molecular balance between differentiation and self-renewal of HSCs. While CBX7 is expressed by HSCs, and its overexpression enhances self-renewal inducing leukemia, overexpression of CBX2, 4 and 8 results in differentiation and exhaustion of HSCs (Klauke et al., 2013). BMI-1 containing PRC1 represses the B cell lineage master regulators *Ebf1* and *Pax5,* which in-turn results in T-to-B cell conversion (Ikawa et al., 2016).

EZH2 plays a critical role in NK cell development and maturation. Yu *et al*. have shown that conditional deletion of *Ezh2* in NK cells results in a maturation trajectory toward NK cell arrest at the CD11b SP stage 5 (Yu et al., 2021). EZH2

has also been shown be required for germinal centre (GC) formation and is highly expressed in GC B cells (Beguelin et al., 2013, Caganova et al., 2013). In human germinal centres, polycomb protein expression patterns correlate with different B cell differentiation stages and are reflective of GC architecture(Raaphorst et al., 2000). Di Pietro *et al*. have recently explored the role of BMI-1 in humoral responses to chronic viral infection showing that deletion of BMI1 accelerated viral clearance and restored splenic architecture by restoring c-Myc expression in B cells (Di Pietro et al., 2022). Thus, previous studies in various immune cells suggest that polycomb proteins play a crucial role in regulating the development and differentiation of hematopoietic stem cells, NK cells and B cells.

1.9 PRCs and T cell differentiation

The role of polycomb proteins has been studied in the context of generation of T cells in the thymus, survival and differentiation of $CD4^+$ T cells, and the generation of memory $CD8^+$ T cells in the context of infection and cancer. Deficiency of EZH2 or SUZ12 in early lymphoid progenitor cells, results in defect in lymphopoiesis and decrease in overall thymocyte numbers (Jacobsen et al., 2017, Lee et al., 2015). Loss of PRC1 member BMI-1, showed a reduced thymic cellularity and arrested thymocyte development with a higher proportion of double negative thymocytes (van der Lugt et al., 1994). Additionally, CBX2 and BMI-1 has also been shown to be involved in regulating DN3 proliferation and cell death by binding to the *Cdkn2a* locus which involved in cell cycle regulation and maintenance of H3K27me3 indicating the cooperation between PRC1 and PRC2 (Miyazaki et al., 2008). BMI-1 is also involved in regulating mitochondrial function in thymocytes and loss of BMI-1 leads to the increase of reactive oxygen species, arresting thymocyte development (Liu et al., 2009). Further, Heffner et al. showed that $KLRG1^-$ memory precursor cells have increased expression of BMI-1, however the mechanism is not well understood(Heffner and Fearon, 2007). Collectively these reports suggest that PRC1 and PRC2 components are important in T cell development.

PRC2 components have been well studied in the regulation of $CD4^+$ T lymphocyte differentiation. The role of EZH2 containing PRC2 has been studied in the differentiation and survival of peripheral T cells. Silencing of *Ifng*, *Gata3*, and *Il10* loci in naïve $CD4^+$ T cells is dependent on EZH2, and deletion of EZH2 silencing leads to Th1 skewing and IL-10 overproduction (Zhang et al., 2014). Furthermore, EZH2 has also been shown to be crucial for T reg cell differentiation (Yang et al., 2015). MEL-18, BMI-1 and RING1B are essential for the expression of Th2 related cytokines such as IL-4, IL-15 and IL-13 (Jacob et al., 2008, Hosokawa et al., 2006, Kimura et al., 2001, Suzuki et al., 2010). BMI-1 is also important for the maintenance of Th2 cells by regulating the genes associated with cell cycle and apoptosis such as *Cdkn2a* and *Bcl2* (Yamashita et al., 2008). CBX7 has been reported to regulate apoptosis related gene *FasL* in $CD4^+$ T cell upon activation (Li et al., 2014). Together, these reports suggest a role for both PRC1 and PRC2 in regulating $CD4^+$ T cell differentiation and function.

Consistent with these mechanisms having a role to play in the regulation of $CD8^+$ T cell differentiation, a recent study showed that EZH2-containing PRC2 is required for effector $CD8^+$ T cell terminal differentiation, with selective epigenetic silencing of pro-memory genes in the effector T cells underlying this fate decision (Gray et al., 2017). Finally, the role of PRC1 and its components in $CD8^+$ T cells remains elusive and is the focus of this thesis.

1.10. Specific Aims of the study

The work of this PhD thesis attempts to understand the role of canonical PRC1 components in regulating $CD8^+$ T cell differentiation. In particular, we attempted to dissect the role of BMI-1 mediated epigenetic repression in regulating $CD8^+$ T cell fate decisions and to determine the mechanisms underlying this regulation.

Hypothesis: Regulated expression of cPRC1 components modulates $CD8^+$ T cell differentiation.

Specific Aims:

1. To characterise the expression of cPRC1 components during $CD8^+$ T cell differentiation.
2. To determine the impact of BMI-1 mediated epigenetic silencing on $CD8^+$ T cell differentiation.
3. To investigate the mechanism by which BMI-1 regulates $CD8^+$ T cell differentiation.

CHAPTER 2: Materials and Methods.

2.1 Materials

2.1.1 Mice

C57BL/6j mice were obtained from Monash Animal Research Platform (MARP) and OT-I and *Bmi1*$^{fl/fl}$ Lck^{Cre} mice were housed and bred in the Animal Research Laboratory at Biomedicine Discovery Institute at Monash University (Clayton, Victoria, Australia) under specific pathogen-free conditions. All experiments were performed according to the guidelines specified by the animal ethics committee.

Table 2.1: Mice used in the study

Strain	Description
C57BL/6	Male and female, H-2^{b}-resticted CD45.2^{+}, aged between 6-8 weeks. These mice were used for adoptive transfers as well as Wild type (WT) controls for *Bmi1*$^{fl/fl}$ *Lck*^{Cre} mice
OT-I	Male and female, CD45.1^{+} and CD45.2^{+}, aged 8-16 weeks. TCR transgenic mice (V⟨2^{+}, V®5.2^{+}), CD8^{+} T cells specific for DbOVA$_{257-264}$(SIINFEKL) peptide.
Bmi1$^{fl/fl}$ Lck^{Cre}	Male and female, aged between 8-12 week. *Bmi1*$^{fl/fl}$ mice obtained from Prof. Kim Good Jacobson at Monash University. Originally generated by S. Morrison (University of Texas Southwestern) (Mich et al., 2014) and then were crossed to *Lck*^{Cre} mice to get T cell specific deletion of *Bmi1.*

2.1.2 Viruses

Three strains of Influenza A virus were used in this study. A/Puerto Rico/8/34 (PR8), serotype H1N1 (Caton et al., 1982), and A/Hong Kong/X31 (HK x31), serotype H3N2 (Schulman and Kilbourne, 1969, Kilbourne, 1969) . Both viruses contain 6 of the 8 PR8 gene segments (NP, PA, M, NS, PB1, and PB2), and are different in their surface hemagglutinin (HA) and neuraminidase (NA). Serologically

distinct viruses were used to study secondary $CD8^+$ T cell responses in the absence of neutralising antibody specific for the surface proteins HA and NA. Using reverse genetics, recombinant X31 viruses were engineered to contain the OVA257-264 peptide (SIINFEKL) in the NA stalk. The SIINFEKL peptide replaced the 8 amino acids at position 69 of x31 of the NA stalk. The recombinant viruses were created by Dr. Richard Webby at St Jude Children's Research Hospital (Memphis, TN, USA) (Jenkins et al., 2006).

2.1.3 Medias and buffers

Complete Roswell Park Memorial Institute medium 1640 (cRPMI): RPMI (Gibco) 1640 with 10% fetal calf serum, 2mM L-glutamine, 100U/ml penicillin, 0.1mg/ml streptomycin and 50mM b-mercaptoethanol.

Magnetic Activated Cell Sorting (MACS) buffer: HBSS with 0.5% BSA and 2 mM EDTA.

FACS buffer: PBS with 10% BSA and 0.02% sodium azide.

10X Phosphate buffered saline (PBS): 80g NaCl, 2g KCl, 14.4g Na2HPO4 and 2.4g KH2PO4 dissolved in 1L deionised H2O.

ChIP Dilution buffer: 0.01% SDS, 1.1% Triton X-100 (Sigma Cat #T8787-100ml), 1.2mM EDTA, 16.7mM Tris-HCI (pH 8) and 167mM NaCl (5M stock), made up in MilliQ water.

ChIP Lysis buffer: 1% SDS (10% SDS Gibco Cat 315553035), 10mM EDTA (0.5M EDTA Sigma Cat #E7889-100ml) and 50mM Tris-HCl (pH 8) in MilliQ water.

ChIP Low salt buffer: 0.1% SDS, 1% Triton X-100, 2mM EDTA, 20mM Tris HCl (pH 8) and 150mM NaCl, in MilliQ water.

ChIP High salt buffer: 0.1% SDS, 1% Triton X-100, 2mM EDTA, 20mM Tris-HCl and 500mM NaCl, in MilliQ water.
ChIP LiCl buffer: 0.25M LiCl (Sigma), 1% IGEPAL CA-630, 1% deoxycholic acid (Sigma), 1mM EDTA and 10mM Tris-HCl (pH 8) in MilliQ water.

ChIP TE buffer*:* 10mM Tris-HCl (pH 8) and 1mM EDTA in MilliQ water.

ChIP Elution buffer: 1% SDS and 0.1M NaHCO3 in MilliQ water.

Fc block: 2.4G2 supernatant (Section 2.5.1) with 1% normal mouse serum and 1% normal rat serum (Stem cell technologies, Vancouver, Canada). Fc block was diluted 1:2 in MACS buffer for use.

Hanks buffered salt solution (HBSS): 0.14 M NaCl, 0.005 M KCl, 0.001 M CaCl2, 0.0004 M MgSO4-7H2O, 0.0005 M, MgCl2-6H2O, 0.0003 M Na2HPO4-2H2O, 0.0004 M KH2PO4, 0.006 M D-Glucose and 0.004 M NaHCO3. Prepared by Media Preparation Unit from the Biomedicine Discovery Institute at Monash University, Clayton campus.

Lung digestion cocktail: 2.5 mg/mL Type I collagenase (Gibco) and 105 U/mL recombinant DNAse I (Sigma Aldrich) in RPMI-1640 media.

Percoll density gradient media: 63% Percoll (Sigma Aldrich), 7% 10x PBS, 30% 1x PBS and 2 mM EDTA.

Cut and Run NE buffer: 20mM HEPES-KOH (pH7.9) 10mM KCl, 0.5 mM Spermidine, 0.1% Triton X-100, 20%Glycerol.

RIPA buffer: Baxter water with 150 mM NaCl, 1% NP-40 (Sigma), 0.5% Sodium Deoxycholate, 0.1% SDS, 50 mM Tris-HCl pH 8.0, and 1x protease inhibitor cocktail.

1X SDS PAGE Running buffer: 25 mM Tris, 192 mM glycine, 0.1% SDS.

SDS PAGE loading buffer: 4x Laemmli Sample Buffer (#1610747 Biorad) with 10% V/V β-mercaptoethanol

1X SDS PAGE Transfer buffer: 25 mM Tris, 192 mM glycine, 20% (v/v) methanol (pH 8.3)

Tris-Tween Buffered Saline (TBST): 20 mM Tris,150 mM NaCl, 0.1% Tween 20.

2.1.4 Peptides

Table 2.2: Peptides used for *in vitro* stimulation of naïve $CD8^+$ T cells or re-stimulation assays to measure cytokine production.

Abbreviation	Protein	Amino acid sequence
NP366-374	Nucleoprotein	ASNENMETM
PA224-233	Acidic polymerase	SSLENFRAYV
OVA257-263	Ovalbumin	SIINFEKL
Q4	Ovalbumin	SIIQFEKL
G4	Ovalbumin	SIIGFEKL
E1	Ovalbumin	EIINFEKL

2.1.5 Antibodies

Table 2.3: Antibodies used for the *in vitro* stimulation of $CD8^+$ T cells.

Antibody	Clone	Supplier
Anti-CD3e	145-2C11	Hybridoma stocks
Anti-CD8	53.6-72	Hybridoma stocks
Anti-LFA-1	121/7.7	Hybridoma stocks
Anti-CD28	37.51	Biolegend

Table 2.4: Antibodies used for flow cytometry.

Antibody	Clone	Fluorochrome	Supplier
Anti-B220	RA3-6B2	FITC	eBioscience
Anti-CD3e	145-2C11	PerCPCy5.5 APC-Cy7	BD

Anti-CD4	GK1.5	PE, AF700, FITC	Biolegend
Anti-CD5	53-7.3	PE	Biolegend
Anti-CD8α	53-6.7	BUV395, Pacific blue, APC, FITC	BD Biosciences Biolegend
Anti-CD11b	M1/70	FITC	eBioscience
Anti-CD11c	N418	FITC	eBioscience
Anti-CD49d	R1-2	BUV395, AF647	Biolegend
Anti-CD44	IM7	APC-Cy7, PE-Cy7	Biolegend
Anti-CD62L	MEL-14	APC, BV605	Biolegend BD Biosciences
Anti-CD25	7D4	FITC	BD Biosciences
Anti-CD122	TM-b1	FITC, BUV395	eBioscience
Anti-CD127	A7R34	FITC, APC, PECy7, PE	eBioscience
Anti-F4/80	BM8	FITC	eBioscience
Anti-Granzyme A	Sc-33692	FITC	Santa Cruz Biotechnology
Anti-Granzyme B	GB11	Pacific Blue	Biolegend
Anti-IL-2	JES6-5H4	PE	Biolegend
Anti-IFNɣ	XMG1.2	FITC, APC	BD Biosciences
Anti-KLRG1	2F1	FITC, PECy7	eBioscience
Anti-PD-1	29.F.1A12	Percp Cy5.5	Biolegend
Anti-TCRβ	H57-597	APCCy7, AF700	Biolegend
Anti-TCF1	C63D9	AF488	CST
Anti-TNF	MP6-XT22	PE, PECy7, APC	Biolegend
Anti-TOX	TXRX10	PE	eBiosciecne
Anti EOMES	21Mags8	PE-Cy7	eBioscience

Table 2.5: Antibodies for Chromatin Immunoprecipitation (ChIP).

Antibody	Clone	Manufacturer	Catalogue No
Anti-H3K27me3	Rabbit Polyclonal	Millipore	07-449
Anti-H2AK119ub	Rabbit Monoclonal	Abcam	8240
Anti-Cbx7	Rabbit Polyclonal	Abcam	Ab21873

Table 2.6: Antibodies for Western Blotting.

Antibody	Clone	Manufacturer	Catalogue
Cbx7	Rabbit Polyclonal	Abcam	Ab21873
Cbx4	Rabbit Polyclonal	Abcam	Ab139815HM
Bmi1	Rabbit Monoclonal	CST	5856
H3	Rabbit Polyclonal	Abcam	Ab1791
Goat anti-rabbit IgG (H+L) secondary Ab HRP	Goat Polyclonal	Merck	AP307P

2.1.6 Primers

Table 2.7: TaqMan® Primers.

Primer	Assay ID	Species
Cbx7	Mm00520006_m1	Mus musculus
Cbx4	Mm00483089_m1	Mus musculus
Bmi1	Mm03053308_g1	Mus musculus
Poldip3	Mm00724315_m1	Mus musculus
Prdm1	Mm00476128_m1	Mus musculus
Eomes	Mm01351984_m1	Mus musculus
Irf4	Mm00516431_m1	Mus musculus

Tbx21	Mm00450960_m1	Mus musculus
Tcf7	Mm00493445_m1	Mus musculus
Satb1	Mm01268940_m1	Mus musculus
Lef	Mm00550265_m1	Mus musculus

Table 2.8: Primers used for SYBR green qPCR.

Gene	Forward primer	Reverse primer	Exons used	Amplicon Length
Poldip3	GCCCATTGGGACTGTAACC	TGCAAACTTCATCTGCTTGG	2 and 3	118
Ring1	CTCTATGAGCTGCACCGGAC	AGAATGCAGTGACCGAGGC	1 and 2	81
Rnf2	CGCGGATTGTATTATCACAGCC	ATCAAAGTTCGGGTCTGGCC	2 and 3	106
Phc1	TGTGGGCATGAACCTGACTC	GAGGTGGATCTGCTGCTGTT	6 and 7	121
Phc2	CAACACCTCATGCTGCAGAC	TTCCTTGTCTGTTGGCCACC	1 and2	119
Phc3	CCACCATCACCACATCCTCC	AGCCGCGTACATCTGCTG	2 and 3	149
Rybp	ACCATGGGCGACAAGAAGAG	TTCGGCGCTGTTCCTAAAGG	1 and 2	108
Mel18	CTCACGGAGAATGGAGATGGG	TGACGGTCATGGCTGCTG	6 and 7	76
Cbx7	CTGGGAGCCTATGGAGCAAG	AGTTGGCGGTGATGTCAGTC	5 and 6	122
Bmi1	CGCTAATGGACATTGCCTAC	TTTCCAGCTCTCCAGCATTC	9 and 10	138
Cbx4	ATGGGATATCGCAAGAGAGG	AAGCCCAGTCAGAACATTGG	4 and 5	90
Cbx8	AGCCTTTGAGGAAAGGGAAC	ATCCGGATGCCTCTGGTAG	3,4,5	147
Cbx 2	CCGAGGAAACACACAGTCAC	ACTGCTGGATTTGGATTTGG	4 and 5	87
Cbx6	TCGAGTACCTGGTGAAATGG	TGAGCCTCGAATCCAGAATG	2 and 3	109

Table 2.9: Primers used for ChIP and FAIRE

Primer	**Sequence**	**Region of Promoters**
Eomes	F: GCAGGGAGCTTGTAAAGACG	-276 to-384
	R: TTTGAAGTCTGCGAACATGG	
Irf4	F: CTGTAGTCGGGCAGAAGGAG	-276 to-384
	R: GGTCCGCTATCTCAGCATTC	
Prdm1	F: CCAACCTGCCCTTAGGTATG	-99to-48
	R: AGGCAGCTACAATCCGTCTC	
Tbx21	F: GAATTCGCGCTGTATTAGCC	-107to -10
	R: GCCTTTGCTGTGGCTTTATG	

2.2 Methods

2.2.1. Tissue processing

Mice were culled by CO2 asphyxiation prior to tissue collection.

Bronchoalveolar Lavage (BAL)

BAL fluid was collected by making a small incision in the trachea and washing the airways out three times with 1 mL HBSS using an 18-gauge catheter and 1 mL syringe. Cells were collected by centrifugation (1600 rpm, 6 min) and resuspended in 500 µL – 1 mL FACS buffer or cRPMI and passed through a 40 µM sieve before further analysis.

Lungs

Mice were perfused via cardiac injection with 10 mL PBS. Lungs were collected and minced with scissors, then digested with 2.5 mg/mL type I collagenase for 30 min at 37°C. Lung homogenates were then passed through a 70 µM cell strainer and collagenase was quenched with cRPMI. Cells were collected by centrifugation, resuspended in cRPMI and passed through a 70 ⌈M cell strainer before underlaying the cell suspension with 70% percoll. The cell suspension containing the percoll underlay was centrifuged at 800 x g for 20 min at room temperature with minimum deceleration. Lymphocytes at the interface were collected into 10 mL of cRPMI, collected by centrifugation and resuspended in cRPMI for further analysis.

Spleens

Spleens were collected into HBSS. Single cell suspensions were generated by mashing spleens through a 70 µM cell strainer with a 3 mL syringe plunger with 20 mL of HBSS. Cell suspensions were depleted of B cells by incubating cells on tissue culture plates pre-coated with goat anti-mouse IgG and IgM antibodies for 30 minutes-1 hours at 37°C with 5% CO2. Cells were collected and pelleted, then red blood cells (RBCs) were lysed with 2 mL lysis buffer (Red Blood Cell Lysing Buffer Hybri-MaxTM, Sigma-Aldrich, St. Louis, Missouri, USA) for 2 minutes at room temperature. Following lysis of RBCs, cells were washed and resuspended in 1-5 mL of HBSS before filtering through 70 µM filters into cRPMI for further analysis.

Thymus

Thymi were mashed through a 70 µM cell strainer with a 3 mL syringe with MACS or HBSS. Cells were collected by centrifugation, then resuspended in MACS buffer, FACS buffer or cRPMI for further analysis.

2.2.2. Infection with Influenza A

For primary infection, mice were first anesthetised by inhalation of isoflurane and then infected with 1 x 10^4 plaque forming units (pfu) of IAV, either WT strain A/HKx31 (H3N2) or HKx31-Ova in 30 µL PBS via intranasal (i.n) administration. For secondary infections, mice were first primed with 10^4 pfu of A/HKx31 i.n 60-70 days prior to i.n challenge with 1 x 10^3 pfu of A/PR8 (H1N1) or PR8-Ova virus in 30 µL PBS.

2.2.3. Adoptive transfer

lymph nodes from one or two naïve female OT-1 mice were collected and pooled before processing to generate a single cell suspension. The proportion of naïve $CD8^+$ T cells (CD8a+ CD44low) within the suspension was determined by staining a small number of cells with anti-CD44 (PE-Cy7) and anti-CD8 (Pacific Blue) antibodies and performing flow cytometry. Cells were counted, resuspended in PBS, and immediately transferred intravenously into naïve C57BL/6J recipient mice via tail vein or by retroorbital injections (1 x 10^4 cells per mouse, in 200 µL).

2.2.4 Isolation of $CD8^+$ T cells by cell sorting

Cells from spleen were stained with 0.5-1 mL of antibody cocktail containing anti-CD8α FITC, anti-CD44 PE-Cy7, anti-CD62L APC and Aqua Blue live/dead in PBS for 30 minutes on ice in the dark. After washing thoroughly with MACS buffer, cells were filtered through a 70 μM cell strainer and sorted to obtain naïve $CD8^+$ T cells (Aqua blue-, CD8α+, CD44low, CD62Lhigh) using a BD Influx Cell Sorter by the staff at FlowCore, Monash University.

2.2.5 *In vitro* stimulation of naïve CD8$^+$ T cells

For *in* vitro activation of naïve CD8$^+$ T cells by plate bound antibodies, 96 U bottom or 24 well plates (Nunclon) were pre-coated with 1µg/mL α-CD3 (unless otherwise specified), 5 µg/mL α-CD8 and 5 µg/mL µ-LFA-1(CD11a) antibodies diluted in sterile PBS at 4°C overnight, or 37°C for 1 hour. Wells were washed three times with sterile PBS. To each well, 5000-10,000 (for 96 U bottom plates) or 200,000-300,000 (for 24 well plates) cells were seeded in 200 µL or 2 mL cRPMI supplemented with human recombinant IL-2 (10 U/mL). Cells were incubated at 37°C with 5% CO2 for the indicated time points. Naïve OT-1 cells were activated *in vitro* by plating 5000-10,000 (for 96 U bottom plates) or 200,000-300,000 (for 24 well plates) cells/well in 200 µL or 2 mL cRPMI with 1 µM N4 or Q4 or G4 peptides in the presence of IL-2 (10 U/mL) and 5 µg/mL anti-CD28 (where indicated) and incubating at 37°C with 5% CO2 for the indicated time points. Unless otherwise indicated, cells were removed from peptide stimulation at 48 hours, split at 1:2 ratio and further cultured in cRPMI supplemented with IL-2 (10 U/mL).

2.2.6. Flow cytometric assays and analysis

Surface staining

Cells were stained in a U bottom 96 well plate with antibodies in 50 µL FACS buffer for 30 minutes at 4°C in the dark, or 15 minutes at room temperature in the dark. Cells were washed twice with FACS buffer, then analysed on the BD LSR Fortessa at FlowCore, Monash University.

Intracellular cytokine staining after peptide re-stimulation.

For peptide re-stimulation to assess cytokine production, cells were incubated with 1 ⌈M D^bNP_{366}, D^bPA_{224} peptide in cRPMI in the presence of 10 U/mL human recombinant IL-2 with Brefeldin A for 5 hours at 37°C. For no-peptide controls, cells were incubated in cRPMI with 10 U/mL human recombinant IL-2 and Brefeldin A. Following re-stimulation, cells were washed and stained with surface antibodies in a U bottom 96 well plate in 50 µL MACS buffer for 30 minutes at

4°C in the dark, then washed with FACS buffer. Cells were fixed for 20 minutes with 100 µL/well BD Cytofix/Cytoperm (BD Biosciences) at 4°C, then washed twice with perm/wash buffer (diluted 1/10 with MilliQ water) and stained with anti-IFN-γ, anti-TNF and anti-IL-2 in perm/wash buffer for 30 minutes at 4°C in the dark. Cells were washed twice in perm buffer, then two times in FACS buffer and resuspended in FACS buffer for analysis on the BD LSR Fortessa at FlowCore, Monash University.

Intranuclear staining for granzymes and transcription factors.

After surface staining, cells were fixed for 1 hour at 4°C using the FoxP3 intranuclear staining kit according to manufacturer's instructions, then intracellularly stained with anti-GZMA (FITC; 1:50) and anti-GZMB (Pacific Blue; 1:50) antibodies in perm/wash buffer for 30 minutes on ice.

2.2.7. Western Blotting

10^6 naïve or stimulated $CD8^+$ T cells were lysed in 200 µL of Cut and RUN Nuclear extraction buffer. Nuclei were obtained by spinning the cells at 5000 rpm for 10 min at 4°C. Nuclei were resuspended in 50⌠L RIPA buffer and mechanically lysed to obtain the nuclear extract. Total protein was estimated using Pierce BCA assay kit. Equal amount of protein was resolved on 12% SDS-PAGE and transferred to PVDF membrane. Membrane was blocked in 4% skimmed milk for one hour and incubated in specific primary antibody (1:1000 dilution for CBX7 and BMI1 and 1:5000 dilution for H3) overnight at 4°C. Membrane washed three times in 1X TBST (Tris buffered saline 0.1%Tween) and incubated in secondary antibody (1:2000) for 1 hour at room temperature. The membrane was again washed three times with TBST, and image was developed using Enhanced ChemiLuminisence.

2.2.8. RNA extraction and cDNA synthesis

For RNA extraction, either naïve or cultured cells were lysed in 500 µL TRIzol reagent for 5 minutes at room temperature before adding 100 µL chloroform and shaking vigorously for 15 seconds. Samples were centrifuged at 12,000 xg for 15

minutes at 4°C and the aqueous phase was carefully transferred to a new tube. RNA was precipitated by adding 500 µL isopropanol and 1 µL GenElute for 15 minutes at room temperature, then pelleted by centrifuging at 12,000 xg for 15 minutes at 4°C. RNA was washed with 75% ethanol then pelleted by centrifuging at 7500 xg for 5 minutes. After air drying, the RNA pellet was redissolved in nuclease free water on the heat block at 60°C for 10 minutes, and 250-1000ng was reverse transcribed to cDNA using the Protoscript II enzyme NEB kit (New England BioLabs). cDNA was diluted to 20 ng RNA equivalent per 2 µL for TaqMan real time PCR assays described below or SYBR green PCR assay (**section 2.2.13**).

2.2.9. TaqMan real time PCR

TaqMan real-time PCR was conducted with TaqMan primers (FAM labelled), using 20 ng of cDNA and 1 x universal TaqMan PCR master mix (ThermoFisher TaqMan Fast Advanced Master Mix) in a total volume of 10 µL. Each reaction was performed in duplicate and normalised to *Poldip3*. Results are expressed relative to naïve, unless otherwise stated, using the ΔΔCT method (Livak and Schmittgen, 2001) using the CFX Connect Real-Time System.

2.2.10 Chromatin Immuno-precipitation (ChIP):

ChIP protocol was performed as described in Russ et al. (Russ et al., 2014). Naïve or cultured $CD8^+$ T cells were fixed with 0.6% formaldehyde for 10min at room temperature, and the reaction was quenched with 125mM glycine for 10min at room temperature. Cells were washed three times with 15mL Dulbecco's PBS and resuspended in 250µL ChIP lysis buffer and sonicated to yield DNA fragments of 200-1000bp. DNA was pelleted, and supernatants were diluted to the equivalent of $0.5x10^6$ cells/mL with ChIP dilution buffer. 50µL of each sample was stored in -80°C freezer as total input control. 1ml ($0.5x10^6$ cells) were aliquoted and appropriate antibodies (5µg each of H2Ub119 and H3K27me3) were added. 20µL/mL Protein A magnetic beads (Cat#16-661 Merck) were added and incubated overnight at 4°C on a rotor.

Protein antibody complex bound to the beads were washed twice with 900µL Low Salt buffer once with high salt buffer and LiCl and finally washed twice with TE buffer. DNA was eluted in 300µL elution buffer for 30min at room temperature on a rotor wheel, DNA-protein cross-links were reversed for overnight with 0.2M NaCl at 66ºC, proteins digested with 10µg proteinase K at 45ºC for 1 hr and the DNA extracted with an equal volume of phenol:chloroform:isoamyl alcohol (25:24:1). DNA was precipitated at 4ºC for 1hr in 2.5 volumes 100% ethanol, 1/10 volume 3M sodium acetate and 1µL GeneElute. DNA was washed once with 80% ethanol and resuspended in 100-200µL 0.1 TE buffer. 5⌈L DNA was used to analyze the enrichment of specific histone mark on promoters of genes of interest by performing SYBR green qPCR as described in **section 2.2.13**

2.2.12 Formaldehyde-Assisted Isolation of Regulatory Elements.

Samples were fixed and sonicated as described in section 2.2.11. Open chromatin was extracted by adding an equal volume of phenol: chloroform: isoamyl (25:24:1) and precipitated as described for ChIP. DNA were resuspended in 100 - 300µl and used for real-time PCR. Analyses were performed by performing SYBR green qPCR as described below

2.2.13. SYBR green qPCR

SYBR gene qPCR was used for ChIP and FAIRE analysis and RNA expression analysis of various PRC1 components. Each reaction had a total volume of 25 µL. Each reaction contained 1X Power SYBR green buffer (Life Technologies) with forward and reverse primers (100 nM of each) and 5 µL of DNA. PCR was run under the following conditions: 95°C 10 min, 40 cycles of 95°C 15 sec and 60°C 1 min followed by a melt curve consisting of 81 cycles of 55°C for 10 seconds with a 0.5°C temperature increase per cycle. The CFX-Connect Real Time system was used to conduct PCR reactions. Ct values were converted to copy number (# copies=105/2Ct-17). Immunoprecipitation values were normalised to the copy number of the total input control and expressed as a percentage. For RNA expression analysis, results are expressed relative to naïve, unless otherwise stated, using the ΔΔCT method [6]83

2.2.12. RNA-sequencing

RNA samples (in biological triplicate for *Bmi1*$^{fl/fl}$ *Lck*^{Cre} and biological duplicate for WT) were extracted using the RNeasy kit (Qiagen) following manufacturer's instructions. DNAse I digestion was performed on column, as specified, with incubation at 37°C for 20 minutes. Total RNA sequencing (RNA-seq) was carried out according to Russ *et al. (Russ et al., 2014)* and Li *et al. (Li et al., 2021)*on a Hiseq2000 instrument the Micromon Genomics Facility at Monash University, Melbourne Australia. The Degust package (performed by Adele Barugahare Monash Bioinformatics Platform) was used to determine differential gene expression (DEG) with a false discovery rate (FDR) of <0.05 and log2 Fold Change (FC) > 1.5.

ATAC-sequencing

ATAC-seq protocol is adapted from Buenrostro et al. (Buenrostro et al., 2015) and Li et al (Li et al., 2021). This experiment was performed with the help of Daniel Thiele and with the guidance from Dr. Brendan Russ. Two biological replicates were used for each genotype for both naïve and day 10 antigen specific $CD8^+$ T cells. A total of 50 000 sort purified cells were lysed with cold lysis buffer for nuclei extraction. Nuclei were immediately resuspended in transposition reaction mix prepared from the Illumina Nextera DNA Sample Preparation Kit (FC- 121-1030) for 30 minutes at 37 C. Transposed DNA was extracted using the QIAGEN MinElute PCR Purification kit (Cat #. 28004). Resulting DNA was subjected to 5 PCR cycles on the thermocycler using a PCR primer 1 (Ad1_noMX) and an indexed PCR primer 2. An aliquot of each sample was used subsequently in a real-time quantitative PCR for 20 cycles to determine the number of cycles required for library amplification. The amplified DNA was purified using the QIAGEN MinElute PCR Purification kit. Library quality was assessed using the bioanalyzer (Agilent) to ensure that the DNA fragmentation ranges between 50-200bp and the Qubit to determine the overall DNA concentration. ATAC-DNA was sequenced paired end on the Hiseq2500 instrument at the Micromon Genomics Facility at Monash University, Melbourne

Australia. Data was further curated and degust was generated by Adele Barugahare at Monash Monash Bioinformatics Platform.

2.2.13. Statistical analysis

Statistical analysis was performed using GraphPad Prism 9.0 software. Data was analysed using either unpaired, two-tailed t-tests, Mann-Whitney test, one-way ANOVA with Tukey's multiple comparison testing, or two-way ANOVA. Significance is denoted as *P≤0.05, **≤0.01, ***≤0.001 and **** ≤0.0001.

CHAPTER 3

Characterisation of canonical PRC1 components during CD8$^+$ T cell activation and differentiation.

3.1 Introduction

Polycomb Repressive Complexes support both self-renewal and differentiation of stem cells(Morey et al., 2012, O'Loghlen et al., 2012), and as such are crucial for tissue homeostasis. Within stem cells, these seemingly opposing functions are achieved through regulated changes to the composition of PRC1 which occur following stem cell activation (Morey et al., 2012, Gao et al., 2012). CBX proteins act as a switch between self-renewal and differentiation. For instance, CBX7 is a primary chromobox orthologue, and its expression is associated with undifferentiated ESCs, whereas CBX2 and CBX4 are primarily expressed in differentiated ESCs (O'Loghlen et al., 2012). Furthermore, in immature hematopoietic stem cells, BMI-1 is specifically expressed, whereas its paralogue MEL18 increases in expression during maturation (Iwama et al., 2004). Over-expression of CBX7 in HSCs enhances self-renewal and induces leukemia, while in contrast, over-expression of CBX2, CBX4 or CBX8 induces differentiation and HSC exhaustion (Klauke et al., 2013). Thus, the composition of PRC1 confers the molecular balance between self-renewal and differentiation and argues that existence of cell-type specific differentiation-state specific PRC1 subunits within the complex (Lessard et al., 1998, Gunster et al., 2001, Gil and O'Loghlen, 2014).

While it is well established that the composition of PRC1 changes during stem cell maturation, whether such changes underscore differentiation in other cellular contexts, including lymphocyte differentiation is not well understood. This chapter aimed to assess the composition of cPRC1 components in CD8$^+$ T cells during activation and differentiation.

As stated previously, activation of T cell is dependent on the affinity of pMHC and TCR interaction and costimulatory signals (Viola and Lanzavecchia, 1996, Fraser

et al., 1991). This chapter attempts to understand the role of pMHC - TCR signalling and costimulation in regulating the expression of CBX7 and BMI-1. This chapter also aims to address the coordinated mechanism of regulation by PRC1 and PRC2 in regulating the gene expression. To elucidate this, we utilized *in vitro* activation of $CD8^+$ T cells in the presence of small molecule inhibitor GSK J4 (inhibits Kdm6b mediated demethylase activity) coupled with ChIP and FAIRE assay to characterise the potential mechanism by which PRC1 and PRC2 regulate the gene expression.

3.2 Results

3.2.1 Differential expression of PRC1 components following activation and differentiation of virus-specific effector $CD8^+$ T cells.

PRC1 is a large, heterogeneous complex (Figure 3.1A), with different accessory components being important in different cellular contexts (as outlined in section 1.6). As an initial attempt to determine which accessory components are required to regulate $CD8^+$ T cell differentiation, an adoptive transfer model (Figure 3.1 B) was used where 1 x 10^4 naïve OT-1 $CD8^+$ T cells (OT-1s; $CD45.1^+$; $CD8^+$ $CD44^{lo}$ $CD62L^{hi}$) were adoptively transferred into congenic C57BL/6j (B6; $CD45.2^+$) recipients, which were infected intranasally 24 h later with 1 x 10^4 p.f.u. A/HKx-31 OVA influenza A virus (IAV, A/H3N2)(Jenkins et al., 2006). This virus has been engineered to express the SIINFEKL peptide from chicken ovalbumin, for which the OT-1 TCR is specific. Naïve (day0), and IAV specific cells were sort purified based on the congenic marker CD45.1 at day10 after infection, and expression of various PRC1 components was assayed by qPCR before and after a brief (5 h) peptide stimulation.

Among the three Polyhomeotic like protein (Phc) coding genes, *Phc3* was the most strongly expressed across all conditions assayed, indicating that within $CD8^+$ T cells, PHC3 is likely to be the PHC component (Figure 3.1 C). The PCGF component of Canonical PRC1 is comprised of *Mel18* or *Bmi1 (Gao et al., 2012)*. We found that *Bmi1* was most highly expressed in our assays and was strongly upregulated upon stimulation of naïve and effector cells, suggesting that BMI1 is

the PCGF component (Figure 3.1 D). The catalytic subunit of PRC1 is encoded by either *Ring1* or *Rnf2,* both of which were found to be expressed in $CD8^+$ T cells, albeit that *Rnf2* is more strongly expressed across the conditions assayed (Figure 3.1E). Moreover, neither gene was regulated between resting and stimulated states, suggesting that either or both may be determinants of PRC1 mediated regulation of $CD8^+$ T cell immune responses.

Canonical PRC1 complexes contain is the presence of one of the five Chromobox containing CBX proteins (encoded by (*Cbx2*, *Cbx4*, *Cbx6*, *Cbx7*, and *Cbx8*). Among all these genes, *Cbx4* and *Cbx7* were the most strongly expressed, with each being downregulated upon stimulation. Finally, the Noncanonical PRC1 is characterised by the presence of the DNA binding component, RYBP, which was expressed to a similar extent across the conditions tested (Figure 3.1G).

Taken together, these data suggest that the canonical PRC1 within naïve and effector $CD8^+$ T cells consists of RING1 B, BMI-1, PHC3 and CBX4 or CBX7. Among all these components, only CBX4*,* CBX7 and BMI-1 have a regulated transcriptional profile. It is noteworthy that transcript levels of *Bmi1* is upregulated with the TCR stimulation while *Cbx* genes are downregulated. These results also do not rule out the possibility that there are different complexes within the same cell, or between cells.

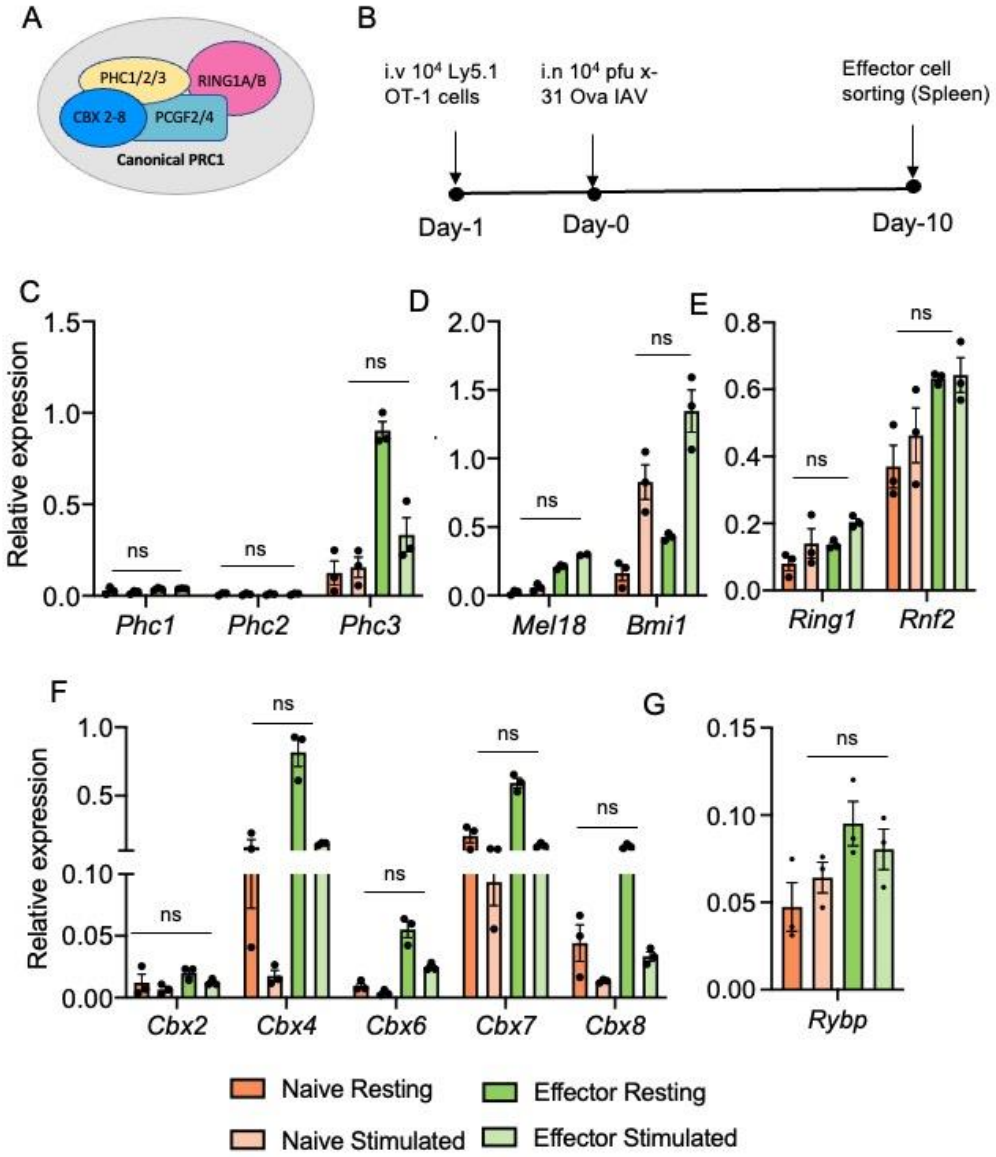

Figure 3.1: Expression of various PRC1 components during CD8⁺ T cell differentiation: A) Various components of canonical and non-canonical PRC1. B) Adoptive transfer model was used to generate Day10 effector cells. 10^4 naïve Ly5.1$^+$ OT-1 cells were transferred into B6 mice. Mice were infected with 10^4 pfu X31 Ova virus. Naïve (Day 0) and Effector cells (Day 10) were harvested 10 days post infection and were used to extract RNA and cDNA synthesis. Transcript levels of various PRC1 components (C-F) were determined using specifically designed primers. Data is represented as relative expression and each of gene expression is normalised to *Poldip3*. (Error bars show ± SEM, n=3 biological replicates. Two-way ANOVA was performed between groups.

3.2.2 TCR signalling induces the expression of BMI-1 and CBX7.

The data presented above demonstrates that expression of PRC1 components is regulated in response to TCR stimulation and differentiation state. To further define the relationship between TCR stimulation and expression of *Bmi1* and *Cbx7*, which were regulated in response to TCR, naïve OT-1 T cells were stimulated with cognate peptide (SIINFEKL) for 24 h and following the removal of the peptide by thorough washing of the cells, cultures were rested in IL-2 up to 5 days (Figure 3.2A). At various time-points cultures were sampled to assay transcript and protein levels (Figure 3.2B, C).

Suggesting a direct relationship between TCR stimulation and gene transcription, *Cbx7* was downregulated within 5hrs of stimulation, with expression remaining low until the peptide was removed, at which time expression increased, reaching naïve levels within 48 h (72 h post initiation of the cultures). However, *Bmi1* transcript levels were at least partly independent of TCR, because while they increased rapidly after stimulation (~4-fold in 5 h), they were approximately equivalent to naïve at 24 h (e.g., before removal of the peptide).

However, surprisingly, while levels of *Cbx7* and *Bmi1* transcripts were inversely correlated, the protein levels of both CBX7 and BMI-1 increased within 5 h of stimulation, peaking at 24 h, and slowly reducing following removal of the peptide. Thus, while *Bmi1* transcript and protein levels were directly correlated, *Cbx7* transcript levels were inversely proportional, suggesting that *Cbx7* is subject to both transcriptional and translational regulation, while BMI-1 expression appears to be regulated predominantly at the transcriptional level.

To further understand the relationship between TCR stimulation and expression of CBX7 and BMI-1, naïve $CD8^+$ OT-1 T cells were stimulated with SIINFEKL for 96 h, with expression measured as above at various time-points (Figure 3.2 D, E). Confirming the role of TCR signalling in the downregulation of *Cbx7* transcripts, transcript levels were reduced ~4-fold within 24 h of stimulation, with expression remaining low at 96 h. In contrast, *Bmi1* transcripts were found to be

independent of TCR stimulation, showing a similar expression pattern regardless of peptide withdrawal (compare Figures 3.2 B and 3.2 E). However, while CBX7 protein levels increased with stimulation and remained constant to 96 h, BMI-1 protein levels increased with stimulation, and slowly reduced after 48 h, consistent with transcript levels and consistent with expression levels following peptide withdrawal (compare Figures 3.2 C and 3.2 F). These results show that the CBX7 and BMI-1 are induced in response to TCR stimulation even though the transcript levels were inversely correlated.

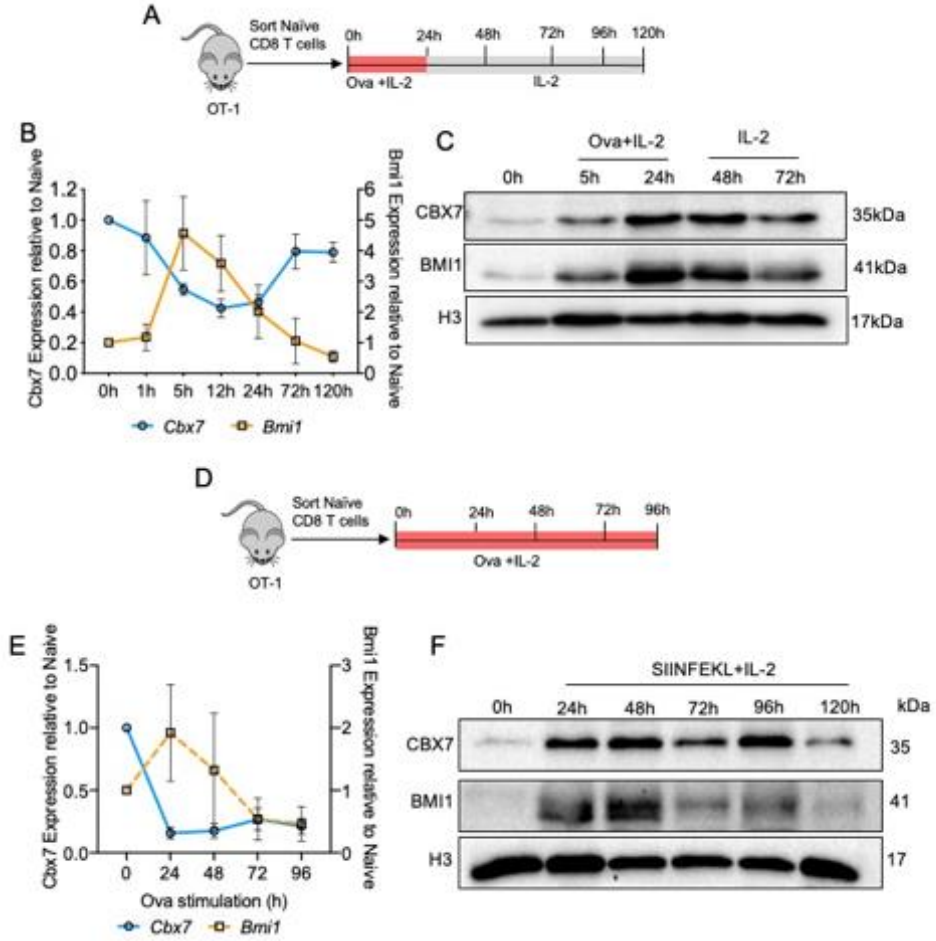

Figure 3.2. BMI-1 and CBX7 expression are regulated in response to TCR signaling (A and D) Experiment layout: Sort-purified naïve (CD44 ^{lo}, CD62L ^{hi}, CD8^{+}) CD8^{+} T cells from OT-1 mice were stimulated with IL-2 (10U/ml) and SIINFEKL(1uM) for 24 h (A) After 24 hours, stimulation was removed, and cells were rested in IL-2 for up to 120 hours. Alternatively sort purified CD8^{+}T cells were stimulated with IL-2 and SIINFEKL for 96 h (D). Cells were harvested at indicated time points for RNA extraction. (B and E) Expression of *Cbx7* and *Bmi1* was determined by real-time PCR and the expression values were normalized to *Poldip3.* Data is represented as expression level relative to Naïve CD8^{+} T cells. (C and F) Protein levels of CBX7 and BMI-1 was assessed by western blotting, H3 was used as a nuclear lysate loading control. (Error bars show ± standard error of mean, n=3 biological replicates)

3.2.3 *Cbx7* and *Bmi1* transcript levels are regulated in accordance with TCR signal strength.

TCR signal strength determines whether T cells become activated, while also regulating differentiation outcomes (King et al., 2012). Having found that CBX7 and BMI-1 expression is regulated in response to TCR-mediated activation, we next determined whether their expression is regulated in accordance with TCR

signal strength, and as such whether their expression may have a role to play in determining the consequences of TCR signals.

As an initial test of the relationship between TCR signal strength and expression of PRC1 components, sort-purified naïve $CD8^+$ T cells from B6 mice were stimulated with titrated doses of anti-CD3 antibody in the presence of α-CD8 antibody and co-stimulation with anti-CD28 and anti-CD11a. Expression of PRC1 components were analysed by qPCR (Figure 3.3A). Transcript levels of *Cbx7* was strongly repressed at higher doses of anti-CD3 but not at the lower doses. Similarly, *Bmi1* was induced at the higher doses of anti-CD3.

Based on the observations described above, we predicted that the expression of PRC1 components is dependent on TCR signal strength. To test this, naïve OT-1 T cells were stimulated with doses of SIINFEKL peptide ranging between 10^{-6}M and 10^{-16}M for 5hrs before *Cbx7* and *Bmi1* transcript levels were assayed as above. We found that at ~10^{-12}M, transcript levels of *Cbx7* were no longer repressed, while *Bmi1* transcript levels were no longer induced (Figure 3.3A). Thus, it appeared that both genes are regulated in accordance with TCR signal strength, although it was possible that this data reflects limiting peptide availability at lower concentrations. To test this latter possibility directly, serial dilutions of a lower affinity SIINFEKL variant SIIQFEKL (Q4) was used. The Q4 variant has been shown to induce OT-1 T cell activation *in vivo* after *L. monocytogenes* infection[13]. Different doses of altered peptide ligands (APLs) N4 and Q4 peptide was used for stimulation of naïve $CD8^+$ T cells form OT-1 mice. Since Q4 has lower affinity to the TCR compared to the wildtype N4 peptide, a higher peptide concentration was required for activation. Final concentration of 10^{-11}M Q4 was found to be the threshold concentration at which transcript levels of *Cbx7* were not repressed and *Bmi1* transcript level was not induced (Figure 3.3B).

Thus, these results reflect the role of TCR signaling in regulating the expression of PRC1 components and suggested that PRC1 may have role in regulating the T cell activation.

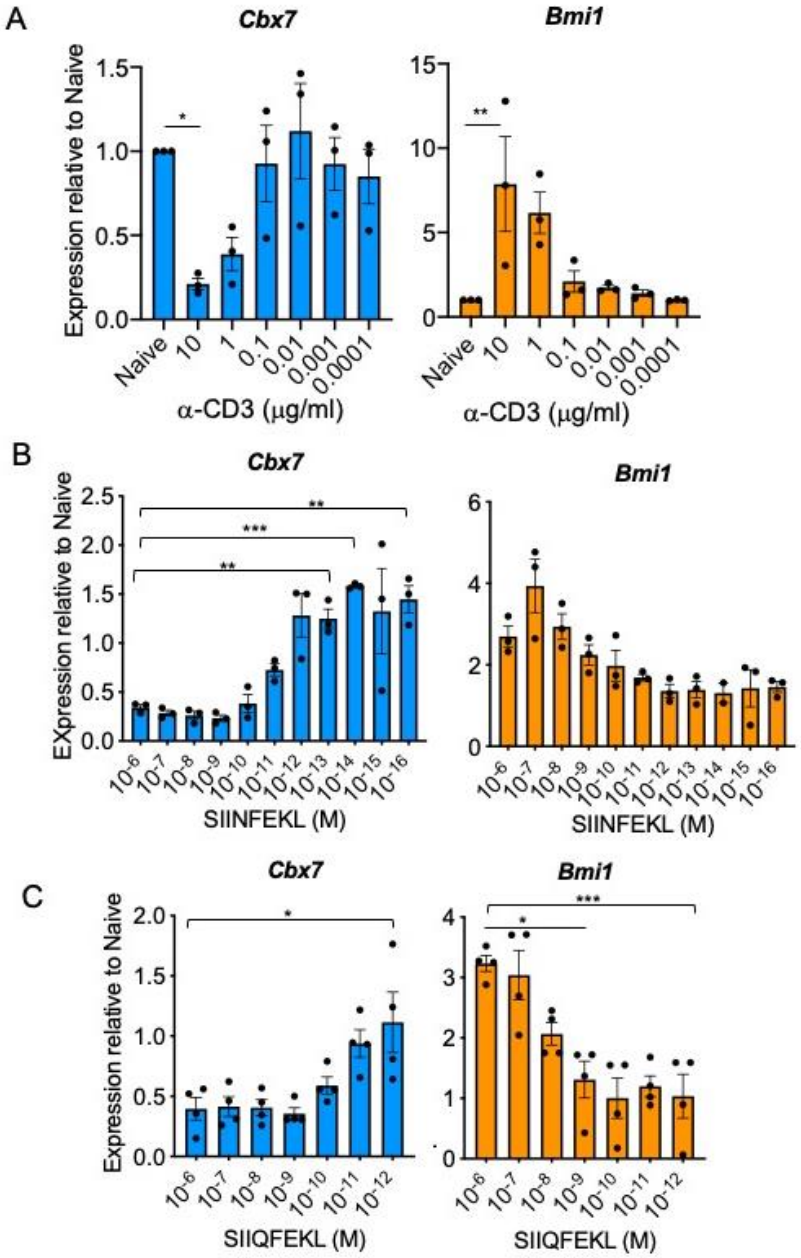

Figure 3.3:TCR signal strength regulates the expression of PRC1 components: A) Naïve $CD8^+$ T cells from C57Bl6 mice were stimulated with various doses of anti-CD3 antibody and 10μg/ml anti-CD8, 5μg/ml anti-CD11a and 2.5μg/ml anti-CD28 antibody for 5 h. B-C) Sort-purified naïve ($CD44^{lo}$, $CD62l^{hi}$, $CD8^+$) $CD8^+$ T cells from OT-1 mice were stimulated with IL-2 (10U/ml) and SIINFEKL(N4), SIIQFEKL (Q4) at indicated doses for 5 h. Cells were harvested for RNA extraction and subsequent cDNA synthesis. Expression of *Cbx7* and *Bmi1* was determined by real-time PCR using specific primer probes and the expression values were normalized to *Poldip3.* (Error bars show ± SEM, n=4 biological replicates. Two-way ANOVA was performed between groups. All values were compared to either naïve (Fig 3.3A) or 10^{-6} (Fig 3.3B and C)

Statistical significance was reported only in the cases of p value<0.05 ($^{*}p < 0.05$ $^{**}p < 0.01$, $^{***}p < 0.001$)

3.2.4 CBX7 and BMI-1 expression is regulated in accordance with TCR affinity.

The data described above demonstrates that *Cbx7 and Bmi1* expression is exquisitely sensitive to TCR signal strength. To directly examine whether their expression is associated with TCR affinity, we utilised SIINFEKL (N4) altered peptide ligands SIIGFEKL(G4) and EIINFEKL (E1) which have been described as partial agonists (Jameson et al., 1993, Hogquist et al., 1994). Sort-purified naïve $CD8^{+}$ T cells were cultured with APLs, N4, Q4, G4 and E1 at a high dose concentration (10^{-6} M) for 5hrs, before *Cbx7* and *Bmi1* transcript levels were assessed by qPCR, and protein levels were measured by western blotting. We found that *Cbx7* and *Bmi1* transcript levels were directly correlated *(Cbx7) and anticorrelated (Bmi1)* with peptide affinity (Figure 3.4A), consistent with our observations described above. Moreover, CBX7 and BMI-1 protein was only detectable in nuclear extracts by western blotting following stimulation with N4 and Q4 peptides, but not with the lower affinity G4 and E1 peptides (Figure 3.4B). It can be concluded from these results that both transcripts are regulated in response to TCR affinity, as is their protein expression. Thus, the regulatory mechanisms that determine expression of each gene are downstream of TCR. Further, *Bmi1* is regulated at both a transcriptional and translational level. A reduced affinity for TCR and decreased signal strength promotes $CD8^{+}$ T cell memory formation over terminal differentiation (Solouki et al., 2020). Thus, these results suggest that cPRC1 components may play a role in regulating the balance between terminal differentiation and memory formation.

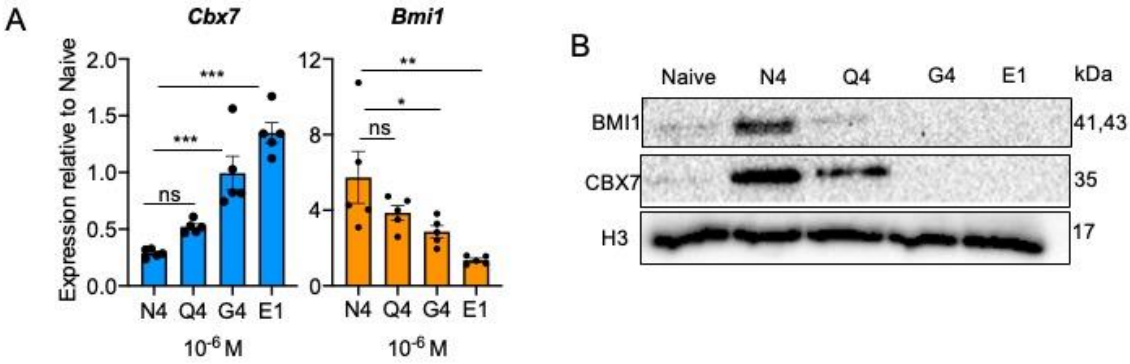

Figure 3.4: TCR affinity regulates the expression of PRC1 components: Sort-purified naïve (CD44 ^{lo}, CD62L ^{hi}, CD8$^+$) CD8$^+$ T cells from OT-1 mice were stimulated with IL-2 (10U/ml) and 10^{-6}M SIINFEKL(N4), SIIQFEKL (Q4), SIIGFEKL (G4) EIINFEKL (E1) for 5 h (for RNA) 24 h (for protein). Cells were harvested for RNA and protein extraction. A) Expression of *Cbx7* and *Bmi1* was determined by real-time PCR and the expression values were normalized to *Poldip3.* Data is represented as expression level relative to Naïve CD8$^+$ T cells. (Error bars show ± standard error of mean, n=5 biological replicates. Two-way ANOVA was performed between groups. ($^*p < 0.05$ $^{**}p < 0.01$, $^{***}p < 0.001$) B) Protein levels of CBX7 and BMI1 was assessed by western blotting, H3 was used as a nuclear lysate loading control.

3.2.5 Costimulation does not influence *Cbx7* or *Bmi1* transcript levels during early CD8$^+$ T cell activation.

CD8$^+$ T cell differentiation outcomes are influenced by signals other than TCR ligation, including CD28 costimulation (Signal 2) which impacts both clonal expansion and the functional capacity of activated T cells (Viola and Lanzavecchia, 1996, Fraser et al., 1991, Tuosto and Acuto, 1998). For instance, the Turner laboratory has previously shown that OT-1 CD8$^+$ T cells cultured with anti-CD28 antibody were able to produce more IFNγ, TNFα and IL-2 compared to CD8$^+$ T cells cultured without costimulation (Hayley Croom, Ph.D. thesis, 2017).

Based on these observations, we aimed to determine whether the phenotypic consequences of costimulation might result from impacts on transcription of PRC1 components. To test this, naïve CD8$^+$ T cells were sorted either from B6 mice or OT-1 mice and cells were stimulated with anti-CD3 or N4 peptide, respectively, in the presence or absence of costimulation (anti-CD28, or anti-CD28 and anti-CD11a), with transcripts measured at time-points to 48hrs. The

results of these experiments demonstrated that *Cbx7* and *Bmi1* transcript levels are not influenced by CD28 and/or CD11a costimulation (Figure 3.5A-D)

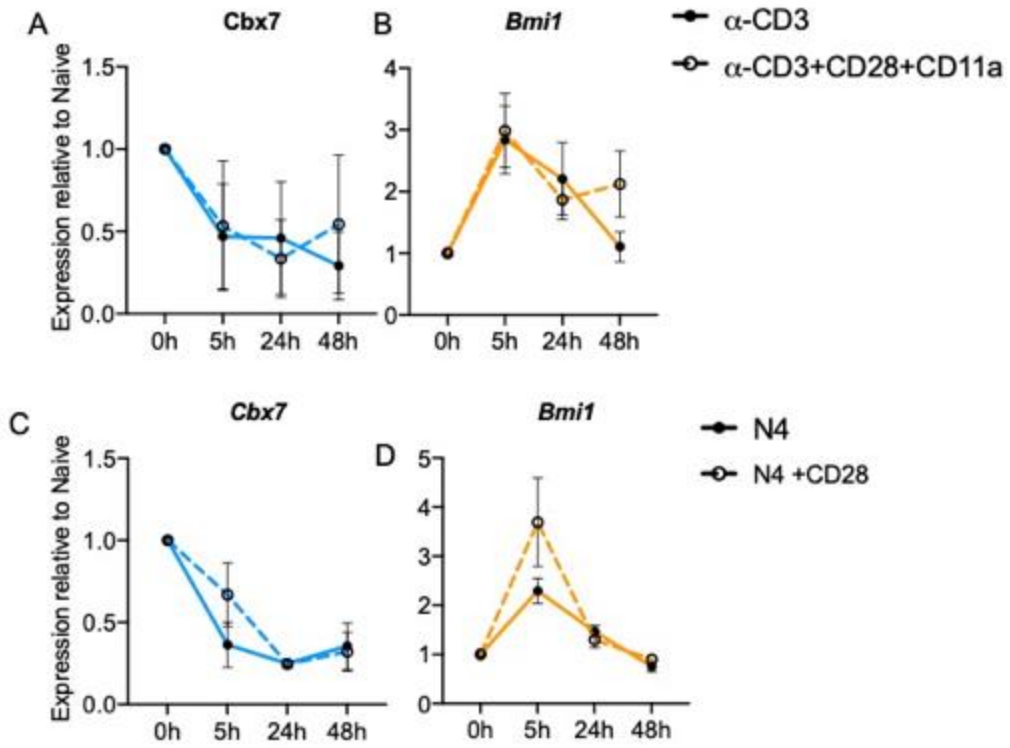

Figure 3.5: Effect of Costimulation on expression of PRC1 components: A) Sort purified naïve (CD44 ^{lo}, CD62L ^{hi}, CD8^{+}) CD8^{+} T cells from B6 mice were stimulated with 1μg/ml of α-CD3 antibody and 10μg/ml α-CD8 and +/- 2.5μg/ml α-CD28 antibody for 5hrs. Cells were harvested for RNA extraction. B) Similarly, sort purified naïve CD8^{+} T cells from OT-1 mice were stimulated with IL-2 (10U/ml) and SIINFEKL(1uM). Expression of *Cbx7* and *Bmi1* was determined by real-time PCR and the expression values were normalized to *Poldip3.* Data is represented as expression level relative to Naïve CD8^{+} T cells. (Error bars show ± standard error of mean, n=3 biological replicates)

3.2.6 cPRC1 activity correlates with PRC2 mediated trimethylation at the promoters of genes that drive CD8^{+} T cell activation.

Transcriptional changes associated with CD8^{+} T cell differentiation are choreographed in part through modulation of histone modifications (Russ et al., 2014). Our finding that core components of cPRC1 are regulated early after activation was consistent with an earlier finding that loss of H3K27me3 at genes encoding transcription factors that drive T cell differentiation (e.g., *Prdm1,*

Eomes, Irf4 and Tbx21) also occurred rapidly following activation (Li et al., 2021, Russ et al., 2014). Thus, to determine whether the dynamics of cPRC1 mediated monoubiquitination was similar that of H3K27me3 after T cell activation, ChIP was performed on OT-1 $CD8^+$ T cells at various time-points after peptide stimulation. Sort-purified naïve OT-1 $CD8^+$ T cells (CD8a+ CD44lo) were stimulated with SIINFEKL peptide for various time-points, and chromatin was immunoprecipitated with H3K27ac-, H3K27me3- or H2AK119Ub-specific antibodies.

We examined the enrichment of histone modifications at the promoters of *Prdm1, Eomes, Irf4* and *Tbx21*, finding that overall, the pattern of enrichment of H2AK119Ub and H3K27me3 was similar at naïve and 24 h time-points, while H3K27me3 (but not H2AK119Ub) appeared to be regained at 48 h (Figure 3.6A and B). This supports the idea that H2AK119ub is may be downstream of H3K27me3 and the re-enrichment of H2AK119ub may happen at a later time point. Further, and as expected, deposition of the activating H3K27ac modification showed a pattern inverse to that of H3K27me3, most noticeably at 24 h (Figure 3.6C), and directly correlated with patterns of gene transcription of *Irf4* and *Tbx21* (Figure 3.6D). Interestingly, the *Eomes* gene promoter was less dynamically regulated than other promoters, consistent with EOMES being expressed later during T cell differentiation, and while the *Prdm1* locus showed dynamic histone modification addition and removal, the gene was only weakly transcribed relative to *Irf4* and *Tbx21*. This latter result is also consistent with PRDM1 being expressed later in T cell differentiation than IRF4 and TBX21. Taken together, these results suggest that within naïve $CD8^+$ T cells, cPRC1 acts in concert with PRC2 to repress genes that drive effector T cell differentiation.

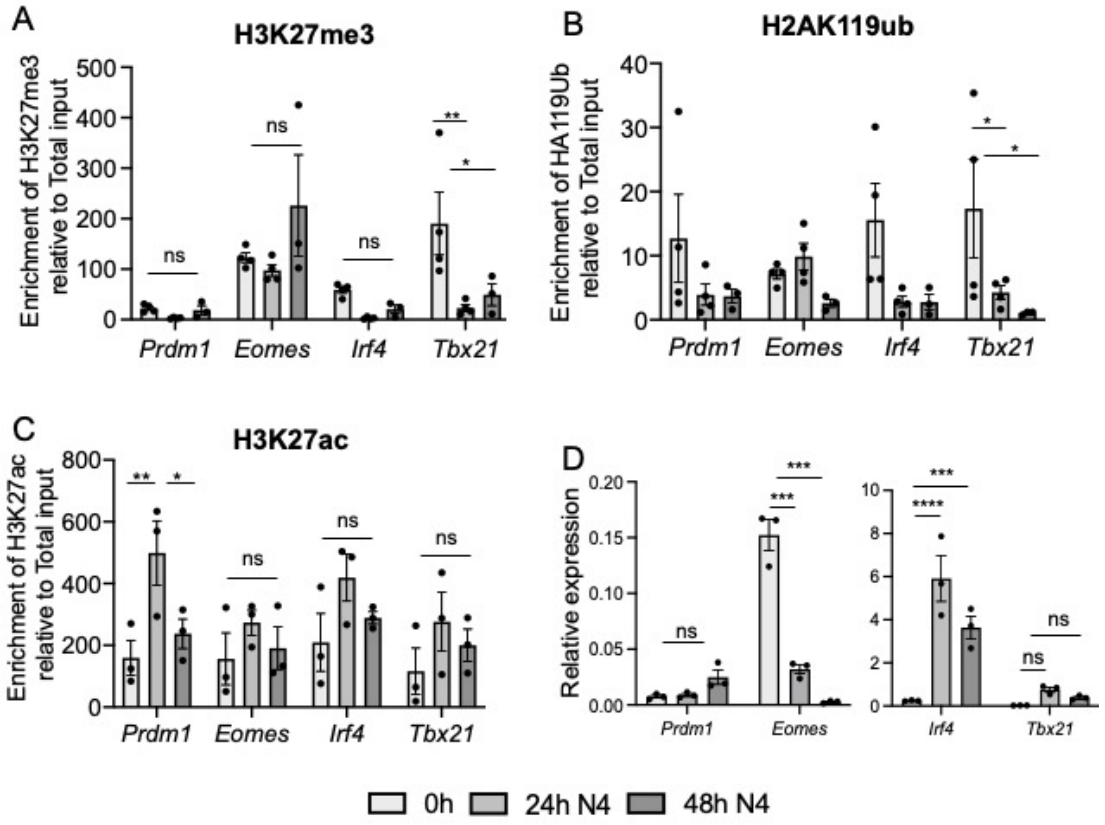

Figure 3.6: Co-deposition within naïve CD8⁺ T cells of H2AK119ub and H3K27me3 at transcription factor encoding genes that drive effector differentiation: Naïve CD8⁺ T cells from OT-1 mice were sort-purified (CD44^{lo}, CD62l^{hi}, CD8⁺) stimulated with IL-2 (10U/ml) and SIINFEKL (1uM) for 24 and 48hrs. Chromatin immunoprecipitation was then performed with H3K27ac (A), H3K27me3 (B) or H2AK119Ub (C) antibodies, and their enrichment on promoters of *Prdm1, Eomes, Irf4, Tbx21,* was determined by qPCR. (D) Expression of these genes at their transcript levels in naïve and activated states were analysed by real time PCR. Data is represented as relative expression and were normalized to *Poldip3* (Error bars show ± SEM, n=3 biological replicates. Two-way ANOVA was performed between groups. ($^{*}p < 0.05$ $^{**}p < 0.01$, $^{***}p < 0.001$, $^{***}p < 0.001$)

3.2.7 cPRC1 does not directly regulate expression of stemness genes within naïve CD8+ T cells.

The stemness of naïve CD8⁺ T cells is maintained by expression of transcription factors including *Tcf7, Lef1* and *Satb1* which must be repressed to allow T cell differentiation (Russ et al., 2012),(Kaech and Cui, 2012). Having found that cPRC1 represses genes that drive T cell differentiation within naïve CD8⁺ T cells, we next asked whether cPRC1 targets stemness genes in CD8⁺ T cells by performing ChIP experiments as above, and assaying enrichment at *Tcf7, Lef1*

and *Satb1* gene promoters. As illustrated in figure 3.7A, there was no significant change in the (activating) H3K7ac modification, despite transcript levels for each gene decreasing within 24hrs of stimulation (Figure 3.7D). Moreover, H3K27me3 enrichment was stably maintained, albeit from a low base (Figure 3.7B). Similarly, and importantly, enrichment of H2AK119 was also stable across the time-course (Figure 3.7C), suggesting that cPRC1 does not directly repress expression of $CD8^+$ T cell stemness genes.

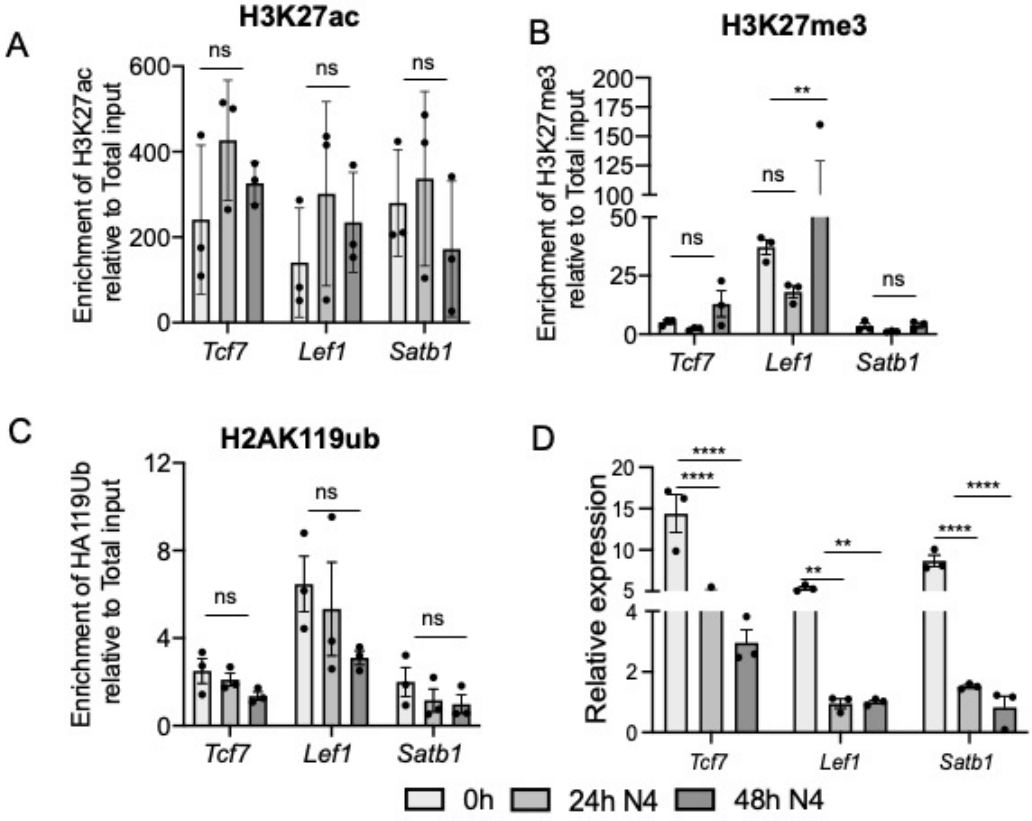

Figure 3.7: **H2AK119ub enrichment does not change on stemness genes:** Naïve $CD8^+$ T cells from OT-1 mice were sort-purified (CD44 ^{lo}, CD62L ^{hi}, $CD8^+$) stimulated with IL-2 (10U/ml) and SIINFEKL (1uM) for 24 and 48hrs. Cells were harvested and fixed with 0.6% formaldehyde, sonicated and chromatin was immunoprecipitated with H3K27ac (A), H3K27me3 (B) or H2AK119Ub (C) antibody and their enrichment on promoters of *Tcf7, Lef1, Satb1* was determined by qPCR. (D)Expression of these genes at their transcript levels in naïve and activated states were analyzed by real time PCR. Data is represented as relative expression and were normalized to *Poldip3* (Error bars show ± SEM, n=3 biological replicates. Two-way ANOVA was performed between groups. ($^*p < 0.05$ $^{**}p < 0.01$, $^{***}p < 0.001$, $^{***}p < 0.0001$)

3.2.8 Differential targeting of CBX7 during CD8$^+$ T cell activation.

The data presented above suggested that in the absence of T cell stimulation, cPRC1 specifically represses genes within naïve T cells that may otherwise drive differentiation, and further, this repression is removed rapidly following activation. To gain further evidence that H2AK119Ub enrichment at transcription factor encoding genes is cPRC1 dependent, CBX7 binding was assessed by ChIP, as above, using naïve OT-1 cells, and cells cultured with peptide for 24hrs. As CBX7 is a primary recruiter of cPRC1 to H2K27me3 decorated chromatin, we reasoned that CBX7 could be used as proxy for cPRC1 occupancy.

Consistent with the finding that H2A119Ub was enriched at the promoters of *Prdm1, Eomes, Irf4* and *Tbx21*, within naïve cells (Figure 3.6B), CBX7 was also strongly enriched at the same regions in naïve cells, with enrichment lost completely following 24hrs of stimulation, consistent with the loss of H2A119Ub with stimulation (Figure 3.8A). A notable exception was the *Eomes* promoter, where CBX7 was lost at 24 h, while H2A119Ub was maintained at this time-point (Figure 3.6B). Further, it was interesting to note that at the *Tcf7, Lef1, and Satb1* loci, which have low levels of H2AK119ub across the timepoints assayed, there was minor CBX7 enrichment within naïve cells, which increased at the *Lef1* and *Satb1 loci* upon stimulation (Figure 3.8 B). Taken together, these results suggest that within naïve CD8$^+$ T cells, cPRC1 mediates repression of transcription factors that drive differentiation, and may be retargeted following activation to repress genes that maintain stemness.

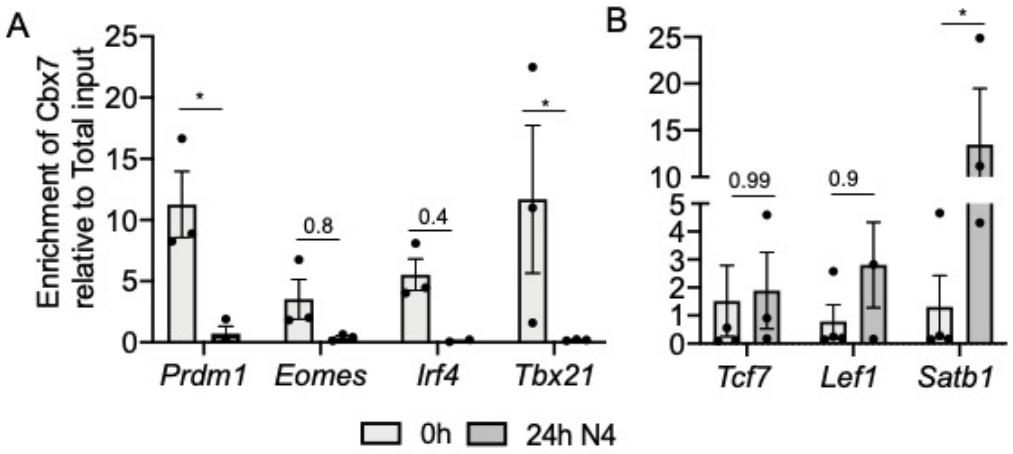

Figure 3.8: **CBX7 is targeted differentially on the promoters of crucial transcription factors in naïve and activated CD8⁺ T cell**: Sort-purified naïve ($CD44^{lo}$, $CD62L^{hi}$, $CD8^{+}$) $CD8^{+}$ T cells from OT-1 mice were stimulated with IL-2 (10U/ml) and SIINFEKL (1uM) for 24 h. Chromatin was immunoprecipitated with anti- CBX7 antibody. Enrichment of CBX7 on promoters of *Tcf7, Lef1, Satb1* and bivalent genes, *Prdm1, Eomes, Irf4 and Tbx21 and* was determined by qPCR. (Error bars show ± SEM, n=3 biological replicates. Two-way ANOVA was performed between groups. ($^{*}p < 0.05$) exact p values are given where significance threshold wasn't reached.

3.2.9 Inhibition of H3K27me3 demethylation prevents removal of H2AK119ub.

Our lab has previously shown that KDM6B is rapidly upregulated upon T cell activation and is responsible for H3K27me3 demethylation at genes required to drive T cell differentiation, including those characterised above(Li et al., 2021). Given that binding of CBX7 to H3K27me3 activates monoubiquitination of H2AK119, we hypothesised that inhibiting the histone demethylase activity of KDM6B would prevent removal of ubiquitination following T cell activation. KDM6B GSK-J4 is a small-molecule-inhibitor that binds to the catalytic pocket of KDM6B, inhibiting its demethylase activity(Kruidenier et al., 2012). Previously Li *et al*. showed that GSK-J4 prevents the removal of H3K27me3 from the promoters of *Tbx21, Irf4* and *Irf8,* preventing their transcriptional upregulation (Li et al., 2021). To assess the effect of KDM6B mediated demethylation on ubiquitination and chromatin accessibility, we pre-treated OT-1 $CD8^{+}$ T cells with KDM6B inhibitor (10uM final concentration) for 2hrs before assaying H3K27me3

and H2AK119ub enrichment immediately, or 24hrs after stimulation (Li et al., 2021).

Consistent with the hypothesis, GSK-J4 prevented removal of H2AK119ub from the promoters of *Prdm1, Irf4* and *Tbx21,* although not *Eomes* (Figure 9A). Additionally, using Formaldehyde Assisted Isolation of Regulatory Elements (FAIRE) to assay chromatin accessibility, we found that where deubiquitination had been prevented (as measured by ChIP), chromatin accessibility was maintained at a low level, consistent with repressed transcription of these genes in naïve cells (Figure 9B). These findings suggest that inhibition of demethylation of H3K27me3 after T cell activation prevents the removal of H2AK119ub, and hence increased chromatin accessibility required for upregulation of genes that drive T cell differentiation.

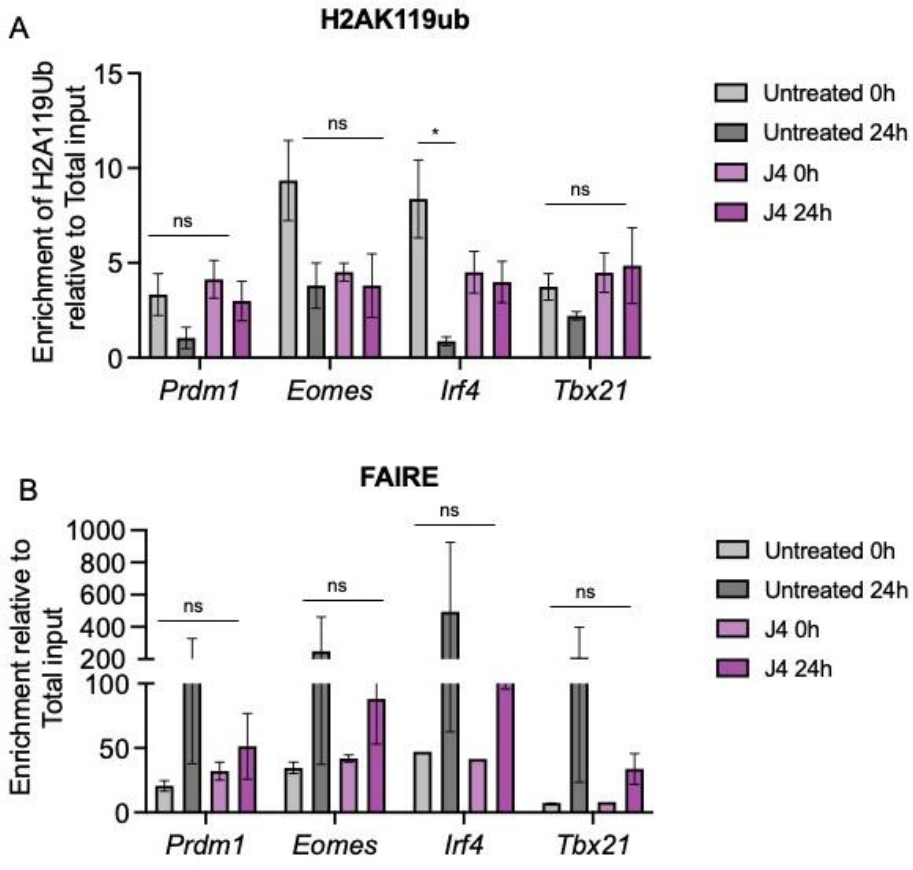

Figure 3.9: Inhibition of H3K27me3 demethylation prevents the removal of H2AK119ub and subsequent decrease in chromatin accessibility: Sort-purified naïve (CD44 ^{lo}, CD62L ^{hi}, CD8^{+}) CD8^{+} T cells from OT-1 mice were either left untreated (mock) or treated with 10 mM of the GSK-J4 for 2h in the presence of IL-2 before activating with the N4 peptide for 24h. Cells were then processed

for ChIP-qPCR analysis for H2AK119ub enrichment (A) and FAIRE (B) at the promoters of *Prdm1, Eomes, Irf4* and *Tbx21.* (Error bars show ± SEM, n=3 biological replicates. Two-way ANOVA was performed between groups.) Comparisons were not made where the significant thresholds were not met.

3.3 Discussion

Canonical PRC1 (cPRC1) is a heterogenous complex with variants playing distinct roles depending on cellular context, and this has been best demonstrated in studies of embryonic stem cells (**Section 1.6.1**). However, the broader biological relevance of the existence of diverse cPRC1 complexes is not well understood. This chapter provides insights into the composition of cPRC1 within $CD8^+$ T cells, and regulation of the expression of those components following TCR stimulation and T cell differentiation. By analysing variant PRC1 component RNA expression, we determined that within $CD8^+$ T cells, cPRC1 is composed of RING1B, PHC3, BMI-1 and CBX7 or CBX4, and found that expression of these components was regulated in accordance with differentiation state (Figure 3.1), and further, within hours of stimulation of naïve T cells (Figure 3.2). Together, these data suggested that cPRC1 regulates $CD8^+$ T cell differentiation and may orchestrate gene expression changes occurring early after T cell activation, and which control $CD8^+$ T cell differentiation outcomes. Indeed, we focussed our study on cPRC1 because of their dependency on H3K27me3, deposition of which is regulated to modulate early changes in gene transcription that both license and direct $CD8^+$ T cell differentiation (Russ et al., 2012, Li et al., 2021, Gray et al., 2017). For instance, Li *et al*. showed that within a few hours of activation of naïve T cells, the H3K27Me3 demethylase KDM6B targets genes such as *Irf4* and *Tbx21*, enabling their transcriptional upregulation, and subsequently driving effector differentiation (Li et al., 2021).

As mentioned, among the various CBX coding genes, we saw a differential regulation of CBX4 and CBX7 following T cell activation, suggesting that, indeed, there may be two cPRC1 variants contributing to gene regulation in $CD8^+$ T cells. In the future, single cell RNA sequencing and FACS experiments could be

performed to determine whether these complexes operate within a single cell, or within distinct subpopulations of the bulk populations that we studied here.

We focussed on understanding the regulation of CBX7 expression, as the chromodomain of CBX7 has a high affinity for H3K27me3 and H3K9me3, whereas CBX4 bind H3K9me3 alone (Bernstein et al., 2006b). Interestingly, we found that *Cbx7* transcripts were downregulated early after activation, while CBX7 protein levels increased, suggesting that CBX7 expression is subject to transcriptional and translation control, and may further suggest that expression is subject to feedback inhibition. Consistent with CBX7 and BMI1 forming part of the same complex, BMI-1 protein was detectable within 24 hours of activation, consistent with the findings of Heffner *et al*. who also reported the increased BMI-1 expression upon $CD8^+$ T cells activation (Heffner and Fearon, 2007). Indeed, upregulation of cPRC1 components upon T cell differentiation of naïve T cells is consistent with the reports showing that chromatin modifiers including SATB1, SUV39h and PRC2 components are upregulated upon $CD8^+$ T cell activation, to coordinate the transcriptional changes that underpin transition of naïve T cells to effector and memory (Gray et al., 2017, Pace et al., 2018, Stephen et al., 2017). TCR activation has been shown to be essential in establishing the epigenetic states of effector/memory differentiation (Henning et al., 2018). Increase in the expression of CBX7 and BMI-1 protein upon T cell activation might suggest the fact that cPRC1 regulates the $CD8^+$ T cell activation and differentiation.

TCR signal strength and the affinity of peptide-MHC interactions are determinants of $CD8^+$ T cell differentiation outcome (Wherry et al., 2002, Viola and Lanzavecchia, 1996). For instance, weak pMHC-TCR interactions, which limit TCR signal strength, may be sufficient to enable memory T cell differentiation, while being too weak to facilitate a functional effector pool (Rosette et al., 2001). Conversely, high affinity interactions result in the formation of both effector long-term memory populations (Corse et al., 2011, Gourley et al., 2004), although the mechanisms governing the translation of TCR signal strength to differentiation outcome are not entirely clear. For instance, it is known that the TF IRF4 is

induced in a TCR signal strength dependent manner, and that IRF4 then binds genomic targets that enable the metabolic reprogramming required to facilitate clonal expansion (Man et al., 2013). However, for TFs to be able to impart their function, they need to be able to access binding sites within chromatin. Hence, epigenetic chromatin regulation may require meeting specific signal thresholds to enable chromatin remodelling, thereby allowing TFs to mediate their effects. Consistent with this idea, we observed a TCR dose-dependent regulation of *Cbx7* and *Bmi1* transcription and translation, with translation only observed following stimulation with high affinity peptides and suggesting that part of the mechanism or mechanisms that translate TCR signal strength into differentiation outcome (this hypothesis is addressed experimentally in later chapters).

Molecular mechanisms by which PRC2 and cPRC1 regulates the gene silencing remain a matter of debate (Francis et al., 2004, Blackledge and Klose, 2021, Tamburri et al., 2020, Chan and Morey, 2019). We used H3K27me3 and H2AK119ub ChIP to understand whether the cooperation of the two complexes is required for the gene silencing in naïve and activated $CD8^+$ T cells. Interestingly, we saw co-deposition of H3K27me3 and H2AK119ub on the gene loci of TFs that drive effector differentiation, but not on those that maintain stemness, suggesting that the two collaborate to restrain activation of naïve T cells. Modulation of permissive or repressive histone modifications have been shown to play a pivotal role in $CD8^+$ T cell differentiation and acquisition of effector functions (Denton et al., 2011a, Russ et al., 2014, Gray et al., 2014). Our group has demonstrated that the promoters of genes encoding key transcription factors necessary for effector differentiation such as *Tbx21, Irf4*, and *Eomes* are poised in naïve cells, meaning that they have both H3K4me3 and H3K27me3 deposition on their promoter region and lose the H3K27me3 mark within a few hours of activation (Russ et al., 2014). With the result we obtained in our current study, we show that there is a second layer of repression in terms of H2AK119ub in naïve $CD8^+$ T cells. This data was also corroborated by CBX7 ChIP, where there was a clear binding of CBX7 to the gene loci that drives the differentiation in naïve cells which was lost upon activation. Upregulation of EZH2 has been

shown decrease the expression of TCF1, stemness marker in $CD8^+$ T cells (Gray et al., 2017) suggesting that H2AK119ub may also be enriched at loci encoding stemness functions following T cell activation, although this was not observed. Perhaps this discrepancy in H3K27me3 and H2AK119ub enrichment can be attributed to the timing with which the expression is regulated, and an extension of the time-course performed in this study could be used to test this idea formally. Indeed, CBX7 was enriched on the stemness maintaining TFs after activation, which may which indicate that these loci are primed for ubiquitination with extended differentiation.

Inhibition of KDM6B to prevent H3K27me3 demethylation also inhibited H2AK119ub deubiquitination at loci encoding TFs that drive effector differentiation, suggesting that H3K27me3 must be removed in order to allow deubiquitination following T cell activation. Furthermore, KDM6B inhibition also prevented an increase in chromatin accessibility, as expected, although it is unclear whether this is due to the failure to demethylate H3K27, or to deubiquitinate H2AK119, thus it would be interesting to repeat the same experiments with inhibition of cPRC1.

Yin *et al*. have shown the association of H2AK119ub and reduced chromatin accessibility in *Arobidopsis* transcriptional regulation hotspots (Yin et al., 2021). Studies have suggested that H2AK119ub is very important in maintaining the repression at gene loci (Tamburri et al., 2020). Absence of BAP, a ubiquitin c-terminal hydroxylase, leads to the accumulation of H2AK119ub which in turn reduces global gene expression (Conway et al., 2021, Fursova et al., 2021). These studies support the hypothesis that the presence of H2AK119ub reduces the chromatin accessibility and hence expression. Our preliminary results show that in activated $CD8^+$ T cells, maintained Ubiquitination on genes driving the differentiation leads to the chromatin accessibility.

Taken together, this chapter has provided an important insight into the expression and characterisation of cPRC1 in naïve and activated $CD8^+$ T cells. We have explored the role of TCR signalling and costimulation on the expression pattern

of CBX7 and BMI-1. Finally, we have also showed the coordination between PRC2 and cPRC1 in maintaining gene repression of crucial transcription factors in naïve cells. Considering the lack of studies exploring cPRC1 in $CD8^+$ T cells, it would be interesting to further investigate this complex and its function in more detail. Coimmunoprecipitation assay would be useful in understanding the recruitment and assembly of the complex in naïve and activated $CD8^+$ T cells. Global CBX7 and H2AK119ub ChIP seq will also provide an idea on the targets and the impact of ubiquitination in detail.

CHAPTER 4

Understanding the impact of epigenetic silencing by BMI-1 during CD8$^+$ T cell differentiation.

4.1 Introduction

In the previous chapter we established that the cPRC1 components CBX7 and BMI-1 are induced upon CD8$^+$ T cell activation. Further, chromatin immunoprecipitation-qPCR experiments suggested that cPRC1 mediated ubiquitination maintains the stemness of naïve CD8$^+$ T cells by repressing transcription factors that would otherwise promote effector differentiation. Indeed, this hypothesis is consistent with studies of hematopoietic stem cells (HSCs), where BMI-1, which regulates the ubiquitination activity of cPRC1, is needed to maintain HSC multipotency (Oguro et al., 2010). BMI-1 may also play a similar role within developing and mature lymphocytes, where loss of BMI-1 leads to impairment of B cell development (Cantor et al., 2019). A recent study by Di Pietro *et al*. showed that BMI-1 upregulation within germinal centre B cells during chronic viral infection results in the generation of a skewed antibody response. Blocking the function of BMI-1 via small molecular inhibitors resulted in restoration of functional B cell responses and clearance of persistent infections (Di Pietro et al., 2022). Importantly, BMI-1 expression has also been implicated in CD8$^+$ T cell differentiation. For example, over-expression of BMI-1 in LCMV-specific CD8$^+$ T cells has been shown to be necessary to limit T cell senescence and maintain memory T cell recall capacity (Heffner and Fearon, 2007). Genetic depletion of *Bmi1* or transient depletion using the inhibitor PTC209 perturbs the epigenetic landscape of Treg cells, which exhibit a TH1/TH17-like proinflammatory phenotype as a result. This indicates a role for BMI-1 in suppressing proinflammatory gene networks that are required to maintain Treg identity (Gonzalez et al., 2021). However very little has been done to understand the role of BMI-1 in antiviral T cell responses.

Given the data and studies described above, we predicted that deleting *Bmi1* from CD8$^+$ T cells would interfere with maintenance of quiescence within naïve cells, and ultimately T cell fate decisions. To address this, we used mice which have a T cell specific deletion of *Bmi1* to study CD8$^+$ T cell responses to Influenza A virus (IAV) infection - an infection model which has been well characterised by our group and others (Jenkins et al., 2006, Denton et al., 2011b, Flynn et al., 1998). Figure 4A shows the quantification of BMI-1 protein in the naïve and stimulated CD8$^+$ T cells from WT and *Bmi1$^{fl/fl}$Lck^{Cre}*.

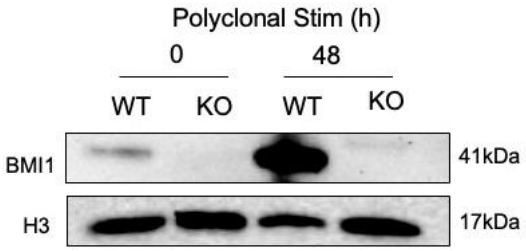

Figure 4A: Quantification of BMI-1 protein in WT and *Bmi1$^{fl/fl}$Lck^{Cre}* mice: Sort-purified naïve (CD44 ^{lo}, CD62L ^{hi}, CD8$^+$) CD8$^+$ T cells from WT and *Bmi1$^{fl/fl}$Lck^{Cre}* mice were stimulated with 5μg/ml of α-CD3 antibody and 10μg/ml α-CD8 for 48 h. Cells were harvested for protein extraction. Protein levels of and BMI1 was assessed by western blotting, H3 was used as a nuclear lysate loading control.

4.2 Results

4.2.1 Increased thymic cellularity in the absence of BMI-1.

BMI-1 is crucial for the growth of the thymic epithelial cells (Guo et al., 2011) as well as for thymocyte proliferation induced by pre-T cell receptor signalling (Miyazaki et al., 2008). Further, BMI-1 mediated repression of the *Cdkn2a* locus is required for the survival of activated pre-T cells, and is essential for the Double Negative (DN, CD8- and CD4-) to Double Positive (DP, CD8+ CD4+) transition (Miyazaki et al., 2008). As a result, global *Bmi1$^{-/-}$* mice have reduced thymic cellularity overall, but an increased proportion of DN cells. Consistent with BMI-1 having a role in the DN to DP transition, we found that in WT B6 mice (Figure 4.2 A), *Bmi1* transcripts were reduced ~4-fold in DP thymocytes relative to DN thymocytes.

To understand the T cell intrinsic role of BMI-1 during thymic T cell development, a phenotypic characterisation was performed on thymi from *Bmi1*$^{fl/fl}$*Lck*^{Cre} using flow cytometry. *Bmi1*$^{fl/fl}$*Lck*^{Cre} mice had significantly higher thymic cellularity compared to WT mice (Figure 4.1 B), consistent with a role for BMI-1 in thymocyte proliferation**.** Dissection of the DN population based on developmental stage (gating in Figure 4.2 C) showed a decreased proportion of DN4 thymocytes in *Bmi1*$^{fl/fl}$*Lck*^{Cre} mice (Figure 4.2 D). Further, the increased cellularity was due to an increased number of DP cells in *Bmi1*$^{fl/fl}$*Lck*^{Cre} mice (Figure 4.2 D-F), although this was not reflected by proportion (Figure 4.2 G). Thus, the decreased proportion of DN4 together with the finding of increased numbers of DP T cells, suggests DN4 stage thymocytes might transition to DP more readily in the absence of BMI-1(Miyazaki et al., 2008). Taken together, these results indicate a T cell intrinsic role for BMI-1 in regulating thymic cellularity and development.

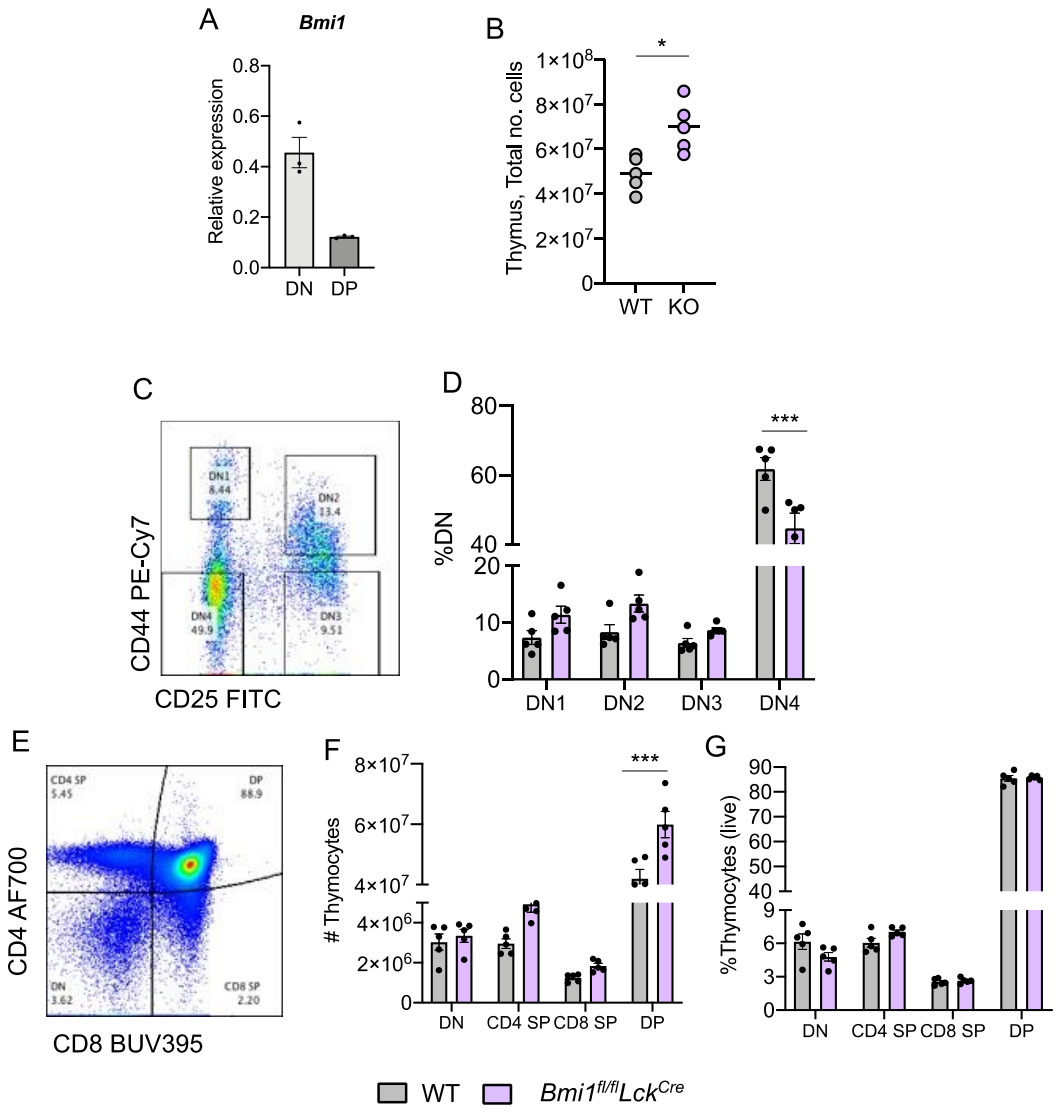

Figure 4.1: BMI-1 ablation increases thymus cellularity and T cell development: A) Relative expression of *Bmi*1 in DN and DP cells. *Bmi*1 expression is normalized to Poldip3. B) Total thymocyte counts. C) Representative flow cytometry plots of gating strategy for various DN population D) Proportion of various subsets of double negative thymocytes from WT and *Bmi1*$^{fl/fl}$*Lck*^{Cre} mice E) Representative flow cytometry plots of gating strategy for single positive, double positive and double negative thymocytes. F-G) Number and proportion of thymocyte subsets. Data shown are representative of 1-3 independent experiment. Error bars show ± SEM, n=5. Two-way ANOVA was performed between groups. ($^{*}p < 0.05$ $^{**}p < 0.01$, $^{***}p < 0.001$)

4.2.2 Deletion of BMI-1 perturbs CD8$^+$ T cell naïvety.

Given the alterations to thymic development observed in *Lck*^{Cre} x *Bmi*$^{fl/fl}$ mice, we predicted that deleting BMI-1 would disrupt the naïve T cell compartment. This hypothesis was addressed by performing a broad phenotypic characterisation of uninfected *Lck*^{Cre} x *Bmi*$^{fl/fl}$ mice (*Bmi1*$^{fl/fl}$*Lck*^{Cre} herein) by flow cytometry.

We found that the total number of splenocytes were decreased in *Bmi1*$^{fl/fl}$*Lck*^{Cre} mice relative to the WT (Figure 4.2 A), and this was reflected by a reduction in the proportion and number of CD4$^+$ and CD8$^+$ T cells (Figure 4.2 B-C). Moreover, and consistent with the hypothesis that BMI-1 maintains CD8$^+$ T cell quiescence, the reduction in total CD8$^+$ T cells was attributable to a loss of naïve cells (defined as CD44low CD49Dlow; Figure 4.2 D-F). Although there was an increase in the proportion of virtual memory T (T_{VM}) cells (defined as CD44high CD49Dlow), this was not reflected in the number of T_{VM}, and no change in the proportion and number of conventional memory T cells (T_{MEM}) was observed. Together, these data suggest that BMI-1 is required to maintain CD8$^+$ T cell naïvety.

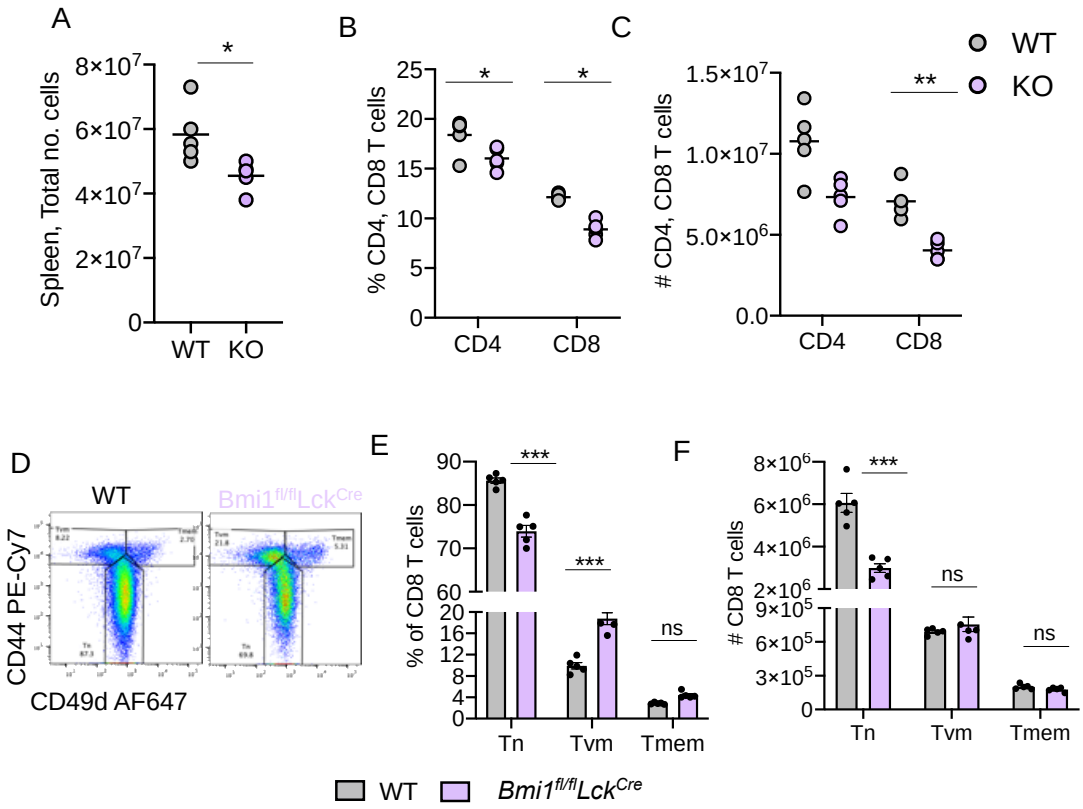

Figure 4.2: Lack of BMI-1 leads to the disruption of naïve CD8⁺ T cell compartment: A) Total splenocyte counts. B-C) Number and proportion (of live lymphocytes) of splenic CD4⁺, CD8⁺ T cells. D) Representative flow cytometry plots of gating strategy for naïve (T_N), virtual memory (T_{VM}) and conventional memory (T_{MEM}) CD8⁺ T cells. E-F) Number and proportion (of CD8⁺ T cells) of T_N, T_{VM} and T_{MEM} cells in the spleens of WT and *Bmi1*$^{fl/fl}$*Lck*^{Cre} mice. Data shown are representative of 1-3 independent experiment. Error bars show ± SEM, n=5. Two-way ANOVA was performed between groups. (*p < 0.05 **p < 0.01, ***p < 0.001)

4.2.3 BMI-1 regulates CD8⁺ T cell proliferation.

BMI-1 regulates cellular proliferation and senescence by repressing *Ink4a*, a tumour repressor and regulates the cell cycle in mouse embryonic fibroblasts.(Jacobs et al., 1999) BMI-1 is a key regulator of proliferative capacity of leukemia stem cells and progenitor cells. Lessard *et al*. have shown that leukemia stem cells lacking *Bmi1* have compromised proliferative potential and this leads to proliferation arrest and differentiation and apoptosis(Lessard and Sauvageau, 2003). CD8⁺ T cell proliferation leads to the acquisition of effector functions and the extension of proliferation determines the T cell polyfunctionality (Denton et al., 2011a).

In the previous chapter it was established that *Bmi1* upregulation was influenced by TCR activation strength. To test whether deletion of BMI-1 from naïve $CD8^+$ T cells alters their proliferative capacity, sort purified naïve $CD8^+$ T cells from WT and $Bmi1^{fl/fl}Lck^{Cre}$ mice were labelled with Cell Trace Violet (CTV) and stimulated with titrated concentrations of plate-bound anti-CD3 antibody along with anti-CD8 and anti-CD11a in the presence of recombinant human IL-2 for 3 days (Figure 4.3A). We found that $CD8^+$ T cell cultures lacking BMI-1 proliferated to a greater extent compared to WT cells, regardless of stimulation strength (Figure 4B-C). Thus, BMI-1 upregulation restrains naïve T cell activation and proliferation, whereby loss of BMI-1 increases sensitivity of naïve $CD8^+$ T cells to stimulation.

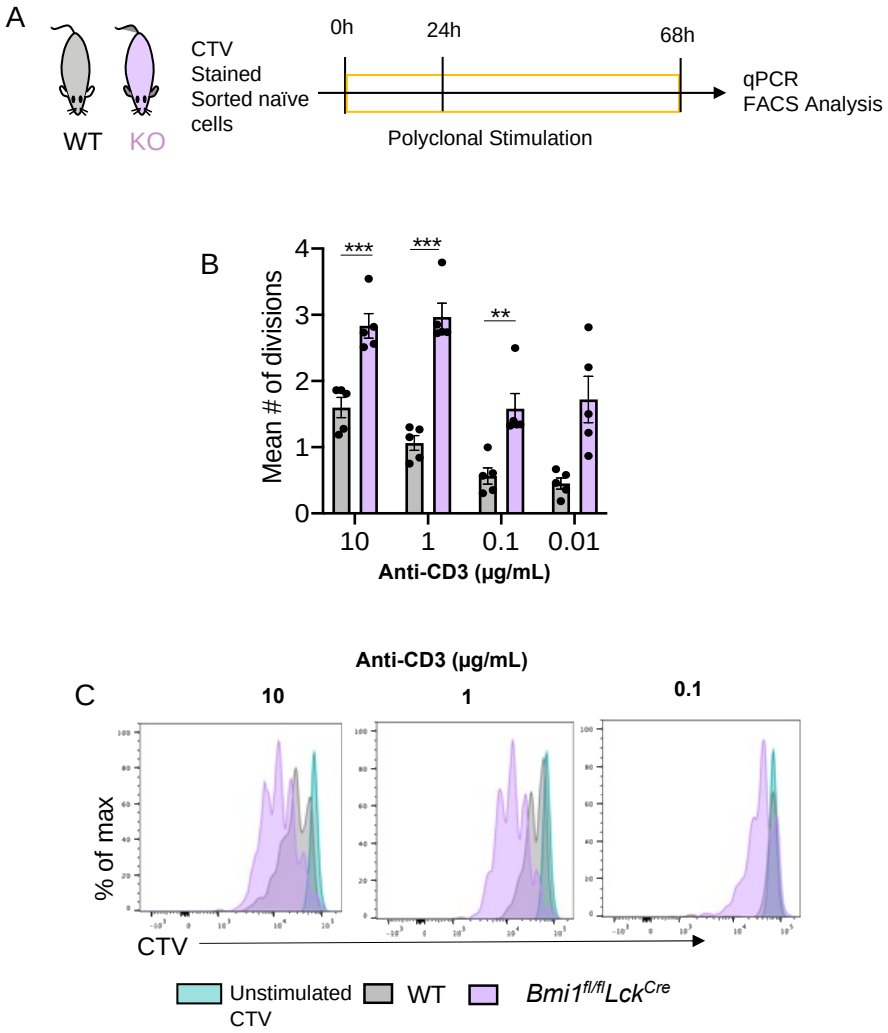

Figure 4.3: BMI-1 deficient CD8⁺ T cells have an increased proliferative capacity. A) Naïve CD8⁺ T cells from WT and *Bmi1*$^{fl/fl}$*Lck*^{Cre} mice were labelled with CTV and and stimulated polyclonally for 68hrs and then FACS analysis was done to analyse CTV dilution. (B) Frequency of division of CD8⁺ T cells upon stimulation with various concentrations of CD3. (C) representative FACS plot showing the dilution of CTV. Data shown are mean ± SEM of 2 independent experiment. Student t-test was performed for analysing statistical significance. n=5 (**p < 0.01, ***p < 0.001)

4.2.4 Increased expansion of CD8⁺ T cells lacking BMI-1 following Influenza A virus infection.

To understand the role of cPRC1 in regulating virus-specific T cell responses, WT control and *Bmi1*$^{fl/fl}$*Lck*^{Cre} mice were challenged with 10^4 PFU of A/HKx31 virus, and antigen specific CD8⁺ T cell primary responses were assessed at day 10 (Figure 4.4 A). We did not observe any change in the weight loss between two genotypes

post infection, although there was a trend towards the *Bmi1*$^{fl/fl}$*Lck*^{Cre} mice regaining weight faster than the WT (Figure 4.4 B). At day 10 post infection, CTLs specific for immunodominant IAV epitopes H-2D^{b}NP$_{366\text{-}374}$ (D^{b}NP) and H-2D^{b}PA$_{224\text{-}233}$ (D^{b}PA) were enumerated using specific tetramers and sampling the spleen (Figure 4.4C) and BAL fluid.

The proportion and number of D^{b}NP and D^{b}PA specific cells were comparable between both genotypes at the site of infection in BAL (Figure 4.4 D). However, in spleen there was a significant increase in the proportion of D^{b}NP-specific CTLs (~7% in *Bmi1*$^{fl/fl}$*Lck*^{Cre} compared to ~3% in WT) and a trend towards increased numbers in the spleen of *Bmi1*$^{fl/fl}$*Lck*^{Cre} mice (Figure 4.4E). These results suggest that loss of BMI-1 from T cells leads to the increased expansion of antigen specific cells upon IAV infection, consistent with the increased proliferative capacity of BMI-1 deficient CD8^{+} T cells described in the previous section.

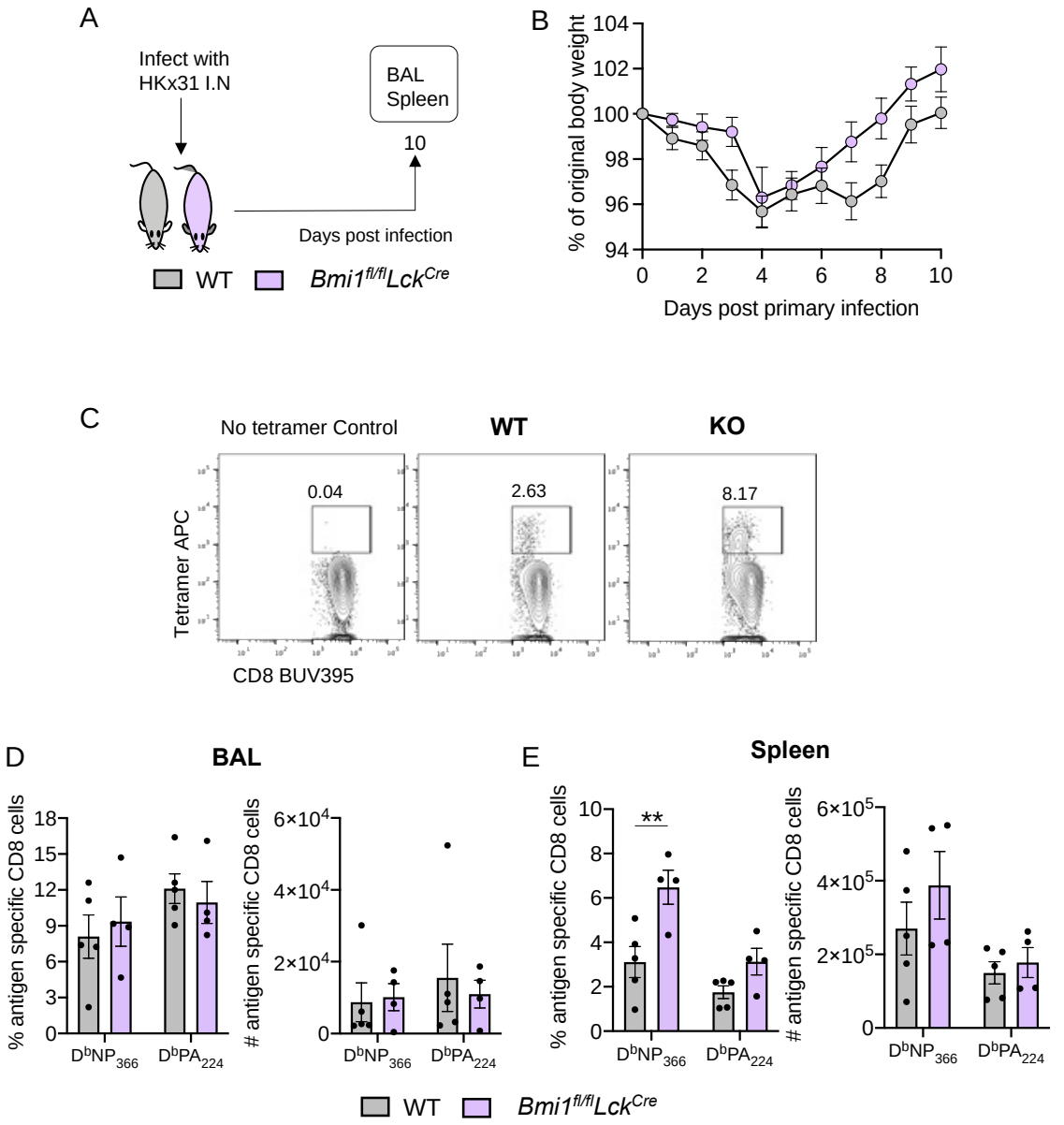

Figure 4.4: Increased epitope specific cells following primary IAV infection: A) WT and *Bmi1*$^{fl/fl}$*Lck*^{Cre} mice were infected with 10^4 PFU of HKx31 strain of Influenza A virus. At day10 (Effector) BAL, and spleen were harvested. B) The proportion weight loss after IAV infection compared between WT and *Bmi1*$^{fl/fl}$*Lck*^{Cre} mice. C) Representative flow plot showing the gating of CD8$^+$T cells specific for the H-2D^{b}NP$_{366\text{-}374}$ (NP) and H-2D^{b}PA$_{224\text{-}233}$ (PA). D-E) The proportion and number of antigen specific cells in BAL and Spleen of WT and *Bmi1*$^{fl/fl}$*Lck*^{Cre} mice were enumerated. Data shown are mean ± SEM of 3 independent experiment. n=5, (5 mice per group) Two-way ANOVA was performed between groups (**p < 0.01).

4.2.5 Increased Granzyme A expression in BMI-1 deficient effector T cells.

Previous work from our lab has shown that acquisition of Granzyme expression is hierarchical during $CD8^+$ T cell differentiation, with GZMB expression being acquired early after activation, while GZMA expression requires more extensive proliferation, characteristic of terminally differentiated cells(Moffat et al., 2009, Jenkins et al., 2008). We have shown that the BMI-1 deficiency results in increased proliferation of naïve $CD8^+$ T cells, which would suggest increased proportions of terminally differentiated effector cells and more GZMA expression.

To test this, expression of GZMA and GZMB was analysed by intracellular staining of splenocytes sampled at d10 post infection (gating strategy is explained in Figure 4.5 A). A greater proportion of NP and PA specific cells from *Bmi1*$^{fl/fl}$*Lck*^{Cre} mice expressed GZMA (*~40%)*, (Figure 4.5B), and on a per cell basis, they produced more GZMA (approximately 1.5-fold) (Figure 4.5 C). However, GZMB production was unaltered (Figure 4.5 C-D). Thus, the increased frequency of antigen specific cells producing GZMA is suggestive of a more terminally differentiated phenotype for *Bmi1*$^{-/-}$ Ag-specific CTL.

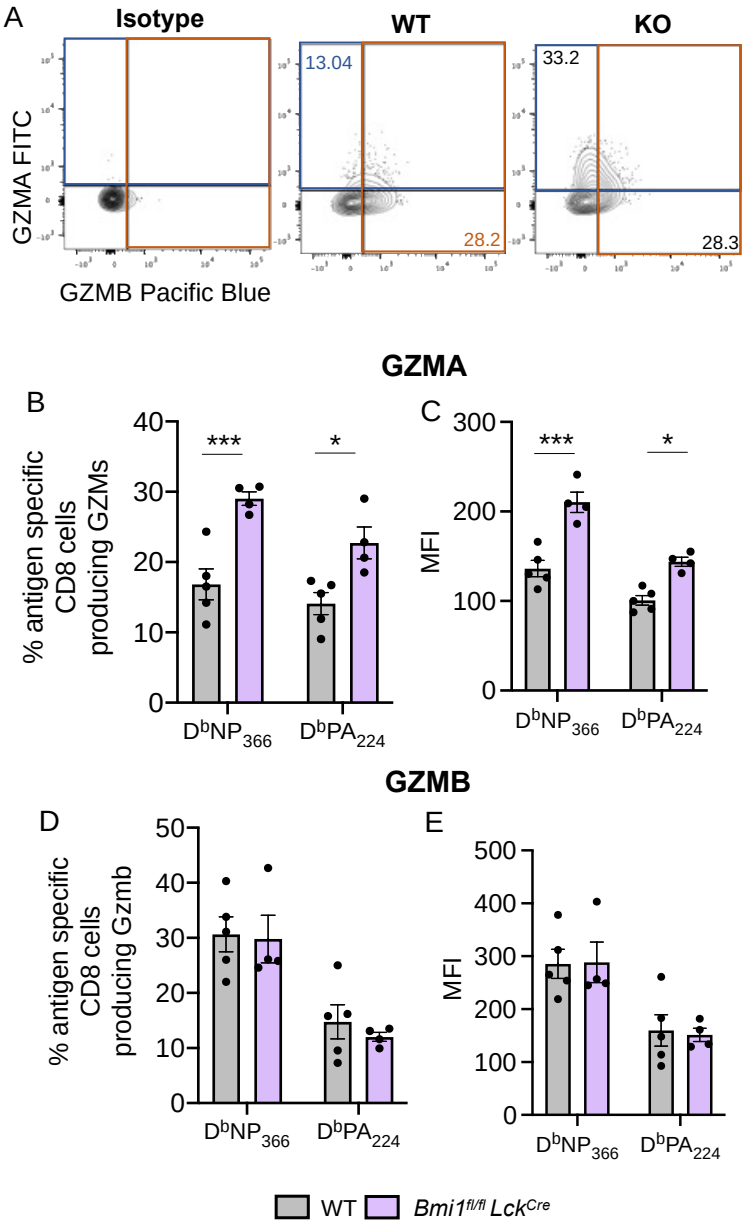

Figure 4.5: Lack of BMI-1 leads to the increased Granzyme A expression: A) Representative flow plot showing GZMA and GZMB expression by antigen specific cells day 10 post IAV infection. B and D) Proportion of antigen specific cells in the spleen expressing GZMA and GZMB. C and E) MFI of GZMA and GZMB in WT and *Bmi1*$^{fl/fl}$*Lck*^{Cre} mice. Data shown are mean ± SEM of 2 independent experiment. n=5. Two-way ANOVA was performed between groups. n=5 (*p < 0.05 **p < 0.01, ***p < 0.001)

4.2.6 BMI-1 deficient effector CD8$^+$ T cells have reduced polyfunctionality.

While a characteristic of CD8$^+$ T cell effector differentiation is the acquired production of antiviral cytokines (Denton et al., 2011a, Morris et al., 1982, Gett and Hodgkin, 1998, La Gruta et al., 2004), our lab has previously shown that extensive proliferation of CD8$^+$ T cell is associated with loss of polyfunctional cytokine production(Denton et al., 2011a). As data presented in the previous section suggested that that CTLs lacking *Bmi1* have an increased likelihood of becoming terminally differentiated, based on increased GZMA expression, we predicted ed that CTLs from *Bmi1$^{fl/fl}$Lck^{Cre}* mice would have a reduced capacity to produce multiple cytokines. To assess this, production of effector cytokines (IFN-**γ**, TNF**α** and IL-2) was measured in WT and *Bmi1$^{fl/fl}$Lck^{Cre}* splenocytes from day 10 post infection with IAV. Intracellular cytokine assays were performed after a 5hr restimulation with NP or PA peptides (gating strategy used is detailed in Figure 4.6 A).

We found that the frequency of NP-specific CTLs producing IFN-**γ** was increased ~2-fold in *Bmi1$^{fl/fl}$Lck^{Cre}* mice (Figure 4.6 B). This was also reflected by production on a per cell basis, where BMI-1 deficient CTLs produced ~30% more IFN-**γ** on average (Figure 4.67 C). However, the proportion of IFN-**γ**+ antigen specific CD8$^+$ T cells that also produced TNF**α** (Figure 4.6 D), or TNF**α** and IL-2 (Figure 4.6 E) was significantly reduced in the *Bmi1$^{fl/fl}$Lck^{Cre}* mice. Taken together with the observation that virus specific effector CTL from *Bmi1$^{fl/fl}$Lck^{Cre}* mice produce more GZMA, these data suggest that the effector CD8$^+$ T cells from *Bmi1$^{fl/fl}$Lck^{Cre}* mice are more terminally differentiated.

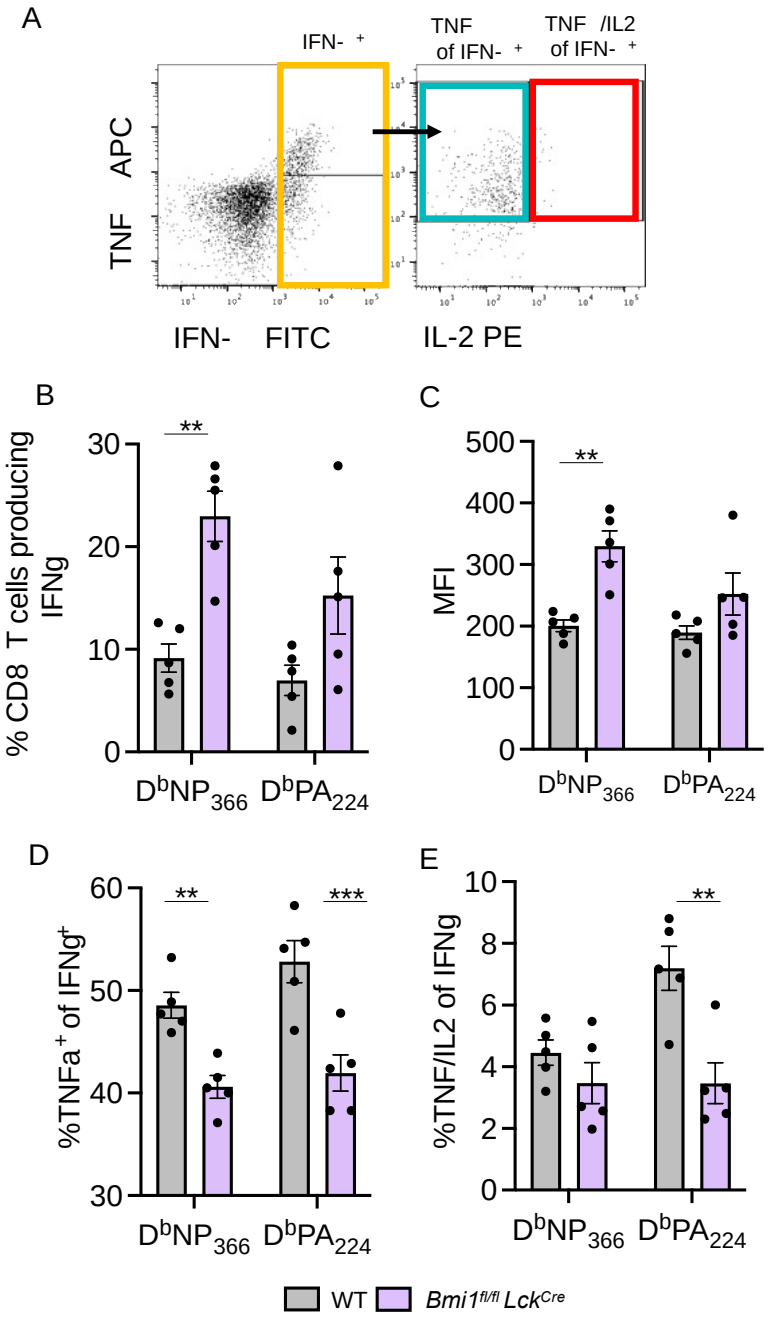

Figure 4.6: Loss of polyfunctional cytokine expression in *Bmi1$^{fl/fl}$Lck^{Cre}* mice: A) Representative flow plot showing the proportion of antigen specific cells expressing IFN-**γ**, TNF**α** and IL-2 from spleens of WT and *Bmi1$^{fl/fl}$Lck^{Cre}* mice. B) Proportion of antigen specific cells expressing IFN**γ** and the C) MFI of IFN-**γ**. D) Proportion of IFN-**γ** producing cells that also produces TNF**α**. E) Proportion of IFN-**γ** producing cells that produces both TNF**α** and IL-2. Data shown are mean ± SEM of 2 independent experiment. n=5. Two-way ANOVA was performed between groups. n=5 (*p < 0.05 **p < 0.01, ***p < 0.001

4.2.7 BMI-1 upregulation restrains terminal differentiation.

The **i**ncreased GZMA expression and decreased polyfunctionality of effector CTLs lacking BMI-1 is indicative of extensive proliferation and terminal differentiation. Among the antigen specific cells, KLRG1^{+} cells are known to have lost replicative capacity and are terminally differentiated (Voehringer et al., 2002, Voehringer et al., 2001), while CD62L marks precursors of central memory at the effector time point (Kaech and Cui, 2012). Therefore, we next measured KLRG1 and CD62L expression on antigen specific splenic CD8^{+} T cells 10 days after IAV infection, as described in Figure 4.7A. Consistent with our previous observations, we found an increased proportion of KLRG1+ $D^{b}NP_{366}$ and $D^{b}PA_{224}$ specific cells in *Bmi1$^{fl/fl}$Lck^{Cre}* mice (~5%), indicating increased terminal differentiation (Figure 4.7B), while there was no change in the proportion of CD62L^{+} cells (Figure 4.7B). Further we also assessed the expression of TCF1. KLRG1+ terminally differentiated cells also lack TCF1 and are unable to form memory(Kim et al., 2020). TCF1 is a master regulator of T cell differentiation and is necessary for restraining the naïvety and memory formation (Jeannet et al., 2010, Danilo et al., 2018). We found that the frequency of $D^{b}NP_{366}$ and $D^{b}PA_{224}$-specific CTLs producing TCF1 was decreased ~1.5-fold in *Bmi1$^{fl/fl}$Lck^{Cre}* mice (Figure 4.7E). This was also reflected by production on a per cell basis, where BMI-1 deficient CTLs produced ~40% less TCF1 on average (Figure 4.67 C-D). Thus, taken together, these results are consistent with a role for BMI-1 in restraining terminal differentiation of CD8^{+} T cells during viral infection.

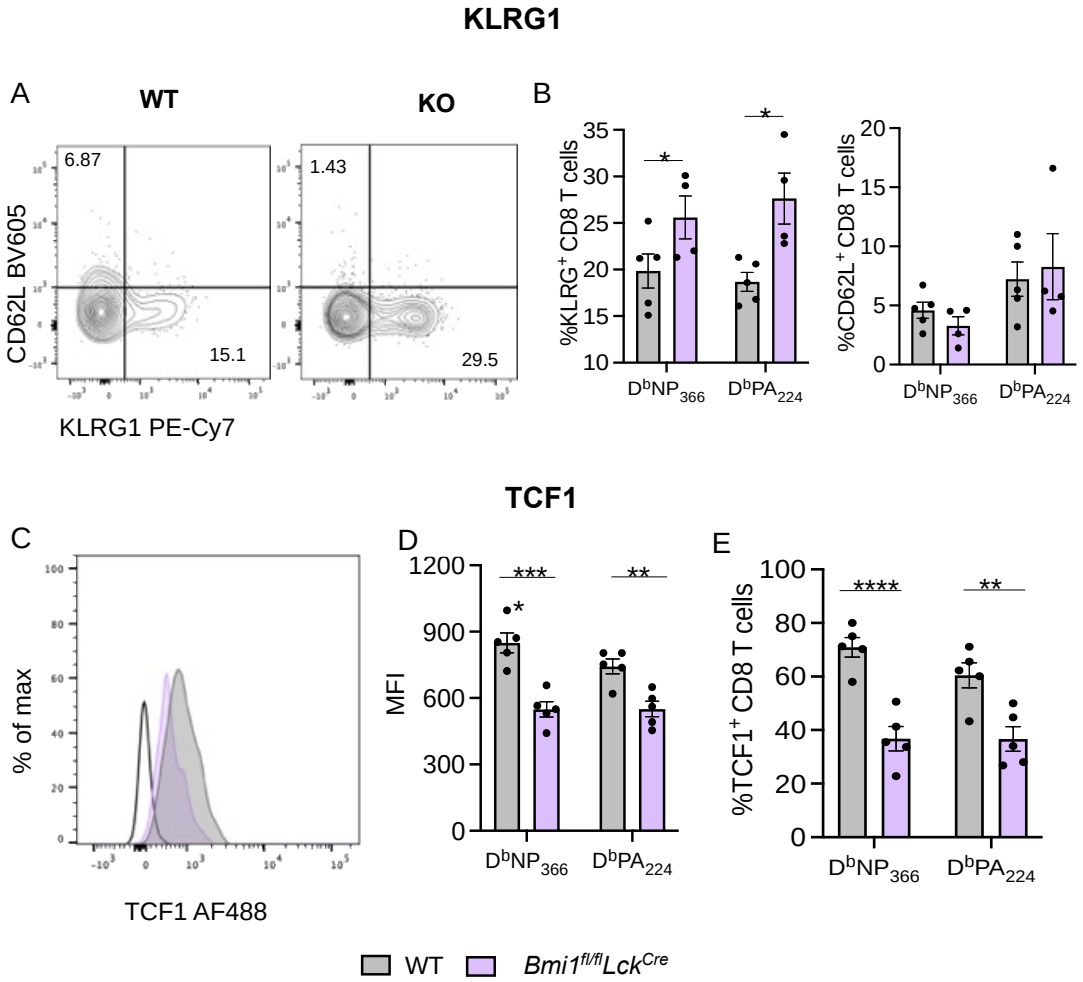

Figure 4.7: BMI-1 restrains terminal differentiation: A) Representative flow plot showing KLRG1 and CD62L expression by antigen specific cells from day 10 post IAV infection. B) Proportion of antigen specific cells expressing KLRG1 and CD62L in spleens of WT and *Bmi1*$^{fl/fl}$*Lck*^{Cre} mice (Analysis was focussed on KRLG1+ CD62L- and KRLG1- CD62L+ subsets). C) Representative histogram of TCF1 expression D) MFI of TCF1 in antigen specific cells. E) proportion of antigen specific cells expressing TCF1. Data shown are mean ± SEM of 2 independent experiment. n=5. Two-way ANOVA was performed between groups. n=5 (*p < 0.05 **p < 0.01, ***p < 0.001)

4.2.8 BMI-1 prevents apoptosis of antigen specific effector CD8$^+$ T cells following IAV infection.

After clearance of pathogens, 90-95% effector CD8$^+$ T cells undergo apoptosis and rest of them survive to become long living memory cells (Kaech et al., 2002b, Williams and Bevan, 2007). Expression of BMI-1 protects against apoptosis in a number of cellular contexts by inducing expression of anti- apoptotic BCL2 family members, including MCL1 (Wu et al., 2021). As BCL2 is an essential regulator of T cell contraction and survival (Grayson et al., 2006), we hypothesised that the increased number of effector T cells observed following IAV infection of *Bmi1*$^{fl/fl}$*Lck*^{Cre} mice may result from a disrupted apoptosis. WT and *Bmi1*$^{fl/fl}$*Lck*^{Cre} mice were infected with IAV and at day 10 post infection splenocytes were harvested (Figure 4.8 A). As expected, the proportion of BCL2+ virus-specific CD8$^+$ T cells was reduced (by 1.5-fold) specifically in D^{b}NP$_{366}$ specific CD8$^+$ T cells lacking *Bmi1*. To further assess the apoptosis, Annexin V and Propidium Iodide (PI) staining was performed. Annexin V preferentially binds to phosphatidylserine which are exposed in the outer membranes of apoptotic cells. Propidium iodide binds to necrotic cells. Early apoptotic cells are Annexin positive and late apoptotic cells stains for both Annexin, and PI as explained in Figure 4.8 D and E. The proportion of antigen specific cells that were early and late apoptotic cells were higher in splenocytes lacking *Bmi1*. Taken together, these results suggest that loss of BMI-1 induces apoptosis of antigen specific cells during IAV infection. However, further analysis of other apoptotic molecules is needed to confirm the result.

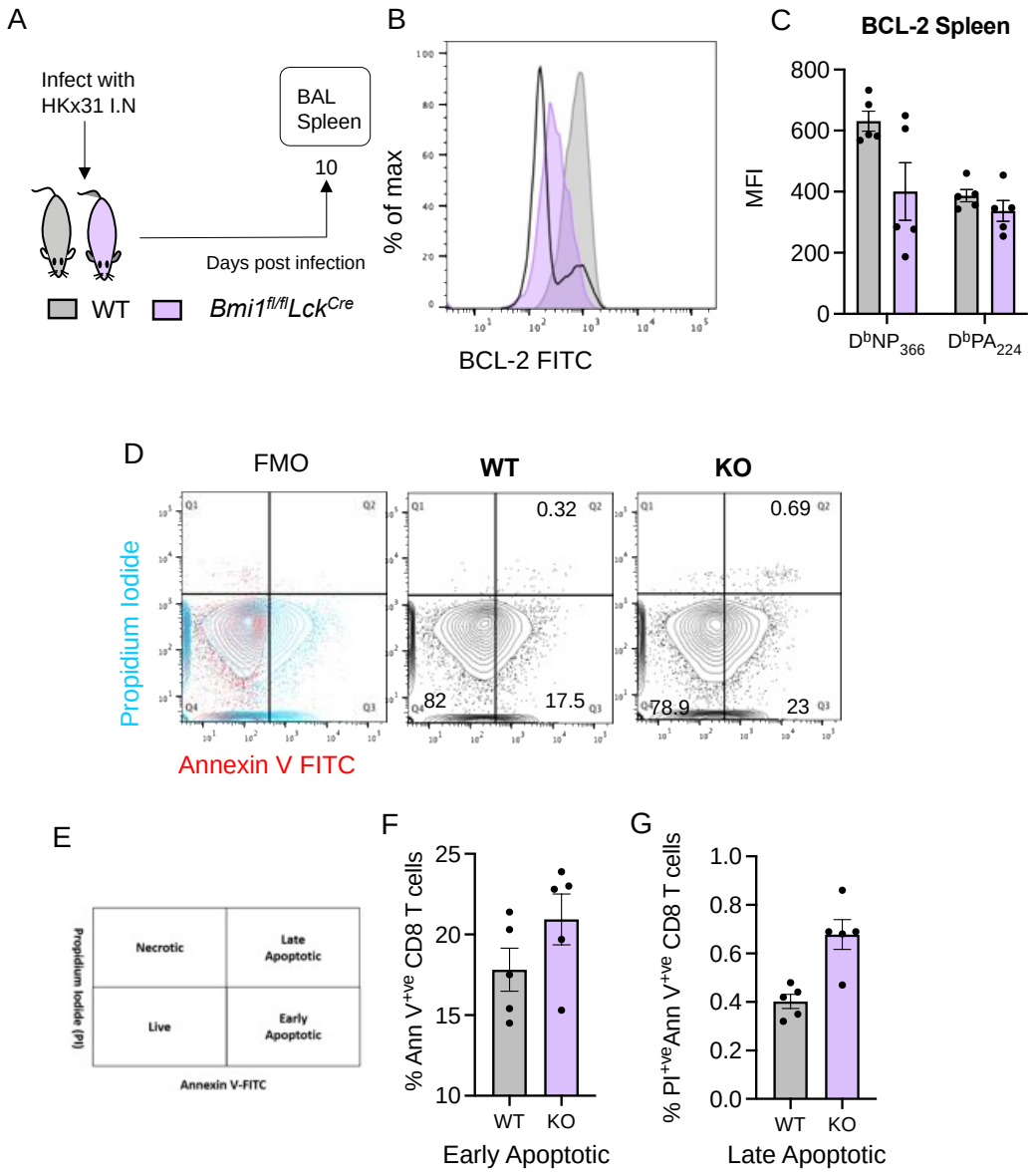

Figure 4.8: BMI-1 supresses apoptosis during IAV infection: A) WT and *Bmi1*$^{fl/fl}$*Lck*^{Cre} mice were infected with 10^4 PFU of HKx31 strain of Influenza A virus. At Day10 (Effector) spleens were harvested. B) Representative histogram of BCL2 expression and C) MFI of BCL2 in antigen specific cells. D) Representative flow plot showing Annexin V and Propidium Iodide staining in antigen specific CD8$^+$ T cells. E) early and late apoptotic cells gating strategy based on Annexin V and Propidium Iodide (PI). F) Proportion of antigen specific cells expressing Annexin V and G) Proportion of antigen specific cells expressing Annexin V and PI. Data shown are mean ± SEM of 2 independent experiment. n=5. Student t-test was performed for analysing statistical significance. n=5 (**p < 0.01, ***p < 0.001)

4.2.9 Reduced virus-specific memory CTLs in *Bmi1$^{fl/fl}$Lck^{Cre}* mice.

Having established that *Bmi1$^{fl/fl}$Lck^{Cre}* mice had an exaggerated effector CD8^{+} T cell response to IAV infection, which was characterised by increased a greater proportion of terminally differentiated CTLs, relative to the WT, we next asked whether the increased effector response came at the expense of memory formation. To test this, *Bmi1$^{fl/fl}$Lck^{Cre}* mice were infected with 1 x 10^4 PFU of A/HKx31 virus and the formation of virus-specific memory CTL was assessed in lungs and spleen 90 days after infection (Figure 4.9A). Antigen specific cells were enumerated by tetramer staining and flow cytometry (Figure 4.9B), and consistent with primary effector expansion coming at the cost of memory formation, we observed a significant reduction in the frequency and number of D^bNP_{366}+ and D^bPA_{224}+ CTLs in both the lung parenchyma (Figure 4.9C) and spleen of *Bmi1$^{fl/fl}$Lck^{Cre}* mice (Figure 4.9D). While in the lungs, the frequency of NP and PA-specific CTLs mice lacking BMI-1 were reduced by ~1.8-fold, in the spleen this difference was more pronounced (~5-fold). Taken together this data suggests that lack of BMI-1 impacts memory formation.

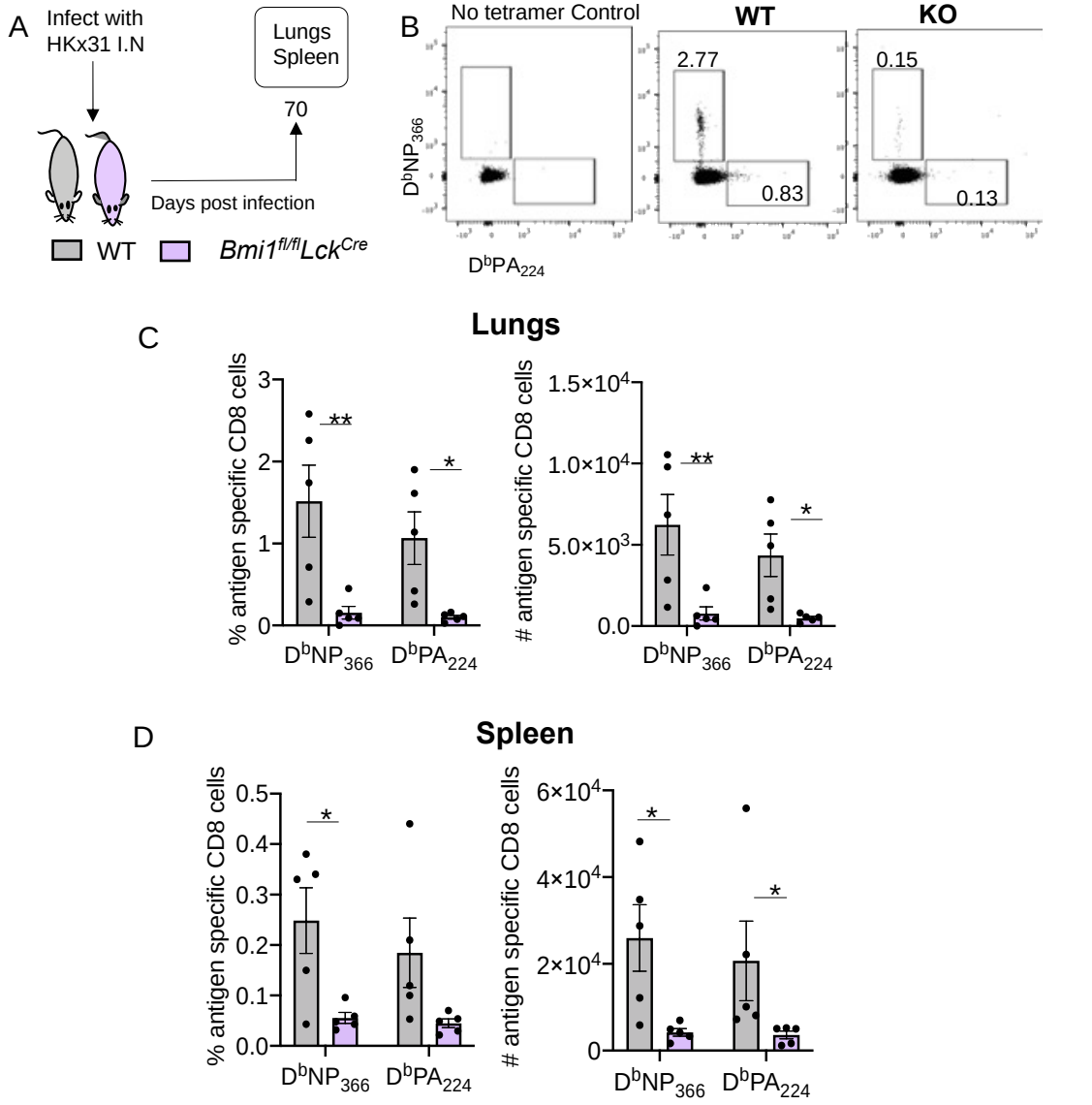

Figure 4.9: Absence of BMI-1 leads to impaired memory formation: A) WT and *Bmi1*$^{fl/fl}$*Lck*^{Cre} mice were infected with 10^4 PFU of HKx31 strain of Influenza A virus. At Day 70 lungs and spleen were harvested. B) Representative flow plot showing the gating of $CD8^+$ T cells specific for the NP and PA epitopes in the lungs of WT and *Bmi1*$^{fl/fl}$*Lck*^{Cre} mice.C-D) The proportion and number of antigen specific cells in lungs and spleen of WT and *Bmi1*$^{fl/fl}$*Lck*^{Cre} mice were enumerated. Data shown are mean ± SEM of 3 independent experiment. n=5 Two-way ANOVA was performed between groups (*$p < 0.05$ **$p < 0.01$)

4.2.10 Mice lacking BMI-1 form poor recall responses after secondary infection with IAV.

Whilst *Bmi1*$^{fl/fl}$*Lck*^{Cre} mice formed an enhanced effector response against primary IAV infection, memory formation was greatly reduced. Indeed, while virus-specific memory cells were detectable after infection of *Bmi1*$^{fl/fl}$*Lck*^{Cre} mice, there were too few to enable phenotypic characterisation of the cells in a resting state. To understand whether the cells that were detectable could be recalled following secondary infection, WT and *Bmi1*$^{fl/fl}$*Lck*^{Cre} mice were infected with IAV HKx31 (H3N2) and at >60 days post infection, mice were re-infected with the serologically distinct IAV strain, A/PR8 (H1N1), and BAL and spleen were collected at 6 days post infection for further analysis (Figure 4.10A).

During secondary infection, the *Bmi1*$^{fl/fl}$*Lck*^{Cre} mice lost slightly more weight compared to WT controls, suggesting a reduced memory CTL recall capacity (Figure 4.10B). Consistent with this, enumeration of tetramer specific cells (Figure 4.10C). showed that both in BAL and spleen, D^bNP_{366} -specific cells were significantly reduced in *Bmi1*$^{fl/fl}$*Lck*^{Cre} mice (approximately 2.5 times), both in number and proportion (Figure 4.10 C-E). However, there was no difference in the proportion and number of D^bPA_{224} which is subdominant relative to D^bNP_{366} following primary and secondary infections (La Gruta et al., 2006). Taken together, these data indicate that Bmi*1*$^{fl/fl}$*Lck*^{Cre} mice generate poor secondary $CD8^+$ T cell responses against IAV infection.

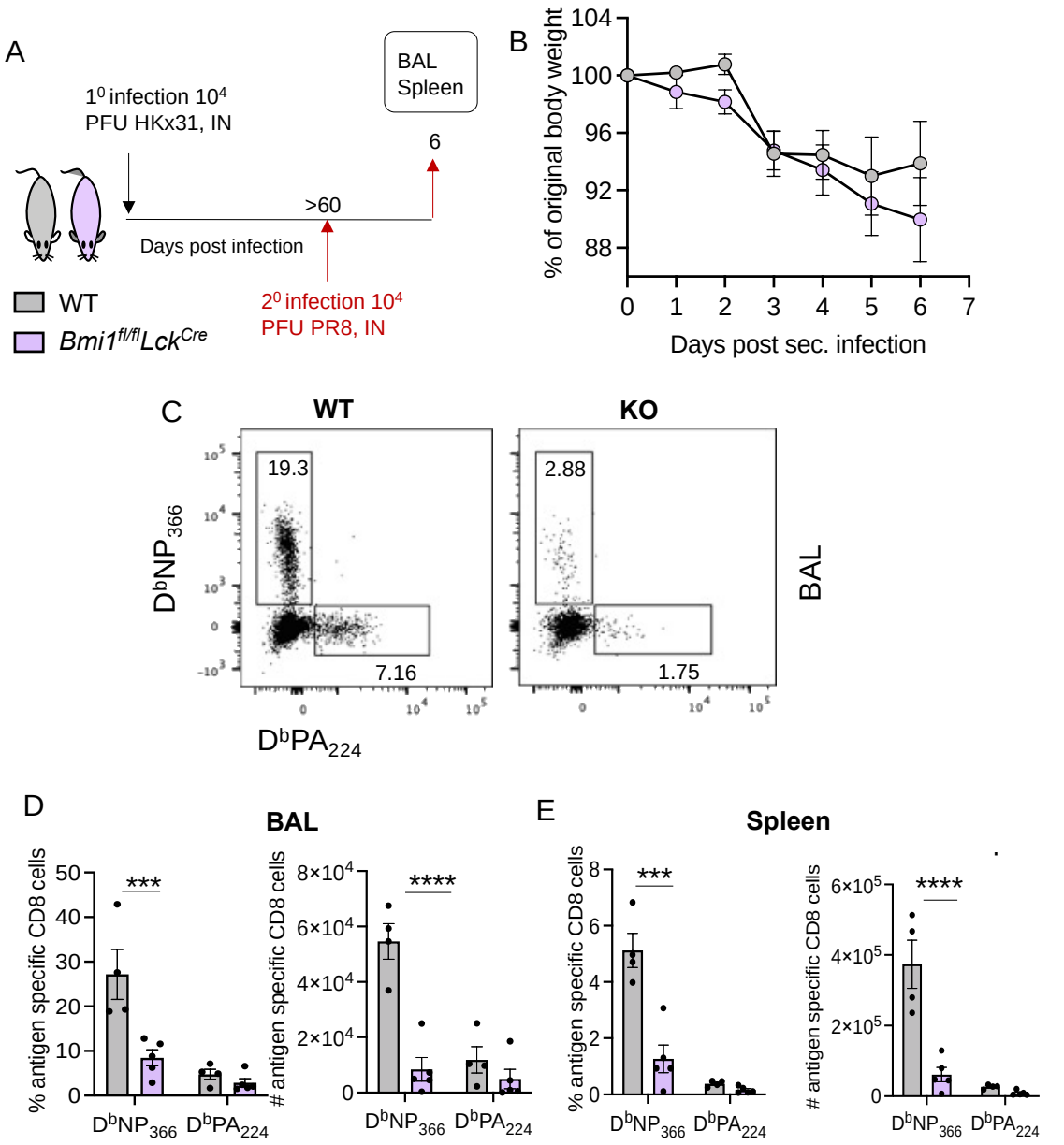

Figure 4.10: *Bmi1$^{fl/fl}$Lck^{Cre}* generate poor secondary immune response: A) WT and *Bmi1$^{fl/fl}$Lck^{Cre}* mice were infected with 10^4 PFU of HKx31 strain of IAV. Day 60 post infection, mice were rechallenged with 10^4 PFU of PR8 strain of IAV. 6 days post-secondary challenge BAL and spleen were harvested for further analysis. B) % weight loss after PR8 IAV infection compared between WT and *Bmi1$^{fl/fl}$Lck^{Cre}* mice. C) Representative flow plot showing the gating of $CD8^+$ T cells specific for the NP and PA. D-E) proportion and number of antigen specific cells in BAL and Spleen of WT and *Bmi1$^{fl/fl}$Lck^{Cre}* mice. Data shown are mean ± SEM of 2 independent experiment. n=5. Two-way ANOVA was performed between groups. n=5 (*p < 0.05 **p < 0.01, ***p < 0.001, **** p < 0.0001)

4.2.11 Virus-specific memory T cells formed in the absence of BMI-1 have decreased functionality following secondary infection.

To further investigate the quality of secondary immune responses in *Bmi1$^{fl/fl}$Lck^{Cre}* mice, following establishment of memory and secondary challenge as described above, expression of cytokines by virus specific CTLs from the spleens of mice was assessed after restimulation with D^bNP_{366} and D^bPA_{224} peptides for 5 hours, by performing an ICS assay (Figure 4.11 A explains the gating from D^bNP_{366} specific cells). We found that the proportion of IFN-**γ** producing D^bNP_{366}-specific cells was significantly decreased (almost 2-fold) in mice lacking BMI-1, as was the TNF**α** and IL-2 producing cells within the IFN-**γ**$^+$ D^bNP_{366} and D^bPA_{224} specific cells (Figure 4.11 B-C). Thus, D^bNP_{366} specific cells had reduced IFN-**γ** production, with cells of both specificities had reduced polyfunctionality, relative to the WT. Consistent with the reduced polyfunctionality, D^bNP_{366} -specific, BMI-1-deficient cells produced less IFN-**γ** on a per cell basis, and D^bPA_{224} -specific cells produced significantly less IL-2 and showed a trend towards reduced TNF**α** production (Figure 4.11 D). Taken together, these results demonstrate that the reduced recall response of virus specific *Bmi1$^{fl/fl}$Lck^{Cre}* CTLs is accompanied by reduced cytokine production.

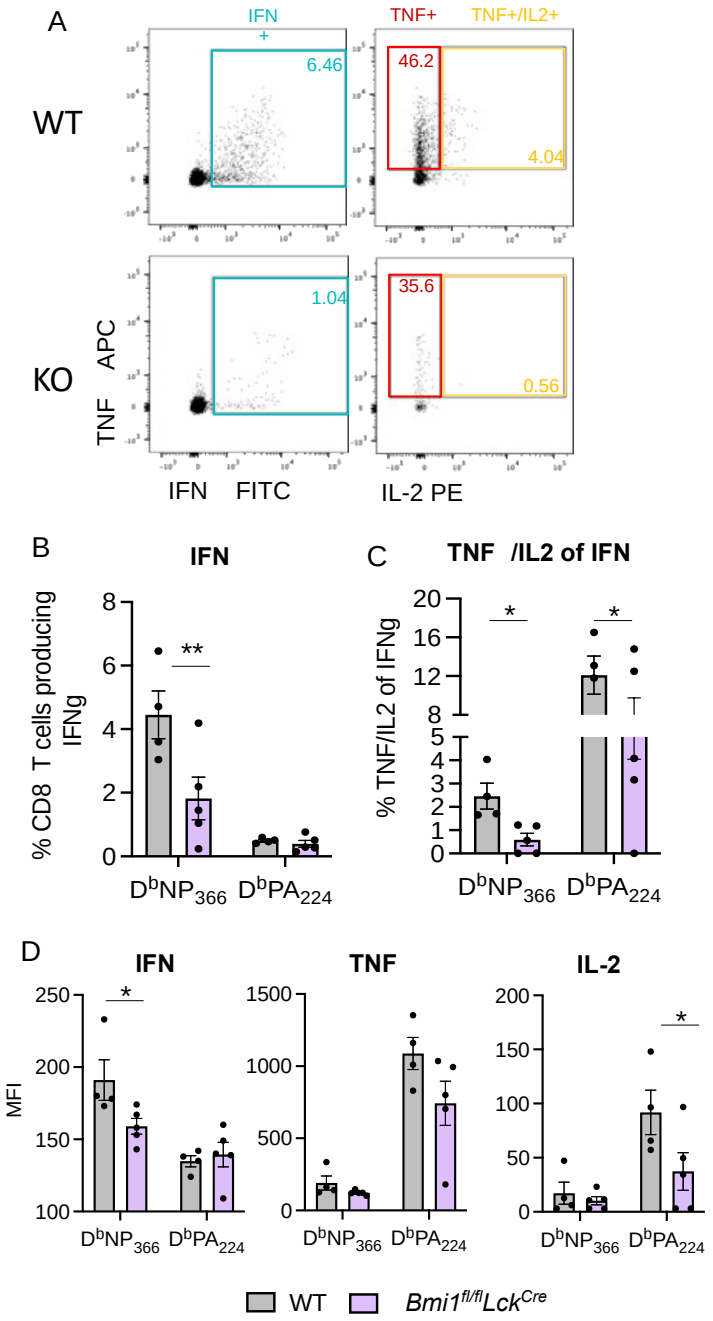

Figure 4.11: *Bmi1$^{fl/fl}$Lck^{Cre}* mice generates decreased amount of cytokine during secondary infection: A) Representative flow plot showing the proportion of D^bNP_{366} -specific cells expressing IFN-**γ**, TNF**α** and IL-2 from spleens of WT and *Bmi1$^{fl/fl}$Lck^{Cre}* mice. B) Proportion of antigen specific cells expressing IFN-**γ** D) Proportion of IFN-**γ** producing cells that produces both TNF**α** and IL-2. E) MFI of IFN-**γ**, TNF**α** and IL-2 from antigen specific cells. Data shown are mean ± SEM of 2 independent experiment. n=5. Two-way ANOVA was performed between groups. n=5 (*p < 0.05 **p < 0.01, ***p < 0.001)

4.2.12 Increased exhaustion marker expression on virus specific CTLs of *Bmi1$^{fl/fl}$Lck^{Cre}* following rechallenge.

The reduced secondary expansion and cytokine production capacity of BMI-1 deficient CTLs in response to secondary challenge is consistent with a T cell exhaustion phenotype (Wherry and Kurachi, 2015, Wherry et al., 2007). As exhaustion is associated with expression of inhibitory receptors including PD-1 (Blackburn et al., 2009, Barber et al., 2006), as well as the TFs EOMES (Paley et al., 2012) and TOX (Khan et al., 2019), we next assessed the expression of these molecules by FACS following secondary challenge, as above.

Consistent with BMI-1-deficient, virus-specific CTLs being exhausted, the proportion of PD1, EOMES and TOX expressing D^bNP_{366} specific CTLs was significantly increased in *Bmi1$^{fl/fl}$Lck^{Cre}* mice, as was the proportion of EOMES and TOX expressing D^bPA_{224} specific cells. (Figure 4.12A-E respectively). While D^bNP_{366} specific cells expressing PD1 was ~15% higher in *Bmi1$^{fl/fl}$Lck^{Cre}* mice (Figure 4.12 A and D), EOMES (Figure 4.12 B and E) and TOX (Figure 4.12 C and F) expressing D^bNP_{366} and D^bPA_{224} specific cells were ~20% and ~10% higher respectively. These results suggest that in the absence of BMI-1, and acute viral infection may drive differentiation of exhausted $CD8^+$ T cells.

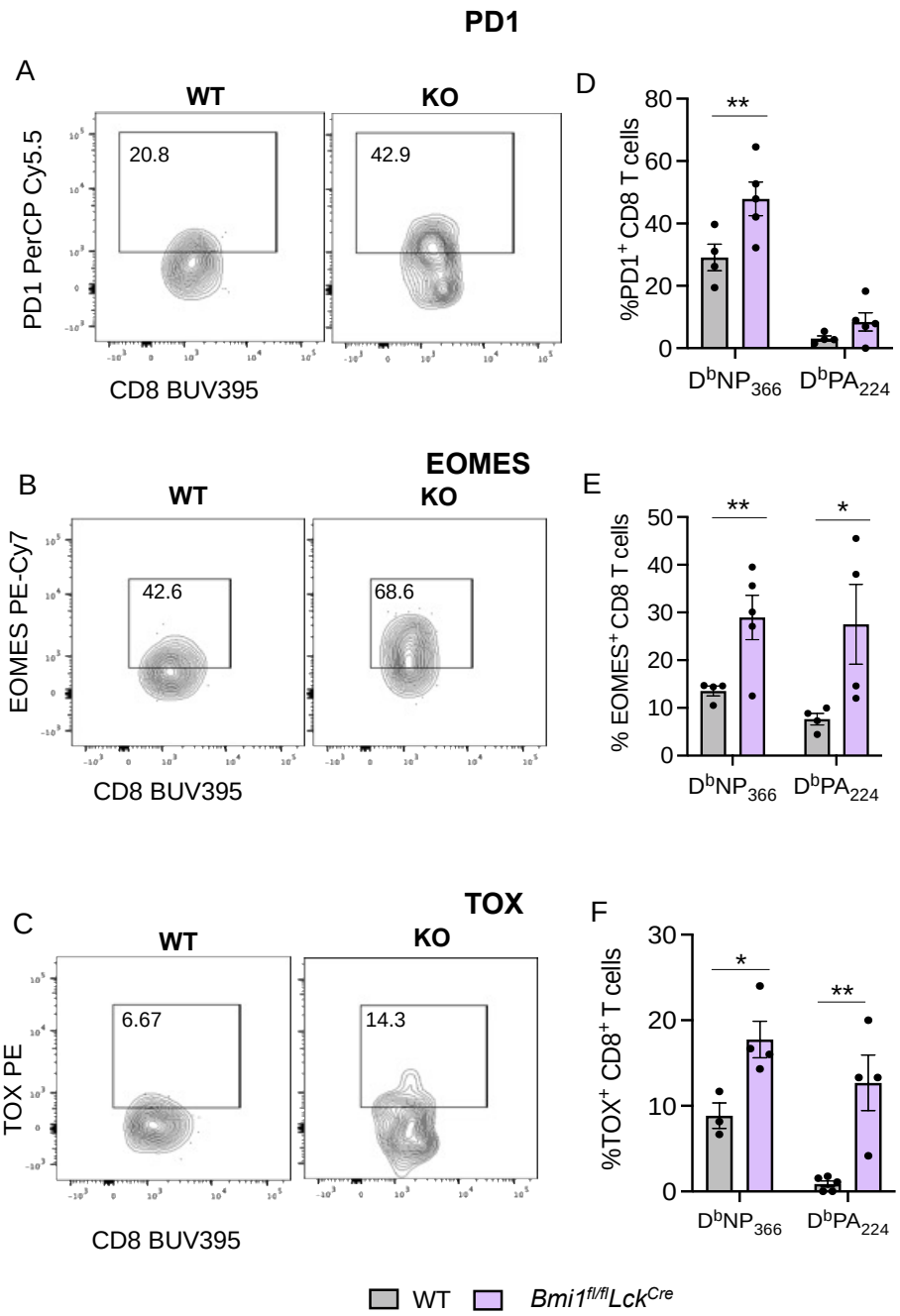

Figure 4.12: Exhaustion marker expression on virus specific CTLs of *Bmi1$^{fl/fl}$Lck^{Cre}* mice is increased following secondary infection: A-C) Representative flow plot showing the gating of antigen specific cells expressing PD1, EOMES and TOX respectively. D-F) Proportion of antigen specific cells expressing PD1, EOMES and TOX respectively.

4.3 Discussion

Although cPRC1 is understood to regulate embryonic stem cell differentiation through its roles in maintaining stemness and self-renewal capacity, it is not clear

whether it plays a similar role in more differentiated cell types, including T cells. This chapter investigated the role of cPRC1 mediated epigenetic repression during $CD8^+$ T cell differentiation using a T cell specific deletion of *Bmi1* - a core component of cPRC1 that regulates its ubiquitination function. The data presented in this chapter demonstrated that BMI-1 has a critical role in maintaining homeostasis of the naïve T cell compartment, with both naïve $CD4^+$ and $CD8^+$ T cells being reduced in mutant mice, consistent with a role in self renewal (Park et al., 2003).

Hematopoietic stem cells and all lymphoid cell subsets were significantly reduced in global $Bmi1^{-/-}$ mice (Park et al., 2003). This study is in accordance with our observation of reduction in naïve $CD8^+$ T cells. $Bmi1^{fl/fl}Lck^{Cre}$ mice also had increased number of thymocytes contributed by increased double positive thymocytes. BMI-1 has been previously shown to be crucial for thymocyte proliferation(Miyazaki et al., 2008, Guo et al., 2011). Our data corroborates these studies suggesting a role for BMI-1 in T cell development. Interestingly, in section 4.2.3. when naïve $CD8^+$ T cells from $Bmi1^{fl/fl}Lck^{Cre}$ mice were cultured in the presence of titrated concentrations of anti-CD3 antibody, they proliferated in excess of WT $CD8^+$ T cells, even at the highest dose for activation. This indicates that even though naïve $CD8^+$ T cells are decreased in number in the absence of BMI-1, they have a higher proliferative potential which indicates that BMI-1 mediated ubiquitination has a role in regulating the differentiation outcome.

A key question was whether there is any role for BMI-1 in regulating viral induced $CD8^+$ T cell differentiation. Recent studies show that effector and memory differentiation is associated with increased generation of one differentiation state coming at the cost of the other (Joshi et al., 2007, Roychoudhuri et al., 2016). Acute infection of $Bmi1^{fl/fl}Lck^{Cre}$ mice with IAV lead to the increased expansion of effector $CD8^+$ T cells along with Granzyme A and cytokine production, which suggested that these cells were also more differentiated than WT controls. As expected, increased expansion of effector cells led to the decrease in memory $CD8^+$ T cell formation in $Bmi1^{fl/fl}Lck^{Cre}$ mice (Section 4.2.9). Further, upon

secondary infection, the recall response was greatly diminished relative to the WT, both in terms of secondary expansion and effector functionality. Thus, these data indicate that BMI-1 directly regulates $CD8^+$ T cell fate decisions. Heffner et al. have described that BMI-1 is expressed in both naïve and antigen experienced memory precursor cells ($KLRG1^-$ $CD44^+$) and but not in $KLRG1^+$ $CD44^+$ terminally differentiated $CD8^+$ T cells(Heffner and Fearon, 2007). This suggests subset specific activity of BMI-1 where BMI-1 mediated repression is necessary to maintain the proliferative capacity of memory precursor cells, with this activity being lost in terminally differentiated cells. With the loss of BMI-1 from $CD8^+$ T cells, mice had compromised ability to form virus-specific memory. One possible mechanism that regulate the fate decision is the selective targeting of BMI-1 containing cPRC1 to differentiation-specific genes. By utilising H2AK119ub ChIP in antigen specific cells, it would be possible to demonstrate this mechanism.

An interesting observation was increased terminal differentiation in antigen specific cells lacking BMI-1 during IAV primary infection. This is supported by the observations in section 4.2.7 that there was an increased proportion of $KLRG^+$ cells along with reduced TCF1 expressing cells. Terminal differentiation was also suggested by an increased frequency of IFN-γ+ cells and reduced polyfunctionality characterised by production of TNF and IL-2. However, this observation is counter to earlier observations by Gray *et al*., who showed that EZH2 containing PRC2 is required for differentiation of terminal effector $CD8^+$ T cells, and that in the absence of PRC2, effector $CD8^+$ T cells had more memory precursor like signatures (Gray et al., 2017). It is interesting to see this difference in the fate decision outcome because polycomb mediated gene silencing requires stepwise and hierarchical targeting of gene loci (Piunti and Shilatifard, 2022). However, it could be possible that PRC2 and cPRC1 might have nonoverlapping targets. This can be assessed by performing global enrichment analysis of both H3K27me3 and H2AK19ub in antigen specific cells. Previous studies in this regard support the targeting of PRC2 to the chromatin by PRC1 (Kalb et al., 2014, Blackledge et al., 2015, Moussa et al., 2019) which would explain the difference in the differentiation outcome we have observed to the previous study (Gray et

al., 2017). Further, PRC2 is known to target and regulate the activities of nascent transcripts and linc RNAs independently of cPRC1, which may also account for the differences observed (Blackledge et al., 2015). Our study also showed that absence of BMI-1 leads to an increased apoptosis during IAV infection, consistent with Yamashita et al., who showed that BMI-1 is needed to repress *Noxa* gene expression in order to avoid apoptosis in Th2 memory T cells (Yamashita et al., 2008). This study corroborates with our data where we find reduced number of memory $CD8^+$ T cells during IAV infection. Further experiments need to be performed to confirm the involvement of apoptosis in regulating the $CD8^+$ T cell numbers.

A cardinal feature of memory cells is that they exist in a poised, multipotent state where they can rapidly proliferate and provide protection to a secondary infection without further differentiation (Kaech and Wherry, 2007, Surh et al., 2006). Following PR8 infection, $Bmi1^{fl/fl}Lck^{Cre}$ mice generate a weak response, which was reflected in a reduced number of antigen specific effector cells, and reduced cytokine production relative to the WT (section 4.2.10-4.2.11). However, $Bmi1^{fl/fl}Lck^{Cre}$ mice are less protected against secondary infections due to a reduced number of antigen specific memory $CD8^+$ cells. The adoptive transfer of an equal number of wild type or $Bmi1^{fl/fl}Lck^{Cre}$ memory CD8+ T cells would be a more appropriate experiment to understand this feature. Remarkably, the proportion of PD1, EOMES and TOX expressing antigen specific cells was increased in $Bmi1^{fl/fl}Lck^{Cre}$ mice, suggesting that these cells may either be dysfunctional or functionally exhausted, and consistent with that, they had reduced cytokine production. Recent studies have profiled the epigenetic landscape of exhausted T cells in the context of LCMV infection and tumour specific $CD8^+$ T cells, chromatin architectures uniquely connected with T cell exhaustion, and suggesting an epigenetic basis (Mognol et al., 2017, Sen et al., 2016). Inhibition of EZH2 with specific small molecule inhibitor EZH2i results in induction of exhaustion and dysfunction of tumour infiltrating primary $CD8^+$ T cells which implies a relationship between EZH2 downregulation and exhaustion (Koss et al., 2020). However, a role for cPRC1 components or H2AK119ub mediated

repression has not been studied in the context of T cell exhaustion and it is hard to conclude that the cells lacking BMI-1 acquires exhaustion phenotype with current data alone. Further analysis of exhaustion signature using GSEA analysis is needed to understand the role of cPRC1 in exhaustion during IAV infection.

Higher expression of PD1 and TOX within antigen specific cells lacking BMI-1 after secondary infection, suggest that BMI-1 mediated H2AK119ub may have a role in regulating the chromatin architecture during secondary infection. Thus, with our study we have uncovered that BMI-1 containing cPRC1 might be important in keeping the expression of exhaustion molecules in check during acute infection. Further study in terms of assessment of chromatin accessibility by ATAC-seq might answer whether the BMI-1 directly regulates chromatin landscape.

Indeed, a cardinal feature of T cell-mediated immunity is establishment of immunological memory, where memory $CD8^+$ T cells are capable of rapidly responding to re-infection, thus preventing disease. Given this unique property of cells for rapid effector functions and long life this can be exploited for developing immunotherapies and vaccines. Given the deletion of BMI-1 gives rise to increased expansion and poor memory formation, pharmacological inhibition of BMI-1 can be used in immunotherapies.

Finally, these studies were performed mice lacking BMI-1 in both $CD8^+$ and $CD4^+$ T cells, and therefore, the generation and infection of mixed bone marrow chimeric mice should be performed to establish whether the phenotypes observed are $CD8^+$ T cell intrinsic. Furthermore, this study has focussed on an acute viral infection. Further research in this area should consider infection of these mice with chronic viruses like LCMV clone 13, where the exhaustion is well defined both phenotypically and at a molecular level. Combining molecular and phenotypic analyses of established exhaustion models with influenza infection of BMI-1 deficient mice may, for instance, enable establishment of core features of T cell exhaustion.

CHAPTER 5

Mechanism of epigenetic silencing by which BMI-1 regulates CD8$^+$ T cell differentiation.

5.1 Introduction

In Chapter 4, it was established that BMI-1 regulates CD8$^+$ T cell differentiation, with deletion impacting naïve homeostasis, effector expansion, and memory formation and function. However, the question of the mechanistic basis for these observations remained to be determined.

As outlined earlier (section 1.6.2), a primary way that cPRC1 exerts transcriptional repression is via CBX-mediated recognition of H3K27me3, resulting in targeting and deposition of H2AK119ub through E3 ubiquitin ligase RING1 at specific genomic regions(Blackledge and Klose, 2021, Morey and Helin, 2010). Modulation of permissive or repressive histone modifications have been shown to play a pivotal role in CD8$^+$ T cell differentiation and acquisition of effector functions (Denton et al., 2011a, Russ et al., 2014, Araki et al., 2009), and PRC2 mediated H3K27me3 deposition is one of the key repressive mechanisms that restrains the activation of genes that regulate CD8$^+$ T cell fate. Transcription factors *Prdm1*, *Eomes*, *Tbx21* and *Irf4*, of which play key roles in CD8+ T cell effector differentiation, exhibit enrichment of H3K27me3 within naïve CD8$^+$ T cells, with KDM6B dependent H3K27me3 removal required to initiate the proliferative and differentiation program early after activation(Russ et al., 2014, Li et al., 2021, Araki et al., 2009). Although H3K27me3 deposition catalysed by PRC2 is recognised by cPRC1, H2AK119ub mediated deposition by cPRC1 has not been studied in CD8$^+$ T cells.

To address the question of the role of cPRC1 and H2AK119ub in CD8+ T cell differentiation, we profiled the chromatin and transcriptomes of naïve and virus-specific CD8$^+$ T cells in BMI-1 deficient and sufficient mice, finding that BMI-1

actively maintains $CD8^+$ T cell naïvety and memory potential by directly repressing genes that would otherwise drive terminal effector differentiation.

5.2 Results

5.2.1. Dysregulation of transcription factors that drive differentiation in BMI-1 deficient, naïve $CD8^+$ T cells.

In Chapter 3, we established that cPRC1 mediated ubiquitination acts in concert with PRC2 deposition of H3K27me3 to repress genes that drive effector differentiation, including *Prdm1* (encoding BLIMP1), *Irf4* and *Tbx21* (encoding TBET; Section 3.2.6). Based on this observation, and the decreased proportion and number of naïve $CD8^+$ T cells in mice $Bmi1^{fl/fl}Lck^{Cre}$ mice observed in Chapter 4 (Section 4.2.2), we predicted that BMI-1 maintains T cell naïvety by repressing transcription factors that would otherwise drive T cell differentiation. To test this, RNA transcripts encoded by genes determined to be targeted by PRC1 in chapter 3 were assayed within sort-purified, naïve $CD8^+$ T cells (CD44lo, CD62Lhi) from WT and $Bmi1^{fl/fl}Lck^{Cre}$ mice, either directly *ex vivo*, or after stimulation with anti-CD3 in the presence of anti-CD28 and anti-CD11a for up to 72 hours (Figure 5.1 A-D). RNA was extracted and converted into cDNA, and expression of target genes was determined by qPCR, relative to the housekeeping gene *Poldip3*.

Consistent with our hypothesis, we found that even within naïve cells, *Prdm1* and *Tbx21* transcripts were elevated ~3-fold with BMI-1 deficiency (figure 5.1A and D), while *Eomes* levels were elevated in the same cells between 24hrs and 72hrs post-stimulation (Figure 5.1B). Interestingly, while *Irf4* transcript levels were elevated slightly in naïve, BMI-1-deficient T cells, levels were otherwise equivalent to the WT across the remainder of the time-course (Figure 5.1C).

To gain a mechanistic understanding of BMI-1 mediated regulation of these genes, ChIP and FAIRE assays were performed. We found that enrichment of H2AK119ub at the promoters of each gene was reduced between ~1.5 and 2-fold in BMI-1 deficient naïve cells, and barring the *Irf4* locus, these differences remained after 48hrs of stimulation (Figure 5.1E). Additionally, chromatin

accessibility, measured by FAIRE, was inversely proportional to H2AK119ub enrichment, and directly proportional to gene transcript levels, and as such, accessibility was increased with BMI-1 deficiency (~2 fold) in both naïve and activated CD8$^+$ T cells (Figure 5.1F). Together, these data suggest that BMI-1 maintains CD8$^+$ T cell naïvety by ensuring that genes driving differentiation are repressed via a mechanism whereby BMI-1 mediated ubiquitination reduces chromatin accessibility.

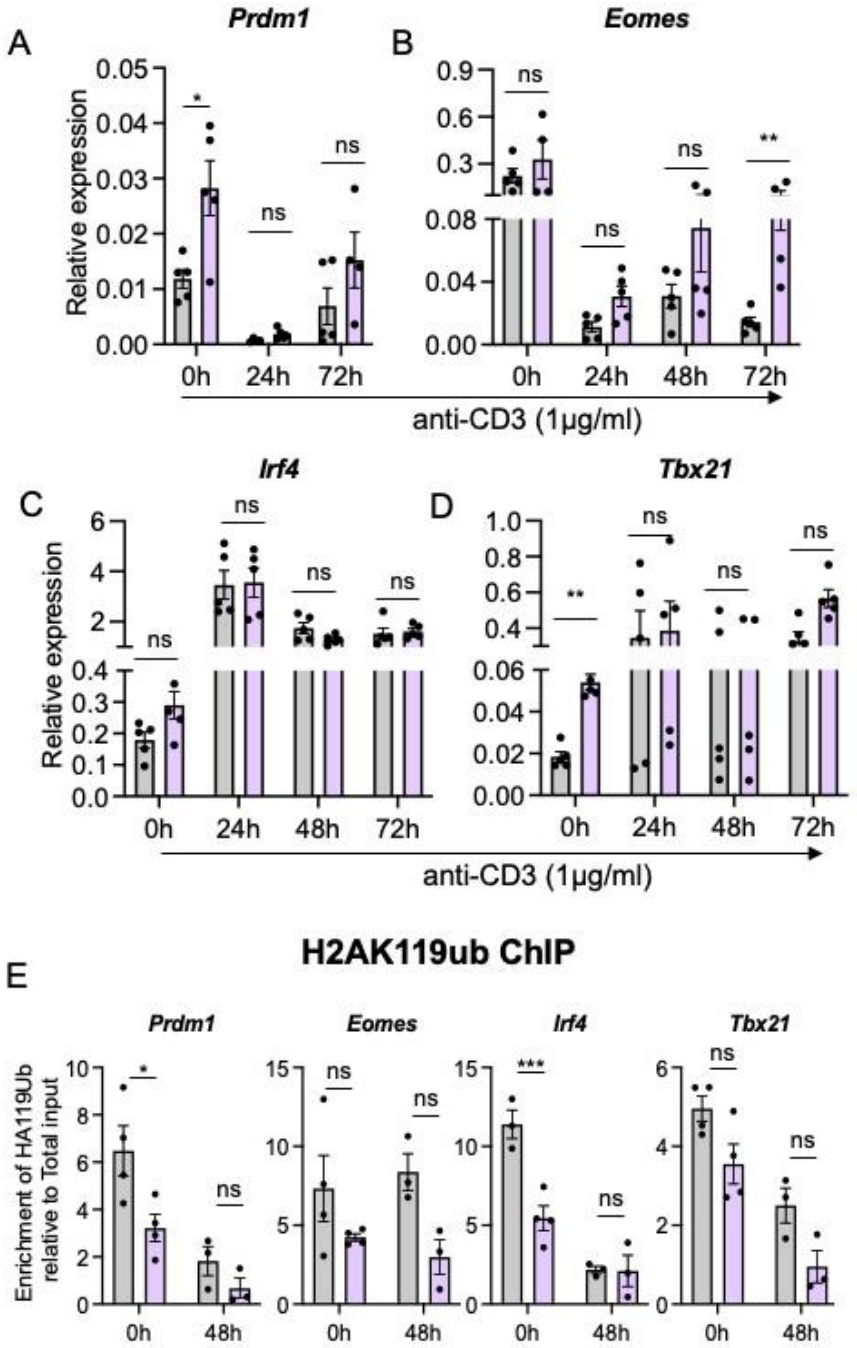

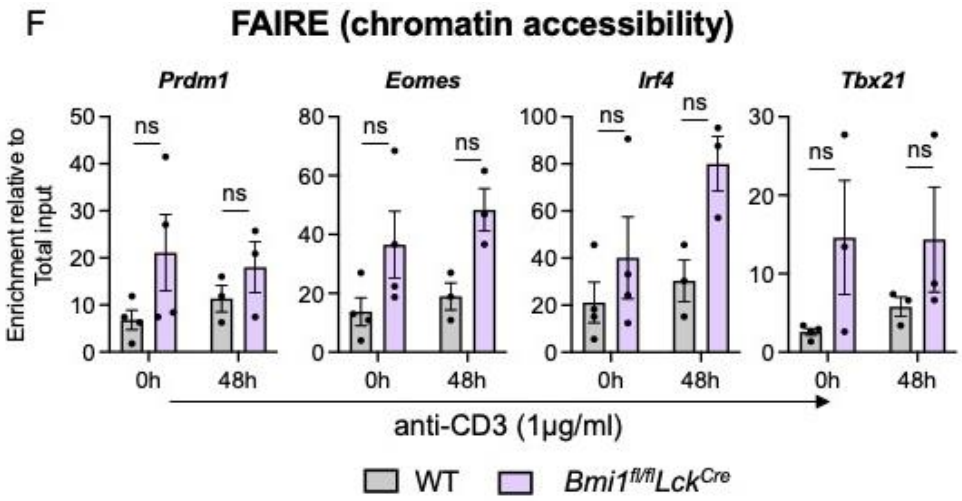

Figure 5.1 BMI-1 targets TFs that drive effector differentiation: Sort purified naïve (CD44 ^{lo}, CD62L ^{hi}, CD8^{+}) CD8^{+} T cells from WT and *Bmi1$^{fl/fl}$Lck^{Cre}* mice were stimulated with 1µg/ml of α-CD3 antibody and 10µg/ml α-CD8 and 2.5µg/ml α-CD28 and 5µg/ml α-CD11a antibody for various time points. Cells were harvested for RNA extraction, ChIP and FAIRE. A-D) Expression of *Prdm1, Eomes, Irf4 and Tbx21* was determined by real-time PCR and the expression values were normalized to *Poldip3.* E) Chromatin immunoprecipitation with H2AK119ub and its enrichment was assessed on promoters of *Prdm1, Eomes, Irf4,* and *Tbx21,* was determined by qPCR. F) Chromatin accessibility was analysed by FAIRE on the promoters of *Prdm1, Eomes, Irf4,* and *Tbx21,* was determined by qPCR. (Error bars show ± standard error of mean, n=3-4)

5.2.2 BMI-1 does not regulate transcription factors required for naïve T cell quiescence.

Having established that BMI-1 represses TFs that drive effector differentiation within naïve T cells, we hypothesised that BMI-1 may be redeployed to repress TFs that maintain stemness following T cell activation. This was further suggested by the finding that EZH2 containing PRC2 was shown to shut-down the expression of *Tcf7* in naïve CD8^{+} T cells (Gray et al., 2017). To test this, we repeated the experiments described in Section 5.1, this time assaying the chromatin landscape and expression of the stemness genes *Tcf7, Lef1* and *Satb1*. We found that within naïve T cells, all three genes showed a trend towards a slightly reduced expression with BMI-1 deficiency, consistent with an increased expression of genes driving an alternative and opposing fate, as seen in Figure 5.1 A-D. Indeed, at most time-points studied, this trend was observed, albeit that

the degree of difference between genotypes appeared to reduce for *Tcf7* and *Lef1* following stimulation (Figure 5.2A-C)

ChIP and FAIRE assays was performed as above, and assaying H2AUb119 enrichment and chromatin accessibility at *Tcf7, Lef1* and *Satb1* gene promoters. As seen in Figure 5.2D, there was no obvious difference in H2AUb119 enrichment between the genotypes in naïve and activated $CD8^+$ T cells, and this was reflective of similar levels of chromatin accessibility (Figure 5.2E). Thus, taken together, these results suggest that BMI-1 does not target directly target the genes that drive the T cell stemness program.

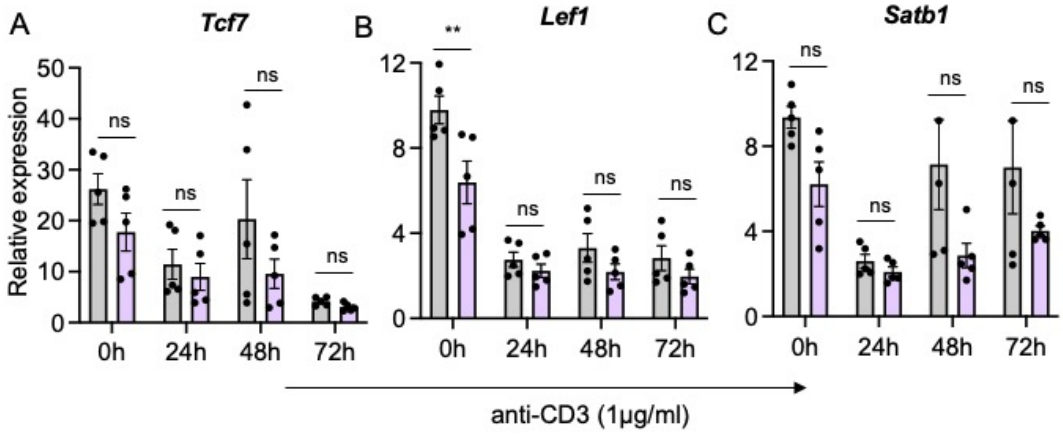

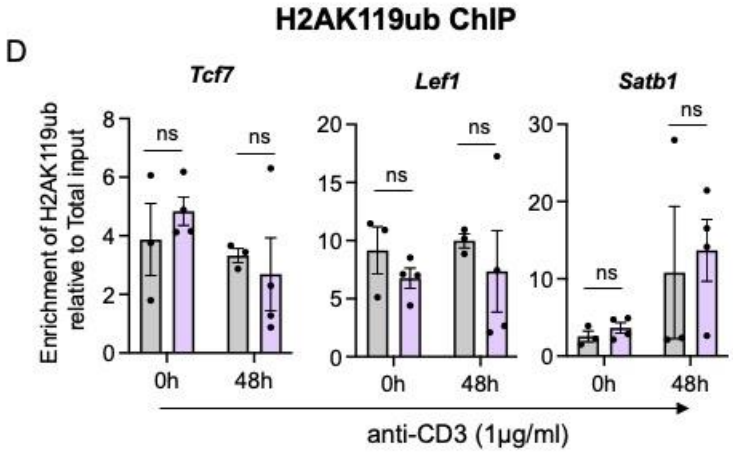

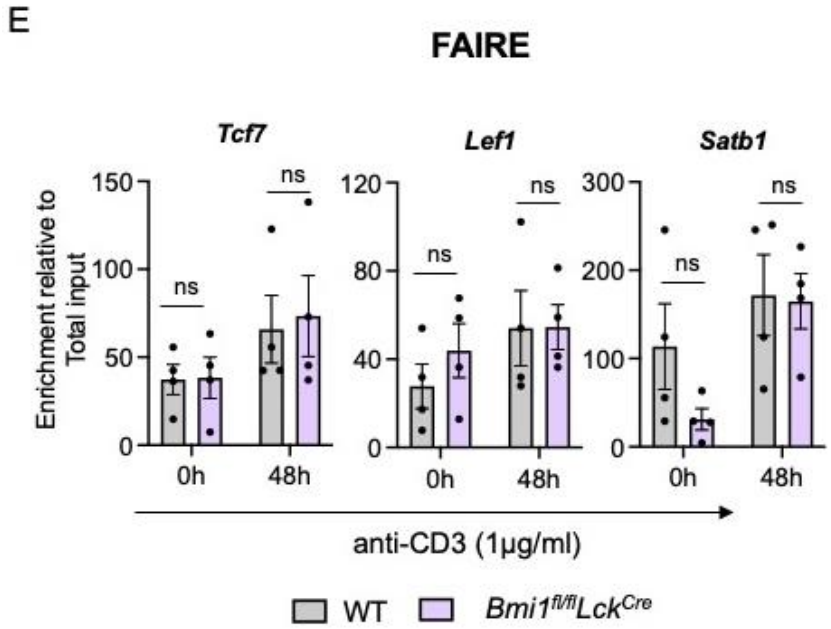

Figure 5.2 BMI-1 does not regulate stemness/quiescence genes: Sort purified naïve (CD44 ^{lo}, CD62L ^{hi}, CD8^{+}) CD8^{+} T cells from WT and *Bmi1$^{fl/fl}$Lck^{Cre}* mice were stimulated with 1µg/ml of α-CD3 antibody and 10µg/ml α-CD8 and 2.5µg/ml α-CD28 and 5µg/ml α-CD11a antibody for various time points. Cells were harvested for RNA extraction, ChIP and FAIRE. A-D) Expression of *Tcf7, Lef1* and *Satb1* was determined by real-time PCR and the expression values were normalized to *Poldip3.* E) Chromatin immunoprecipitation with H2AK119ub and its enrichment was assessed on promoters of *Tcf7, Lef1* and *Satb1,* was determined by qPCR. F) Chromatin accessibility was analysed by FAIRE on the promoters of *Tcf7, Lef1* and *Satb1,* was determined by qPCR. (Error bars show ± standard error of mean, n=3-4)

5.2.3 BMI-1 deficiency leads to small scale changes in the transcriptome of naïve CD8^{+} T cells.

Having found that the expression of key TFs is regulated by BMI-1 mediated H2AK119ub in naïve CD8^{+} T cells, we next aimed to understand the global transcriptional consequences of BMI-1 deficiency.

To do this, mRNA-Sequencing was performed on sort-purified naïve CD8^{+} T cells from WT and *Bmi1$^{fl/fl}$Lck^{Cre}* mice (Figure 5.3A). As an initial assessment of the quality and reproducibility of the data, a Multidimensional Scaling Analysis was performed. This analysis demonstrated that biological replicates from each genotype were clustered closely, but that samples from each genotype clustered

separately from one another, indicating the transcriptional difference resulting from BMI-1 deletion was the major contributor to sample separation in the plot (Figure 5.3B).

Surprisingly, there were only 63 differentially expressed genes (DEGs) between the two genotypes (with an adjusted p value < 0.05 and fold change >1.5x) (shown as a volcano plot and heatmap in Figure 5.3 C-D). However, despite the small number of DEGs, the majority (53) were upregulated in naïve $CD8^+$ T cells lacking BMI-1, as expected given the deletion of a core component of a repressive complex (Detailed in Table 5.1 below). The genes upregulated with BMI-1 deficiency included *Eomes* and *Runx2*, which encodes a TF important for T cell memory formation. Interestingly, *Bmi1* was itself upregulated in the BMI-1 mutant, suggesting that *Bmi1* transcript levels are subject to feedback inhibition, and that reads mapping to *Bmi1* in the mRNA-Seq data came from exons prior to the deletion site (exon 3). Collectively, this data shows that BMI-1 predominantly functions to repress a small number of genes within naïve $CD8^+$ T cells.

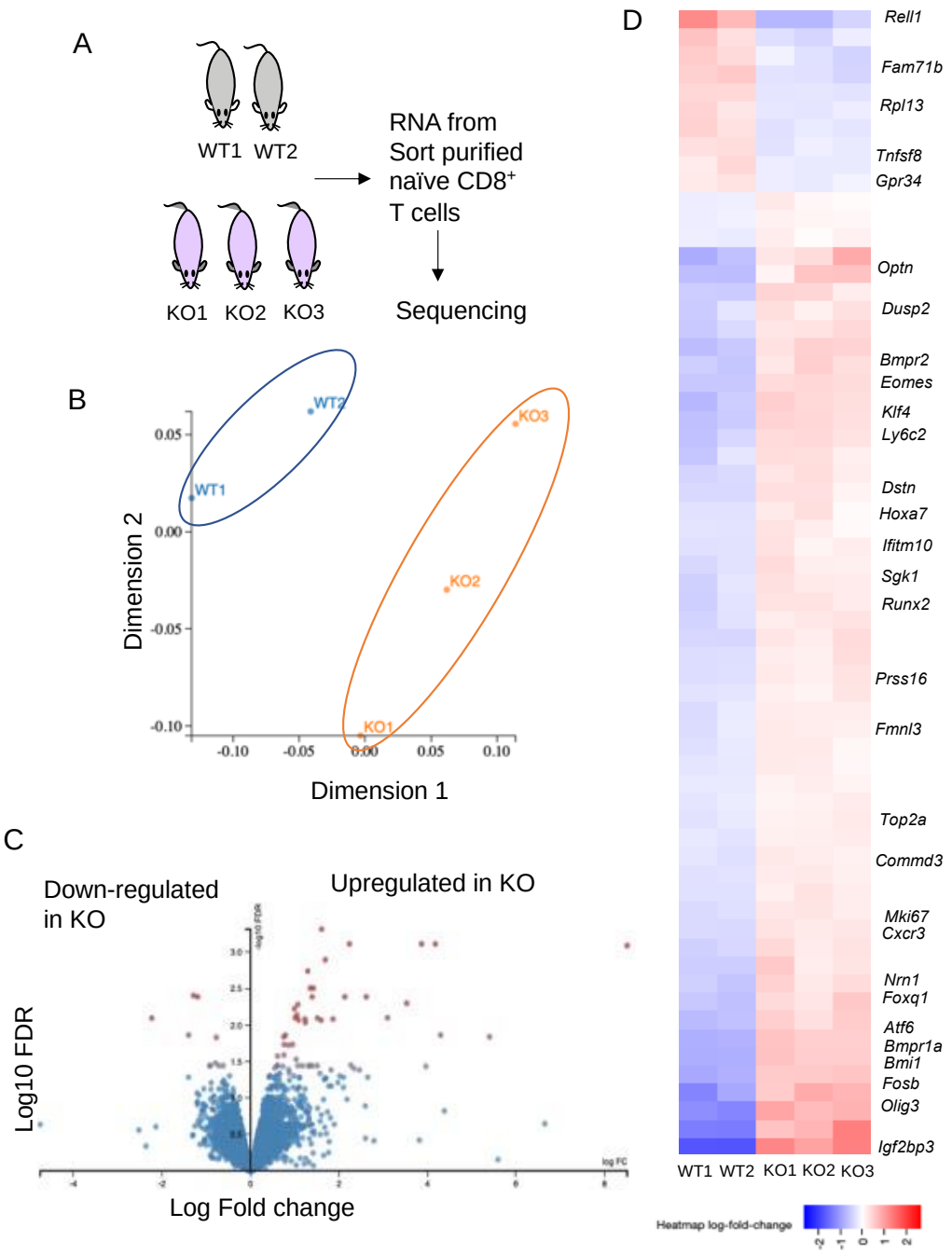

Figure 5.3 BMI-1 represses a small group of genes within naïve CD8⁺ T cells: A) RNA seq analysis was performed was performed on naïve CD8⁺ T cells (CD44 ^{lo}, CD62L ^{hi}, CD8⁺) sorted from 2 WT and 3 *Bmi1*$^{fl/fl}$*Lck*^{Cre} mice (females). B) Multidimension scaling analysis shown for all the replicates. C-D) Volcano plot showing the differentially expressed genes (DEGs). The number of DEGs was determined by comparing the fold difference (>log fold change 1.5X, FDR 0.05) of gene transcripts between WT and KO.

Table 5.1 List of differentially expressed genes between WT and *Bmi1$^{fl/fl}$Lck^{Cre}* mice

Upregulated						Downregulated
Igf2bp3	*Yes1*	*Runx2*	*Gm15459*	*E030030I06Rik*	*F2r*	*Tnfsf8*
Igkv10-96	*Hoxa7*	*Plag1*	*Klf4*	*Rps15a-ps4*	*RP23-477O15.1*	*Rpl13*
Nrn1	*Zfp608*	*Iigp1*	*Igf1r*	*Pisd-ps1*	*Dusp2*	*Rpl3-ps2*
Olig3	*Atf6*	*Pik3r3*	*Mki67*	*Dstn*	*Top2a*	*Gm10073*
Optn	*Cxcr3*	*Arhgef12*	*Ifitm10*	*Ern1*	*H2-Oa*	*Gm11539*
Bmpr1a	*Foxq1*	*Rps2-ps6*	*Gm3362*	*Pmaip1*	*Fmnl3*	*Gpr34*
Prss16	*Casp1*	*Eomes*	*Ly6c2*	*Sfmbt2*	*Commd3*	*Gm5045*
Gm11942	*Bmpr2*	*Pisd-ps2*	*Gm10257*	*Sgk1*	*H2-Q6*	*Fam71b*
Fosb	*Bmi1*	*Cyfip1*	*Eng*	*Gm9320*		*Grm6*
						Rell1

5.2.4 BMI-1 represses genes driving effector differentiation and proliferation.

To further understand the altered transcriptional profile of BMI-1 deficient naïve CD8$^+$ T cells, we performed Gene Ontology (GO) analysis using Metascape (Zhou et al., 2019) and g:Profiler (Raudvere et al., 2019). Enrichment analysis was only performed using genes that were upregulated as there were insufficient downregulated genes to enable robust statistical analyses. According to the metascape analysis, genes that were upregulated were mainly enriched for signalling pathways regulating the pluripotency of stem cells (BMPR1A, BMPR2, BMI1, PIK3R3, KLF4, IGF1R), consistent with a role for BMI-1 in regulating the stemness of naïve T cells (Figure 5.4A). Furthermore, other ontologies that were enriched included *cellular support processes*, *growth factor stimulus* and *regulation of growth*, and *regulation of apoptosis*. When the same analysis was performed using g:Profiler, similar GO terms were observed (Listed in Table 5.2), along with pathways involving regulation of RNA polymerase II activity, and notably, Bone Morphogenic Protein (BMP) pathways, (e.g. *BMP binding*, *BMP receptor activity*) the latter of which have been implicated in regulation of such

processes as cellular differentiation and lineage commitment in various tissues and cell types.

Further, by inspecting the list of DEGs, we found that several genes associated with $CD8^+$ T cell proliferation were upregulated in mutant naïve $CD8^+$ T cells (Figure 5.4 B), consistent with our previous observation that BMI-1 deficient cells are hyperproliferative (Chapter 4 Section 4.2.3). These included Mki67 (encoding Ki-67) (Gerdes et al., 1983, Soares et al., 2010) (upregulated ~2 fold), and the AP-1 family transcription factor *fosb* (encoding FosB; up ~3 fold). Finally, consistent with our data suggesting that *Prdm1, Tbx21, Irf4* and *Eomes* are direct targets of BMI-1/cPRC1 repression in naïve T cells, the expression of each was increased (at least 1.5-fold) in BMI-1 lacking naïve $CD8^+$ T cells (Figure 5.4C-D), while expression of *Tcf7, Lef1* and *Satb*1 was unchanged (Figure 5.4E). Taken together, these data support the idea that BMI-1 selectively targets and represses TFs that drive proliferation and effector differentiation.

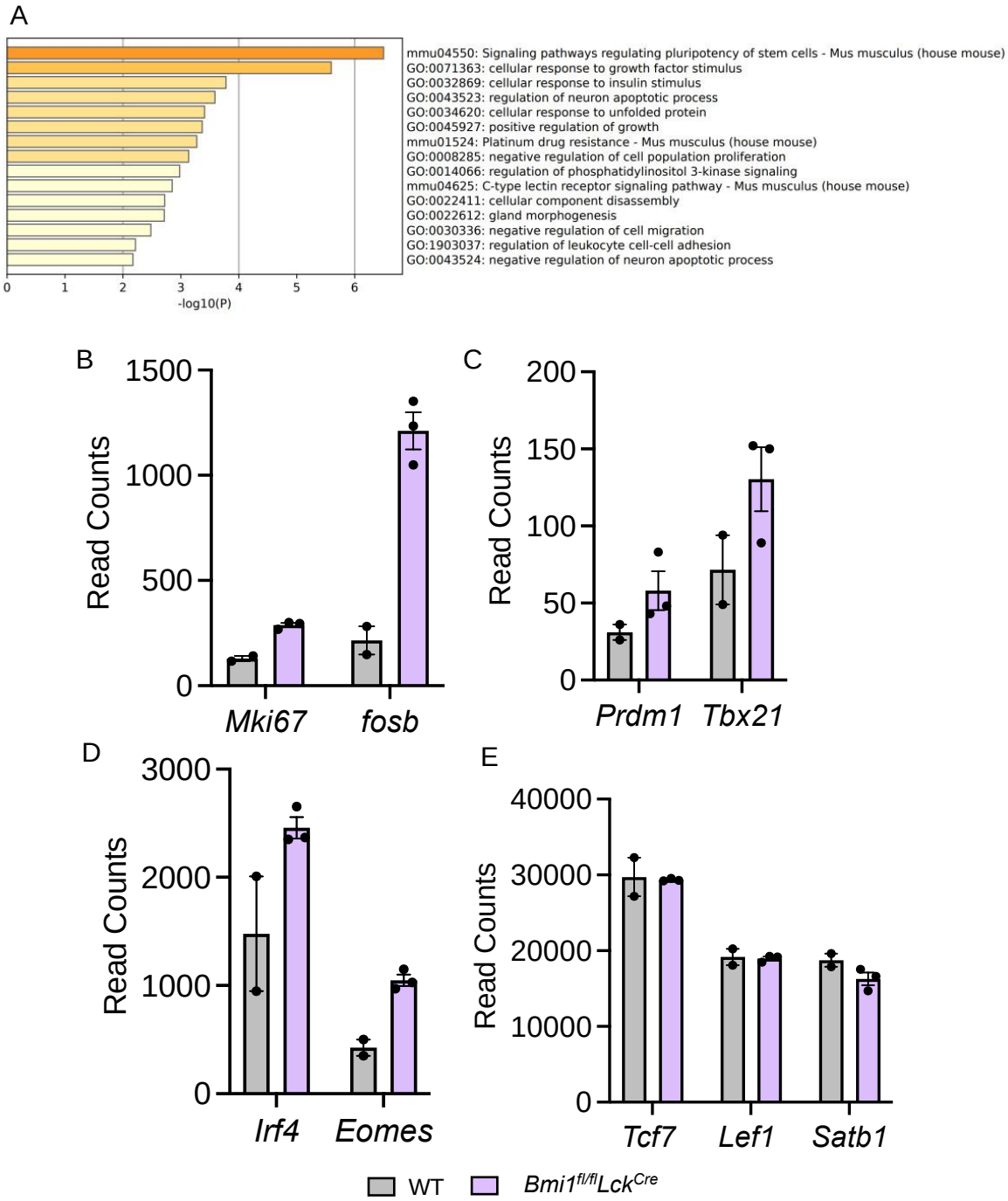

Figure 5.4 BMI-1 represses gene driving proliferation and effector differentiation: A) Gene ontology analysis performed using Metascape analysis showing enriched ontology clusters in upregulated genes in BMI-1 deficient naïve CD8$^+$ T cells. Normalised read counts for various transcription factors in naïve CD8$^+$ T cells from N=2 WT and 3 *Bmi1$^{fl/fl}$Lck^{Cre}* mice, Error bars show ± standard error of mean)

Table 5.2 List of Gene ontology terms obtained from g:Profiler

GO term: Biological Process (Top 10)
anatomical structure morphogenesis
regulation of cellular metabolic process
regulation of gene expression
positive regulation of transcription by RNA polymerase II
positive regulation of RNA metabolic process
positive regulation of cellular metabolic process
regulation of RNA metabolic process
regulation of transcription by RNA polymerase II
positive regulation of transcription, DNA-templated
positive regulation of nucleic acid-templated transcription

GO term: Molecular Functions
transforming growth factor beta-activated receptor activity
BMP binding
transmembrane receptor protein serine/threonine kinase activity
transmembrane receptor protein kinase activity
RNA polymerase II cis-regulatory region sequence-specific DNA binding
cis-regulatory region sequence-specific DNA binding
BMP receptor activity
Protein binding

GO Term: KEGG Pathway
Signalling pathways regulating pluripotency of stem cells

5.2.5 BMI-1 deficiency results in a global increase in chromatin accessibility within naïve and effector CTLs.

In sections 5.2.1 and 5.2.2, we established that, within naïve $CD8^+$ T cells, BMI-1 is crucial for the establishment of transcriptionally repressive chromatin structures at loci encoding TFs that drive effector differentiation. Indeed, BMI-1 deletion largely resulted in aberrant upregulation of gene expression (Figure 5.3),

suggesting that BMI-1 functions to install repressive chromatin structures more generally. Given the profound functional impact of BMI1 deficiency on $CD8^+$ T cell function, the relatively small number of transcriptional differences between naïve WT and BMI1 KO $CD8^+$ T cells was surprising. One explanation might be that the PRC1 plays a more prominent role in regulating chromatin structures, perhaps impacting transcriptional activation upon stimulation. To test this, we measured global chromatin accessibility by performing ATAC-Seq on sort-purified naïve (CD8a+ CD44lo) and tetramer positive (pooled D^bNP_{366} and D^bPA_{224}) effector CTLs isolated from the spleens of mice 10 days post-infection with the A/HKx31 influenza virus (Figure 5.5 A-B).

As an initial assessment of the data, a Multidimensional scaling analysis (MDS) was performed which demonstrated that samples clustered by genotype and differentiation state, with biological replicates clustering most closely to one another. However, naïve and effector CTLs were separated by dimension 1, regardless of genotype, indicating that the largest difference between the samples resulted from differentiation, while samples were separated based on genotype by dimension 2 (Figure 5.5C). We identified 463 differentially accessible regions (DARs) (with an adjusted p value < 0.05) between WT and BMI-1 deficient naïve $CD8^+$ T cells, with 365 regions having increased accessibility in the KO, consistent with the RNA-Seq data indicating that most changes in gene expression with BMI-1 deletion resulted from upregulation (Figure 5.5D). Furthermore, there were 1647 DARs between WT and BMI-1 deficient effector CTLs, with 1078 DARs having increased accessibility in the KO, and 569 DARs being less accessible in the KO (Figure 5.5D). Thus, deletion of BMI-1 results in an overall increase in chromatin accessibility in naïve and effector $CD8^+$ T cells, consistent with the primary mechanism by which BMI-1 regulates gene expression being through instillation of repressive chromatin structures.

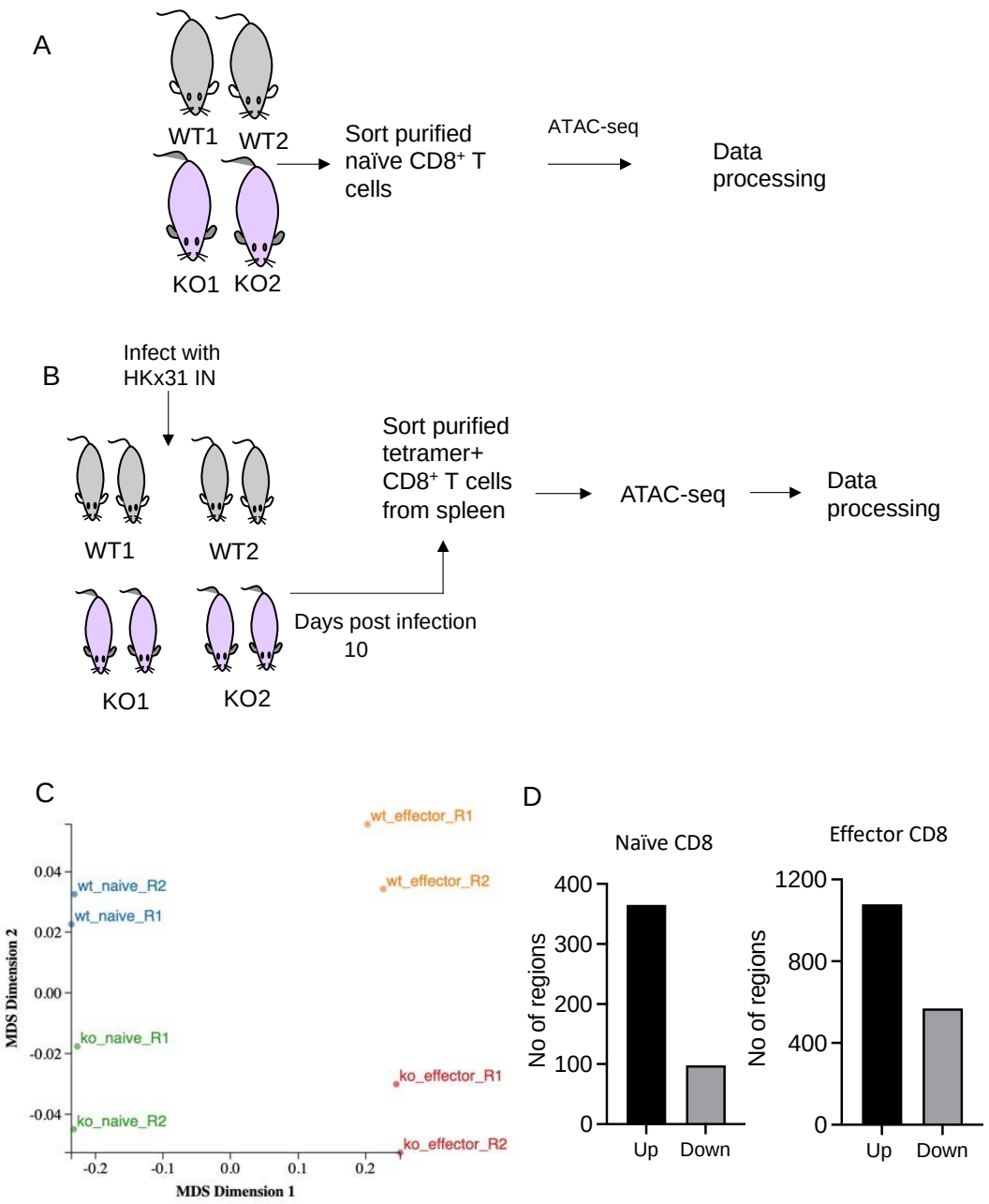

Figure 5.5 BMI-1 deletion increases the global chromatin accessibility: A) ATAC seq was performed on Sort purified naïve CD8⁺ T cells (CD44 ^{lo}, CD62L ^{hi}, CD8⁺) from WT and *Bmi1*$^{fl/fl}$*Lck*^{Cre} mice (2 females from each genotype). B) tetramer positive (pooled D^{b}NP$_{366}$ and D^{b}PA$_{224}$) effector CTLs isolated from the spleens of mice (two mice each per replicate from both WT and *Bmi1*$^{fl/fl}$*Lck*^{Cre} mice) 10 days post-infection with the 10^4 PFU A/HKx31 influenza virus. C) Multidimensional scaling analysis of differentially accessible regions from naïve and effector CTLs. D) Number of differentially accessible regions between WT and BMI-1 deficient naïve and effector CTLs.

5.2.6 GSEA analysis demonstrates strong correlation between de novo chromatin accessibility and gene expression in naïve BMI-1 deficient CD8$^+$ T cells.

To determine whether changes in chromatin accessibility within naïve, BMI-1-deficient CD8$^+$ T cells may be related to the changes in mRNA expression observed in the same cells, Gene Set Enrichment Analysis (GSEA) was performed (Subramanian et al., 2005, Mootha et al., 2003). Analysis was performed using RNA-Seq and ATAC-Seq data from WT and *Bmi1*$^{fl/fl}$*Lck*^{Cre} naïve CD8$^+$ T cells, after assigning ATAC-Seq peaks to the nearest genes using GREAT(Tanigawa et al., 2022, McLean et al., 2010). We observed a significantly positive correlation between the gene expression and open peaks from ATAC-Seq data (Figure 5.7), suggesting that within WT cells, BMI-1 directly targets genes transcriptionally upregulated in the BMI-1 KO to repress them, and repression is by the formation of inaccessible chromatin.

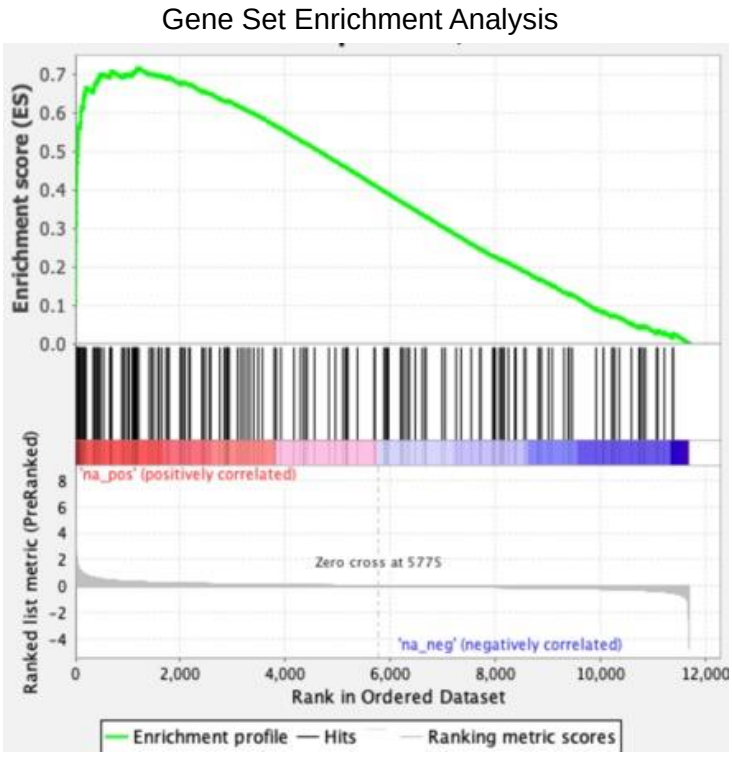

Figure 5.6: **GSEA analysis of open peaks showing the correlation with increased gene expression.**

5.2.7 Differentially accessible regions regulate T cell activation and differentiation.

To better understand the functionality of DARs identified above, gene ontology and functional predictions were performed using Genomic Regions Enrichment of Annotation Tool (GREAT)(Tanigawa et al., 2022, McLean et al., 2010) which is specifically designed for annotation of *cis* regulatory elements.

While there were insufficient regions with reduced accessibility in BMI-1 deficient naïve $CD8^+$ T cells for analyses to be performed, regions showing increased accessibility in the mutant were strongly associated with terms such as positive regulation of T cell activation and regulation of T cell differentiation, consistent with BMI-1 repressing T cell activation and differentiation (Figure 5.7A). Terms relating to chemokine signalling were also enriched, and the most enriched term was *O-glycan processing*, which covers processes that regulate T cell activation and metabolism (recently reviewed in (Pereira et al., 2018)) .

When the same analysis was performed for effector DARs, there was no obvious differences in the types of biological processes enriched in regions that became more and less accessible with deletion of BMI-1 (Figure 5.7B-C). For instance, both described general cellular processes such as *leucocyte cell adhesion*, *leukocyte activation,* and *leukocyte proliferation*, and many of the processes described involved activation, such as *positive regulation of leukocyte activation*. One notable exception to the overlap in terms between regions that became opened and closed in effector CTLs in the absence of BMI-1 was a number of terms relating to proliferation, that were present in the “closed” dataset, but not the “open” dataset (e.g., *regulation of lymphocyte proliferation*). Taken together, these results suggest that BMI-1 regulates a broad set of processes within naïve and effector $CD8^+$ T cells.

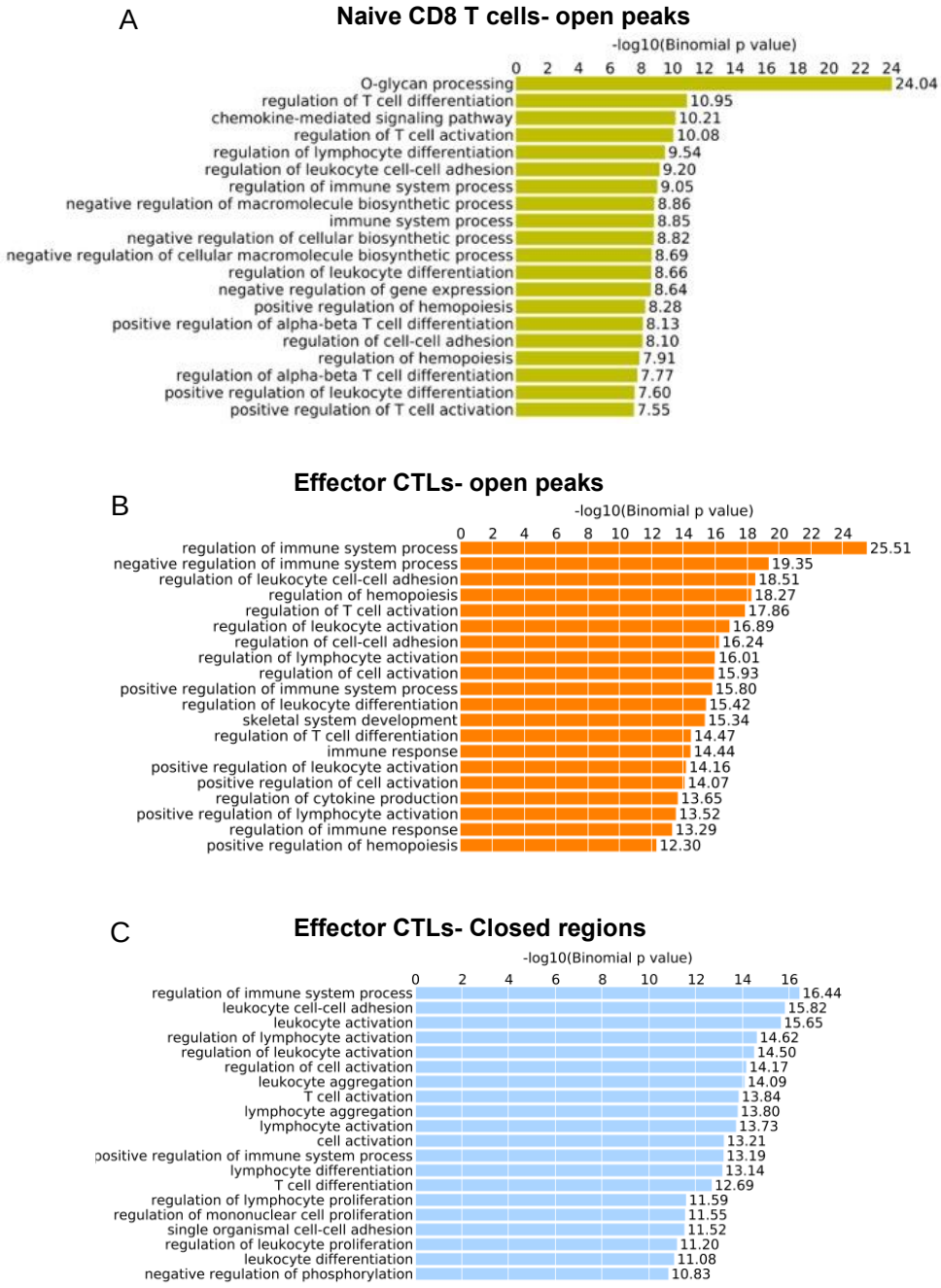

Figure 5.7. Functional interpretation of DARs showed the enrichment of T cell differentiation pathways: A) GREAT analysis of DARS predicting the top 20 Gene ontology biological processes of the open peaks from naïve $CD8^+$ T cells, B) open peaks from effector CTLs and C) closed regions from effector CTLs.

5.2.8 BMI-1 targets genomic regions bound by transcription factors that drive CD8$^+$ T cell differentiation.

To further understand how BMI-1 regulates CD8$^+$ T cell differentiation, we sought to determine which TFs bind the DARs identified by ATAC-Seq. To do this, we used the Cistrome toolkit (Zheng et al., 2019) which performs TF enrichment based on a large set of curated TF ChIP-Seq datasets to find the factors that have significant overlap with input regions. As the Cistrome Toolkit uses datasets from a large number of cell types and lines, we filtered results such that only datasets derived from lymphocytes were included. Using this approach, identified on DARs that became accessible within naïve cells on BMI-1 deletion, the histone acetyltransferase EP300, binding of which characterises active transcriptional enhancers and gene promoters (Ogryzko et al., 1996) was strongly enriched, consistent with BMI-1 having a repressive function (Figure 5.8A). Furthermore, transcription factors crucial for effector differentiation, including TBX21, IRF4 and BATF were also found to bind to the same regions, again, consistent BMI-1 restraining effector differentiation by repressing the activity of genes that drive T cell differentiation.

When the same analysis was applied to regions that became open in effector CTLs following BMI-1 deletion, EP300 was again enriched, as were TFs that drive effector differentiation, consistent with the naïve data described above. These included RUNX3, TBX21, IRF4, and AP-1 family transcription factors including JUND, JUNB, FOSL2, and BATF (Figure 5.8B Upper panel). However, in contrast to regions of opening with BMI-1 deletion, DARs that are less accessible in effector CTLs were found to be bound by TFs known to maintain naïve and memory CD8$^+$ T cell stemness including TCF7, FOXO1, and SATB1 (Figure 5.8B lower panel).

Collectively, these data suggest that BMI-1 functions to inhibit binding of transcription that drive effector CTL differentiation while promoting binding of factors that maintain stemness.

A

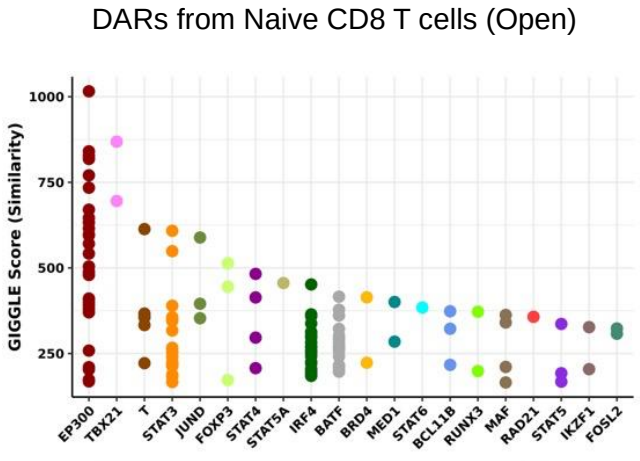

B

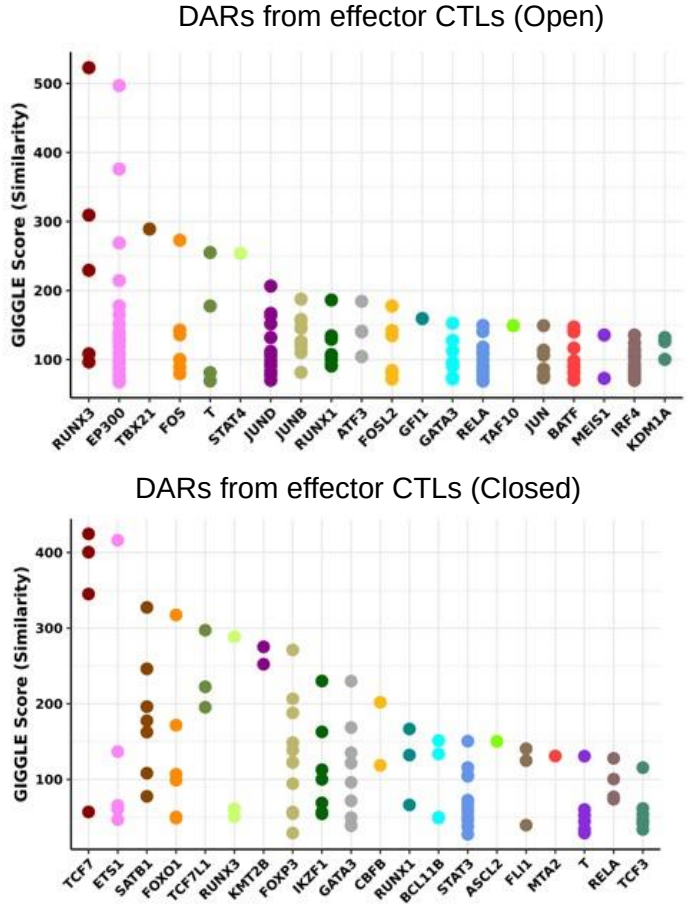

Figure 5.8 Increased chromatin accessibility correlates with increase in gene expression: A) Cistrome toolkit analysis of open peaks demonstrating the possible transcription factors binding to the genomic regions open region from naïve $CD8^+$ T cells. B) Cistrome toolkit analysis of open regions (upper panel) and closed regions (lower panel).

5.3 Discussion

In previous chapters, we determined that BMI-1 is an important regulator of $CD8^+$ T cell differentiation in response to viral infection; we showed that in the absence of BMI-1, acute viral infection resulted in increased primary virus-specific T cell responses, with greatly reduced T cell memory formation, and memory T cells baring the hallmarks of exhaustion. In this chapter, we aimed to understand the molecular basis for these observations. We found that within naïve T cells, BMI-1 targets key drivers of effector T cell differentiation (TBET, BLIMP1, EOMES) for transcriptional repression, with repression correlating with ubiquitination of H2AK119, and decreased chromatin accessibility.

While we observed slightly reduced expression of stemness related genes within naïve, BMI-1 deficient T cells (Figure 5.2 A-C), this appeared to be related to increased expression of effector program genes (e.g., indirect), as expression levels did not correlate with changes in H2AK119ub levels or chromatin accessibility. Thus, BMI-1 directly targets effector genes for repression, with T cell activation resulting in repression of stemness associated genes via means that are apparently independent of BMI-1/cPRC1, suggesting that distinct transcriptional networks are repressed via distinct means during $CD8^+$ T cell differentiation. Indeed, Gray *et al*. have demonstrated that stemness genes are targeted by EZH2 containing PRC2 following acute LCMV infection, resulting in deposition of H3K27me3 at gene loci encoding stemness factors including *Tcf7* and *Foxo1*, and enabling instillation of the effector gene program (Gray et al., 2017). Thus, it appears that following $CD8^+$ T cell activation, PRC1 and PRC2 act independently of one another to repress gene expression, at least at some gene loci, and a mechanistic understanding of this divergence of function remains to be determined. Furthermore, it should also be noted that PRC-independent mechanisms are also required to repress gene transcription following $CD8^+$ T cell activation. For instance, TCF7 is repressed by CpG methylation following T cell activation (Ladle et al., 2016). Moreover, Pace *et al*. found that following Listeria infection, SUV39H1 dependent deposition of H3K9me3 was required to shut-down the stemness program more broadly within effector CTLs, with SUV39H1

deficient CTLs failing to repress genes such as *Satb1, Tcf7 and Il7r*, and ultimately results in sustained survival and increased long-term memory reprogramming capacity (Pace et al., 2018).

Interestingly, deletion of BMI1 from naïve T cells perturbed transcription of only a small number of genes, with most increasing in expression, as expected for deletion of a repressor. This relatively minor effect suggests that genes derepressed by BMI1 deletion are largely targeted by TFs that are induced by TCR engagement and cytokine signals, and indeed, our ATAC-Seq analysis showed that genomic regions which become accessible in BMI-1 deficient naïve T cells are targets of TFs including IRF4 and TBET, which are induced by TCR stimulation, as well as STAT3, STAT4 and STAT6, which are induced/activated by cytokine signals (Morris et al., 2018). Further, consistent with the targets of BMI-1 requiring induction, while there was a small number of genes dysregulated by BMI-1 deletion in naïve T cells, a considerably greater number of regions changed in chromatin accessibility in the same cells, with most becoming open. It is also important to consider that BMI-1 expression is increased after T cell activation, and therefore, performing RNA-Seq after activation of $CD8^+$ T cells may reveal further information about the regulatory networks controlled by BMI-1. Indeed, it appears likely that following T cell activation, BMI-1 targets a broader range of genes based on the increased number of DARs in the effector ATAC-Seq data relative to naïve (Figure 5.5D), and the different array of TFs that bind the DARs (Comparing BMI-1 specific Open regions in naïve and effector; Figure 5.7A and C).

Beyond repressing the effector gene program in naïve T cells, our GO analysis indicated a broad array of functions for BMI-1 including in regulating functions such as metabolic pathways, and responses to growth stimulus and insulin stimulus, which may also regulate the outcomes of T cell differentiation, and thus explain the perturbed differentiation phenotype we observed following infection of BMI-1 deficient mice. Insulin receptor mediated stimulation, for instance, has important roles in providing protective immunity against Influenza by regulating T

cell proliferation and cytokine production and by modulating the cellular metabolism (Tsai et al., 2018).

When considering the results described here, it is important to factor that the analyses were performed on bulk cell populations, and therefore, do not account for the consequence of cellular heterogeneity during $CD8^+$ T cell responses to infection. Indeed, we observed in Chapter 3 that the degree of BMI-1 upregulation following TCR stimulation is dependent on TCR strength, suggesting that within an infection context, different individual T cells will express different levels of BMI-1 following infection. This, in-turn, would result in a spectrum of expression profiles, whereby BMI-1high cells continue to repress the effector transcriptional program and give rise to memory, while BMI-1low cells would give rise to terminal effector. Indeed, this model is consistent with our finding that BMI-1 deletion results in increased effector expansion, and reduced memory formation, and may suggest that the T cell exhaustion characteristics of memory T cells that do form result from unrestrained differentiation in the absence of BMI-1. To test this model, future experiments could combine single-cell ATAC-Seq and RNA-Seq with fate-mapping experiments that make use of *Bmi1* reporter mice.

Performing H2AK119ub and BMI-1 ChIP-seq and integrating the data with available ChIP-seq data for H3K27me3, H3K27ac, H3K4me3 will provide a comprehensive analysis of how cPRC1 and BMI-1 functions integrates with changes in histone PTMs and chromatin accessibility.

CHAPTER 6

General Discussion

This thesis demonstrates an important role for BMI-1 and the canonical PRC1 in maintaining $CD8^+$ T cell naïvety, with deletion of BMI-1 within naïve T cells resulting in loss of homeostasis and increasing the reactivity of naïve cells to antigen. These data add to an emerging literature which describes T cell naïvety as an actively maintained state, rather than a state which persists only because of the absence of signals driving differentiation. For instance, recent papers have described that the loss of the transcription factor BACH2, or the chromatin organising protein SATB1 from naïve T cells results in expression of genes characteristic of differentiated T cells (Roychoudhuri et al., 2016, Nussing et al., 2022). Moreover, loss of the transcription factors TCF1 and LEF1 results in the loss of T cell lineage fidelity, as well as naïvety (Shan et al., 2021). Taken together, these studies suggest that proteins such as BMI-1/cPRC1 can actively restrain a partially autonomous differentiation process, and this thesis provides further mechanistic insight by demonstrating that it is through direct repression of transcription factors that drive the effector gene program that naïvety is maintained. Furthermore, these data demonstrate a link between the naïve chromatin architecture and naïve T cell activation thresholds, with both BMI-1 and CBX7 expression being exquisitely sensitive to TCR signal strength, and BMI-1 deficient naïve T cells have a reduced threshold for activation.

These observations raise the question of why it is necessary to actively restrain T cell activation and differentiation? Such restraint is necessary to prevent autoimmunity resulting from T cell activation in response to weak MHC-self peptide interactions, but likely also to prevent depletion of the breadth of the naïve T cell repertoire and as such, the ability to respond to new infections. However, the observation that perturbation of cPRC1 silencing resulted in aberrant memory formation suggests that restraint may also be required to enable the formation of functional memory. One interpretation of this observation is that loss of the gene expression pattern enforced by BMI-1 within naïve T cells extinguishes a window of opportunity for differentiation towards a memory T cell fate following antigen

encounter. Indeed, this interpretation is consistent with recent findings which suggest that differentiation trajectories toward effector or memory fates are determined very early after T cell activation (Kakaradov et al., 2017). Thus, it may be that effector differentiation is the default trajectory, and that BMI-1 deficient, “naïve” T cells have already differentiated beyond the effector/memory decision point. Furthermore, genes that enforce T cell naïvety overlap with those required for memory formation and homeostasis (Bennett et al., 2020). Therefore, it may be that in the absence of BMI-1 and cPRC1 silencing, genes such as TCF1 cannot be re-expressed to enable formation and maintenance of a memory 1. In either case, it is clear that BMI-1/cPRC1 is an essential regulator of the effector/memory fate decision.

A recent study showed that the epigenomes of NK cells and effector and memory T cells are similarly organised (Lau et al., 2018). Thus, it is interesting to consider that the restraints on naïve T cell activation described in this thesis may underscore some of the major differences between adaptive T lymphocytes and innate lymphocytes, including immediate versus delayed effector function, and the presence and absence of immunological memory. Further, the coincidence of evolution of adaptive clonal receptors and the naïvety argues that the existence of such restraints may have been necessary for the evolution of adaptive immunity.

A particularly intriguing finding of the work presented in this thesis was that in the absence of BMI-1, T cells baring the hallmarks of exhaustion (reduced effector function, reduced secondary expansion, and expression of inhibitory receptors) formed in response to an acute viral infection. This was surprising given that exhaustion is typically associated with instances of antigen persistence, such as following chronic viral infections and cancers, and indeed, antigen persistence is often considered a requisite driver of T cell exhaustion (Blank et al., 2019). Recent studies have identified a population of stem-like, progenitor exhausted T cells (T_{PEX}) following LCMV infection (Utzschneider et al., 2020, Utzschneider et al., 2016). T_{PEX} are maintained long-term, and continuously seed terminally

differentiated, functionally exhausted T cells. These progenitor cells are characterised by high expression of TCF1, which is rapidly and stably repressed following T cell activation in the absence of BMI-1. Therefore, it may be that the reason that T cell exhaustion is observed in the absence of BMI-1 in an acute infection setting is that cells which would become T_{PEX} with intact cPRC1 repression, terminally differentiate in the absence of BMI-1/cPRC1. Given the potential therapeutic significance that insights into mechanisms governing the formation of T cell exhaustion may have, a pressing future direction for this work will be to infect BMI-1 deficient mice with LCMV to determine whether the formation and maintenance of T_{PEX} is BMI-1/cPRC1 dependent. Furthermore, if T cell exhaustion occurs following influenza infection because BMI-1 cannot restrain the further differentiation of T_{PEX}, that implies that the differentiation of T_{PEX} is not solely a characteristic of chronic infection, and thus it would be predicted that T_{PEX} can be identified after influenza infection of WT mice. Aside from virus infection models of T cell exhaustion, a further, pressing future direction for this work is analysis of the consequences of BMI-1 deficiency in cancer settings. This is of particular interest, not only because of the relevance of T cell exhaustion to cancer progression and therapy, but also because of the exaggerated effector response and reduced activation threshold of BMI-1 deficient T cells, which suggests that they may provide more potent anti-tumor responses. Indeed, the reduced activation threshold is of particular relevance as $CD8^+$ T cell cancer epitopes are typically recognised via very low affinity interactions (Hoffmann and Slansky, 2020).

While we observed co-deposition of cPRC1 and PRC2 at genes encoding transcription factors driving the effector gene program within naïve T cells, following activation, PRC2 was retargeted to stemness genes, in the absence of cPRC1 (as determined by lack of H2AUb119 deposition). These data suggest that the two repressive complexes do not always act in concert and may have divergent activities dependent on T cell differentiation state or activation status. Indeed, cPRC1 has been shown to function independently of PRC2 in some contexts (Sawai et al., 2022). Thus, a thorough understanding of the mechanisms

and targets of polycomb mediated gene repression during T cell differentiation requires genome-wide characterisation of H2AUb119 deposition patterns throughout the phases of the T cell response to infection using a technique such as Cut&Run or ChIP-Seq. These data could then be combined with paired H3K27me3 datasets to better understand the consequences of cPRC1/PRC2 collaboration during T cell differentiation. Moreover, understanding of the composition of cPRC1, and its recruitment to target sites will be important in understanding how cPRC1 choreographs T cell differentiation, and this could be addressed through deletion of cPRC1 components and TFs that bind motifs of genomic regions found to become accessible within naïve and effector T cells upon deletion BMI-1.

Finally, the data in this thesis has provided new insights into how cPRC1 acts on the epigenome of $CD8^+$ T cells to regulate differentiation in response to infection. The targeting of epigenetic mechanisms can be used to develop new therapeutic strategies for treating immune-related diseases. For example, drugs that inhibit the methylation of specific genes in T cells have been developed to enhance T cell responses in cancer immunotherapy. Similarly, drugs that modify histone modification patterns in T cells can be used to boost T cell activation in autoimmune disorders. Additionally, the use of epigenetic editing techniques, such as CRISPR, to precisely modify the epigenome of T cells is being explored as a potential treatment for a variety of diseases, including cancer and autoimmune disorders. Overall, the study of cPRC1 in $CD8^+$ T cells has opened up new avenues for the development of therapies that can specifically target this mechanism of immune regulation to modulate the immune system function and improve the efficacy of immunotherapies. For instance, one way that this might be done is by engineering CAR T cells to stably express BMI1, since this study has shown that BMI1 is required to maintain stemness programs in naïve T cells, and that without BMI1, memory T cells become dysfunctional. As such, it may be that as has been shown recently for FOXO1 – a TF that is also required to maintain naivety (Ouyang et al., 2009), and to maintain functional memory (Delpoux et al., 2018) – that forced expression of BMI1 in CAR T cells would

direct their differentiation towards a stable memory fate. Indeed, this is the case with FOXO1 expressing CAR T cells, with the outcome being improved clinical outcomes (Shan et al., 2022, Chan et al., 2024).

Bibliography

AGGER, K., CLOOS, P. A., CHRISTENSEN, J., PASINI, D., ROSE, S., RAPPSILBER, J., ISSAEVA, I., CANAANI, E., SALCINI, A. E. & HELIN, K. 2007. UTX and JMJD3 are histone H3K27 demethylases involved in HOX gene regulation and development. *Nature,* 449**,** 731-4.

AKKAYA, M., KWAK, K. & PIERCE, S. K. 2020. B cell memory: building two walls of protection against pathogens. *Nat Rev Immunol,* 20**,** 229-238.

ALLEN, J. E. & MAIZELS, R. M. 2011. Diversity and dialogue in immunity to helminths. *Nat Rev Immunol,* 11**,** 375-88.

ALOIA, L., DI STEFANO, B. & DI CROCE, L. 2013. Polycomb complexes in stem cells and embryonic development. *Development,* 140**,** 2525-34.

ARAKI, Y., FANN, M., WERSTO, R. & WENG, N. P. 2008. Histone acetylation facilitates rapid and robust memory CD8 T cell response through differential expression of effector molecules (eomesodermin and its targets: perforin and granzyme B). *J Immunol,* 180**,** 8102-8.

ARAKI, Y., WANG, Z., ZANG, C., WOOD, W. H., 3RD, SCHONES, D., CUI, K., ROH, T. Y., LHOTSKY, B., WERSTO, R. P., PENG, W., BECKER, K. G., ZHAO, K. & WENG, N. P. 2009. Genome-wide analysis of histone methylation reveals chromatin state-based regulation of gene transcription and function of memory CD8+ T cells. *Immunity,* 30**,** 912-25.

ARANDA, S., MAS, G. & DI CROCE, L. 2015. Regulation of gene transcription by Polycomb proteins. *Sci Adv,* 1**,** e1500737.

BANERJEE, A., GORDON, S. M., INTLEKOFER, A. M., PALEY, M. A., MOONEY, E. C., LINDSTEN, T., WHERRY, E. J. & REINER, S. L. 2010. Cutting edge: The transcription factor eomesodermin enables CD8+ T cells to compete for the memory cell niche. *J Immunol,* 185**,** 4988-92.

BANNISTER, A. J. & KOUZARIDES, T. 2011. Regulation of chromatin by histone modifications. *Cell Res,* 21**,** 381-95.

BARBER, D. L., WHERRY, E. J., MASOPUST, D., ZHU, B., ALLISON, J. P., SHARPE, A. H., FREEMAN, G. J. & AHMED, R. 2006. Restoring function in exhausted CD8 T cells during chronic viral infection. *Nature,* 439**,** 682-7.

BEGUELIN, W., POPOVIC, R., TEATER, M., JIANG, Y., BUNTING, K. L., ROSEN, M., SHEN, H., YANG, S. N., WANG, L., EZPONDA, T., MARTINEZ-GARCIA, E., ZHANG, H., ZHENG, Y., VERMA, S. K., MCCABE, M. T., OTT, H. M., VAN ALLER, G. S., KRUGER, R. G., LIU, Y., MCHUGH, C. F., SCOTT, D. W., CHUNG, Y. R., KELLEHER, N., SHAKNOVICH, R., CREASY, C. L., GASCOYNE, R. D., WONG, K. K., CERCHIETTI, L., LEVINE, R. L., ABDEL-WAHAB, O., LICHT, J. D., ELEMENTO, O. & MELNICK, A. M. 2013. EZH2 is required for germinal center formation and somatic EZH2 mutations promote lymphoid transformation. *Cancer Cell,* 23**,** 677-92.

BENNETT, T. J., UDUPA, V. A. V. & TURNER, S. J. 2020. Running to Stand Still: Naive CD8(+) T Cells Actively Maintain a Program of Quiescence. *Int J Mol Sci,* 21.

BERNDSEN, C. E. & DENU, J. M. 2008. Catalysis and substrate selection by histone/protein lysine acetyltransferases. *Curr Opin Struct Biol,* 18**,** 682-9.

BERNSTEIN, B. E., KAMAL, M., LINDBLAD-TOH, K., BEKIRANOV, S., BAILEY, D. K., HUEBERT, D. J., MCMAHON, S., KARLSSON, E. K., KULBOKAS, E. J., 3RD, GINGERAS, T. R., SCHREIBER, S. L. & LANDER, E. S. 2005. Genomic maps and comparative analysis of histone modifications in human and mouse. *Cell,* 120**,** 169-81.

BERNSTEIN, B. E., MIKKELSEN, T. S., XIE, X., KAMAL, M., HUEBERT, D. J., CUFF, J., FRY, B., MEISSNER, A., WERNIG, M., PLATH, K., JAENISCH, R., WAGSCHAL, A., FEIL, R., SCHREIBER, S. L. & LANDER, E. S. 2006a. A bivalent chromatin structure marks key developmental genes in embryonic stem cells. *Cell,* 125**,** 315-26.

BERNSTEIN, E., DUNCAN, E. M., MASUI, O., GIL, J., HEARD, E. & ALLIS, C. D. 2006b. Mouse polycomb proteins bind differentially to methylated histone H3 and RNA and are enriched in facultative heterochromatin. *Mol Cell Biol,* 26**,** 2560-9.

BLACKBURN, S. D., SHIN, H., HAINING, W. N., ZOU, T., WORKMAN, C. J., POLLEY, A., BETTS, M. R., FREEMAN, G. J., VIGNALI, D. A. & WHERRY, E. J. 2009. Coregulation of CD8+ T cell exhaustion by multiple inhibitory receptors during chronic viral infection. *Nat Immunol,* 10**,** 29-37.

BLACKLEDGE, N. P. & KLOSE, R. J. 2021. The molecular principles of gene regulation by Polycomb repressive complexes. *Nat Rev Mol Cell Biol,* 22**,** 815-833.

BLACKLEDGE, N. P., ROSE, N. R. & KLOSE, R. J. 2015. Targeting Polycomb systems to regulate gene expression: modifications to a complex story. *Nat Rev Mol Cell Biol,* 16**,** 643-649.

BLANK, C. U., HAINING, W. N., HELD, W., HOGAN, P. G., KALLIES, A., LUGLI, E., LYNN, R. C., PHILIP, M., RAO, A., RESTIFO, N. P., SCHIETINGER, A., SCHUMACHER, T. N., SCHWARTZBERG, P. L., SHARPE, A. H., SPEISER, D. E., WHERRY, E. J., YOUNGBLOOD, B. A. & ZEHN, D. 2019. Defining 'T cell exhaustion'. *Nat Rev Immunol,* 19**,** 665-674.

BOISE, L. H., MINN, A. J., NOEL, P. J., JUNE, C. H., ACCAVITTI, M. A., LINDSTEN, T. & THOMPSON, C. B. 1995. CD28 costimulation can promote T cell survival by enhancing the expression of Bcl-XL. *Immunity,* 3**,** 87-98.

BUENROSTRO, J. D., WU, B., CHANG, H. Y. & GREENLEAF, W. J. 2015. ATAC-seq: A Method for Assaying Chromatin Accessibility Genome-Wide. *Curr Protoc Mol Biol,* 109**,** 21 29 1-21 29 9.

CAGANOVA, M., CARRISI, C., VARANO, G., MAINOLDI, F., ZANARDI, F., GERMAIN, P. L., GEORGE, L., ALBERGHINI, F., FERRARINI, L., TALUKDER, A. K., PONZONI, M., TESTA, G., NOJIMA, T., DOGLIONI, C., KITAMURA, D., TOELLNER, K. M., SU, I. H. & CASOLA, S. 2013. Germinal center dysregulation by histone methyltransferase EZH2 promotes lymphomagenesis. *J Clin Invest,* 123**,** 5009-22.

CAI, S., LEE, C. C. & KOHWI-SHIGEMATSU, T. 2006. SATB1 packages densely looped, transcriptionally active chromatin for coordinated expression of cytokine genes. *Nat Genet,* 38**,** 1278-88.

CANTOR, D. J., KING, B., BLUMENBERG, L., DIMAURO, T., AIFANTIS, I., KORALOV, S. B., SKOK, J. A. & DAVID, G. 2019. Impaired Expression of Rearranged Immunoglobulin Genes and Premature p53 Activation Block B Cell Development in BMI1 Null Mice. *Cell Rep,* 26**,** 108-118 e4.

CAO, J. & YAN, Q. 2012. Histone ubiquitination and deubiquitination in transcription, DNA damage response, and cancer. *Front Oncol,* 2**,** 26.

CAO, R., TSUKADA, Y. & ZHANG, Y. 2005. Role of Bmi-1 and Ring1A in H2A ubiquitylation and Hox gene silencing. *Mol Cell,* 20**,** 845-54.

CAO, R., WANG, L., WANG, H., XIA, L., ERDJUMENT-BROMAGE, H., TEMPST, P., JONES, R. S. & ZHANG, Y. 2002. Role of histone H3 lysine 27 methylation in Polycomb-group silencing. *Science,* 298**,** 1039-43.

CARETTI, G., DI PADOVA, M., MICALES, B., LYONS, G. E. & SARTORELLI, V. 2004. The Polycomb Ezh2 methyltransferase regulates muscle gene expression and skeletal muscle differentiation. *Genes Dev,* 18**,** 2627-38.

CASTRO, F., CARDOSO, A. P., GONCALVES, R. M., SERRE, K. & OLIVEIRA, M. J. 2018. Interferon-Gamma at the Crossroads of Tumor Immune Surveillance or Evasion. *Front Immunol,* 9**,** 847.

CATON, A. J., BROWNLEE, G. G., YEWDELL, J. W. & GERHARD, W. 1982. The antigenic structure of the influenza virus A/PR/8/34 hemagglutinin (H1 subtype). *Cell,* 31**,** 417-27.

CHAN, H. L. & MOREY, L. 2019. Emerging Roles for Polycomb-Group Proteins in Stem Cells and Cancer. *Trends Biochem Sci,* 44**,** 688-700.

CHAN, J. D., SCHEFFLER, C. M., MUNOZ, I., SEK, K., LEE, J. N., HUANG, Y. K., YAP, K. M., SAW, N. Y. L., LI, J., CHEN, A. X. Y., CHAN, C. W., DERRICK, E. B., TODD, K. L., TONG, J., DUNBAR, P. A., LI, J., HOANG, T. X., DE MENEZES, M. N., PETLEY, E. V., KIM, J. S., NGUYEN, D., LEUNG, P. S. K., SO, J., DEGUIT, C., ZHU, J., HOUSE, I. G., KATS, L. M., SCOTT, A. M., SOLOMON, B. J., HARRISON, S. J., OLIARO, J., PARISH, I. A., QUINN, K. M., NEESON, P. J., SLANEY, C. Y., LAI, J., BEAVIS, P. A. & DARCY, P. K. 2024. FOXO1 enhances CAR T cell stemness, metabolic fitness and efficacy. *Nature,* 629**,** 201-210.

CHEUTIN, T. & CAVALLI, G. 2018. Loss of PRC1 induces higher-order opening of Hox loci independently of transcription during Drosophila embryogenesis. *Nat Commun,* 9**,** 3898.

COHEN, I., ZHAO, D., MENON, G., NAKAYAMA, M., KOSEKI, H., ZHENG, D. & EZHKOVA, E. 2019. PRC1 preserves epidermal tissue integrity independently of PRC2. *Genes Dev,* 33**,** 55-60.

CONWAY, E., ROSSI, F., FERNANDEZ-PEREZ, D., PONZO, E., FERRARI, K. J., ZANOTTI, M., MANGANARO, D., RODIGHIERO, S., TAMBURRI, S. & PASINI, D. 2021. BAP1 enhances Polycomb repression by counteracting widespread H2AK119ub1 deposition and chromatin condensation. *Mol Cell,* 81**,** 3526-3541 e8.

CORSE, E., GOTTSCHALK, R. A. & ALLISON, J. P. 2011. Strength of TCR-peptide/MHC interactions and in vivo T cell responses. *J Immunol,* 186**,** 5039-45.

CRUZ-GUILLOTY, F., PIPKIN, M. E., DJURETIC, I. M., LEVANON, D., LOTEM, J., LICHTENHELD, M. G., GRONER, Y. & RAO, A. 2009. Runx3 and T-box proteins cooperate to establish the transcriptional program of effector CTLs. *J Exp Med,* 206**,** 51-9.

CURTSINGER, J. M., JOHNSON, C. M. & MESCHER, M. F. 2003a. CD8 T cell clonal expansion and development of effector function require prolonged exposure to antigen, costimulation, and signal 3 cytokine. *J Immunol,* 171**,** 5165-71.

CURTSINGER, J. M., LINS, D. C. & MESCHER, M. F. 2003b. Signal 3 determines tolerance versus full activation of naive CD8 T cells: dissociating proliferation and development of effector function. *J Exp Med,* 197**,** 1141-51.

DANILO, M., CHENNUPATI, V., SILVA, J. G., SIEGERT, S. & HELD, W. 2018. Suppression of Tcf1 by Inflammatory Cytokines Facilitates Effector CD8 T Cell Differentiation. *Cell Rep,* 22**,** 2107-2117.

DELPOUX, A., MICHELINI, R. H., VERMA, S., LAI, C. Y., OMILUSIK, K. D., UTZSCHNEIDER, D. T., REDWOOD, A. J., GOLDRATH, A. W., BENEDICT, C. A. & HEDRICK, S. M. 2018. Continuous activity of Foxo1 is required to prevent anergy and maintain the memory state of CD8(+) T cells. *J Exp Med,* 215**,** 575-594.

DENTON, A. E., DOHERTY, P. C., TURNER, S. J. & LA GRUTA, N. L. 2007. IL-18, but not IL-12, is required for optimal cytokine production by influenza virus-specific CD8+ T cells. *Eur J Immunol,* 37**,** 368-75.

DENTON, A. E., RUSS, B. E., DOHERTY, P. C., RAO, S. & TURNER, S. J. 2011a. Differentiation-dependent functional and epigenetic landscapes for cytokine genes in virus-specific CD8+ T cells. *Proc Natl Acad Sci U S A,* 108**,** 15306-11.

DENTON, A. E., WESSELINGH, R., GRAS, S., GUILLONNEAU, C., OLSON, M. R., MINTERN, J. D., ZENG, W., JACKSON, D. C., ROSSJOHN, J., HODGKIN, P. D., DOHERTY, P. C. & TURNER, S. J. 2011b. Affinity thresholds for naive CD8+ CTL activation by peptides and engineered influenza A viruses. *J Immunol,* 187**,** 5733-44.

DESAI, D., KHANNA, A. & PETHE, P. 2020. PRC1 catalytic unit RING1B regulates early neural differentiation of human pluripotent stem cells. *Exp Cell Res,* 396**,** 112294.

DI CROCE, L. & HELIN, K. 2013. Transcriptional regulation by Polycomb group proteins. *Nat Struct Mol Biol,* 20**,** 1147-55.

DI PIETRO, A., POLMEAR, J., COOPER, L., DAMELANG, T., HUSSAIN, T., HAILES, L., O'DONNELL, K., UDUPA, V., MI, T., PRESTON, S., SHTEWE, A., HERSHBERG, U., TURNER, S. J., LA GRUTA, N. L., CHUNG, A. W., TARLINTON, D. M., SCHARER, C. D. & GOOD-JACOBSON, K. L. 2022. Targeting BMI-1 in B cells restores effective humoral immune responses and controls chronic viral infection. *Nat Immunol,* 23**,** 86-98.

ESKELAND, R., LEEB, M., GRIMES, G. R., KRESS, C., BOYLE, S., SPROUL, D., GILBERT, N., FAN, Y., SKOULTCHI, A. I., WUTZ, A. & BICKMORE, W. A. 2010. Ring1B compacts chromatin structure and represses gene expression independent of histone ubiquitination. *Mol Cell,* 38**,** 452-64.

FISCHLE, W., WANG, Y., JACOBS, S. A., KIM, Y., ALLIS, C. D. & KHORASANIZADEH, S. 2003. Molecular basis for the discrimination of repressive methyl-lysine marks in histone H3 by Polycomb and HP1 chromodomains. *Genes Dev,* 17**,** 1870-81.

FLYNN, K. J., BELZ, G. T., ALTMAN, J. D., AHMED, R., WOODLAND, D. L. & DOHERTY, P. C. 1998. Virus-specific CD8+ T cells in primary and secondary influenza pneumonia. *Immunity,* 8**,** 683-91.

FRANCIS, N. J., KINGSTON, R. E. & WOODCOCK, C. L. 2004. Chromatin compaction by a polycomb group protein complex. *Science,* 306**,** 1574-7.

FRASER, J. D., IRVING, B. A., CRABTREE, G. R. & WEISS, A. 1991. Regulation of interleukin-2 gene enhancer activity by the T cell accessory molecule CD28. *Science,* 251**,** 313-6.

FURSOVA, N. A., TURBERFIELD, A. H., BLACKLEDGE, N. P., FINDLATER, E. L., LASTUVKOVA, A., HUSEYIN, M. K., DOBRINIC, P. & KLOSE, R. J. 2021. BAP1 constrains pervasive H2AK119ub1 to control the transcriptional potential of the genome. *Genes Dev,* 35**,** 749-770.

GAO, Z., ZHANG, J., BONASIO, R., STRINO, F., SAWAI, A., PARISI, F., KLUGER, Y. & REINBERG, D. 2012. PCGF homologs, CBX proteins, and RYBP define functionally distinct PRC1 family complexes. *Mol Cell,* 45**,** 344-56.

GERDES, J., SCHWAB, U., LEMKE, H. & STEIN, H. 1983. Production of a mouse monoclonal antibody reactive with a human nuclear antigen associated with cell proliferation. *Int J Cancer,* 31**,** 13-20.

GETT, A. V. & HODGKIN, P. D. 1998. Cell division regulates the T cell cytokine repertoire, revealing a mechanism underlying immune class regulation. *Proc Natl Acad Sci U S A,* 95**,** 9488-93.

GIL, J. & O'LOGHLEN, A. 2014. PRC1 complex diversity: where is it taking us? *Trends Cell Biol,* 24**,** 632-41.

GONZALEZ, M. M., BAMIDELE, A. O., SVINGEN, P. A., SAGSTETTER, M. R., SMYRK, T. C., GABALLA, J. M., HAMDAN, F. H., KOSINSKY, R. L., GIBBONS, H. R., SUN, Z., YE, Z., NAIR, A., RAMOS, G. P., BRAGA NETO, M. B., WIXOM, A. Q., MATHISON, A. J., JOHNSEN, S. A., URRUTIA, R. & FAUBION, W. A., JR. 2021. BMI1 maintains the Treg epigenomic landscape to prevent inflammatory bowel disease. *J Clin Invest,* 131.

GOURLEY, T. S., WHERRY, E. J., MASOPUST, D. & AHMED, R. 2004. Generation and maintenance of immunological memory. *Semin Immunol,* 16**,** 323-33.

GRAY, S. M., AMEZQUITA, R. A., GUAN, T., KLEINSTEIN, S. H. & KAECH, S. M. 2017. Polycomb Repressive Complex 2-Mediated Chromatin Repression Guides Effector CD8(+) T Cell Terminal Differentiation and Loss of Multipotency. *Immunity,* 46**,** 596-608.

GRAY, S. M., KAECH, S. M. & STARON, M. M. 2014. The interface between transcriptional and epigenetic control of effector and memory CD8(+) T-cell differentiation. *Immunol Rev,* 261**,** 157-68.

GRAYSON, J. M., WEANT, A. E., HOLBROOK, B. C. & HILDEMAN, D. 2006. Role of Bim in regulating CD8+ T-cell responses during chronic viral infection. *J Virol,* 80**,** 8627-38.

GREER, E. L. & SHI, Y. 2012. Histone methylation: a dynamic mark in health, disease and inheritance. *Nat Rev Genet,* 13**,** 343-57.

GUNSTER, M. J., RAAPHORST, F. M., HAMER, K. M., DEN BLAAUWEN, J. L., FIERET, E., MEIJER, C. J. & OTTE, A. P. 2001. Differential expression of human Polycomb group proteins in various tissues and cell types. *J Cell Biochem Suppl,* Suppl 36**,** 129-43.

GUO, Y., MIYAZAKI, M., ITOI, M., SATOH, R., IWAMA, A., AMAGAI, T., KAWAMOTO, H. & KANNO, M. 2011. Polycomb group gene Bmi1 plays a role in the growth of thymic epithelial cells. *Eur J Immunol,* 41**,** 1098-107.

GUTHMILLER, J. J., UTSET, H. A. & WILSON, P. C. 2021. B Cell Responses against Influenza Viruses: Short-Lived Humoral Immunity against a Life-Long Threat. *Viruses,* 13.

HABERLAND, M., MONTGOMERY, R. L. & OLSON, E. N. 2009. The many roles of histone deacetylases in development and physiology: implications for disease and therapy. *Nat Rev Genet,* 10**,** 32-42.

HEFFNER, M. & FEARON, D. T. 2007. Loss of T cell receptor-induced Bmi-1 in the KLRG1(+) senescent CD8(+) T lymphocyte. *Proc Natl Acad Sci U S A,* 104**,** 13414-9.

HENNING, A. N., ROYCHOUDHURI, R. & RESTIFO, N. P. 2018. Epigenetic control of CD8(+) T cell differentiation. *Nat Rev Immunol,* 18**,** 340-356.

HESS MICHELINI, R., DOEDENS, A. L., GOLDRATH, A. W. & HEDRICK, S. M. 2013. Differentiation of CD8 memory T cells depends on Foxo1. *J Exp Med,* 210**,** 1189-200.

HIRAYAMA, D., IIDA, T. & NAKASE, H. 2017. The Phagocytic Function of Macrophage-Enforcing Innate Immunity and Tissue Homeostasis. *Int J Mol Sci,* 19.

HOFFMANN, M. M. & SLANSKY, J. E. 2020. T-cell receptor affinity in the age of cancer immunotherapy. *Mol Carcinog,* 59**,** 862-870.

HOGQUIST, K. A., JAMESON, S. C., HEATH, W. R., HOWARD, J. L., BEVAN, M. J. & CARBONE, F. R. 1994. T cell receptor antagonist peptides induce positive selection. *Cell,* 76**,** 17-27.

HOSOKAWA, H., KIMURA, M. Y., SHINNAKASU, R., SUZUKI, A., MIKI, T., KOSEKI, H., VAN LOHUIZEN, M., YAMASHITA, M. & NAKAYAMA, T. 2006. Regulation of Th2 cell development by Polycomb group gene bmi-1 through the stabilization of GATA3. *J Immunol,* 177**,** 7656-64.

HWANG, J. R., BYEON, Y., KIM, D. & PARK, S. G. 2020. Recent insights of T cell receptor-mediated signaling pathways for T cell activation and development. *Exp Mol Med,* 52**,** 750-761.

ICHII, H., SAKAMOTO, A., KURODA, Y. & TOKUHISA, T. 2004. Bcl6 acts as an amplifier for the generation and proliferative capacity of central memory CD8+ T cells. *J Immunol,* 173**,** 883-91.

IKAWA, T., MASUDA, K., ENDO, T. A., ENDO, M., ISONO, K., KOSEKI, Y., NAKAGAWA, R., KOMETANI, K., TAKANO, J., AGATA, Y., KATSURA, Y., KUROSAKI, T., VIDAL, M., KOSEKI, H. & KAWAMOTO, H. 2016. Conversion of T cells to B cells by inactivation of polycomb-mediated epigenetic suppression of the B-lineage program. *Genes Dev,* 30**,** 2475-2485.

ITO, S., SHEN, L., DAI, Q., WU, S. C., COLLINS, L. B., SWENBERG, J. A., HE, C. & ZHANG, Y. 2011. Tet proteins can convert 5-methylcytosine to 5-formylcytosine and 5-carboxylcytosine. *Science,* 333**,** 1300-3.

IWAMA, A., OGURO, H., NEGISHI, M., KATO, Y., MORITA, Y., TSUKUI, H., EMA, H., KAMIJO, T., KATOH-FUKUI, Y., KOSEKI, H., VAN LOHUIZEN, M. & NAKAUCHI, H. 2004. Enhanced self-renewal of hematopoietic stem cells mediated by the polycomb gene product Bmi-1. *Immunity,* 21**,** 843-51.

IWASAKI, A. & MEDZHITOV, R. 2015. Control of adaptive immunity by the innate immune system. *Nat Immunol,* 16**,** 343-53.

IWATA, A., DURAI, V., TUSSIWAND, R., BRISENO, C. G., WU, X., GRAJALES-REYES, G. E., EGAWA, T., MURPHY, T. L. & MURPHY, K. M. 2017. Quality of TCR signaling determined by differential affinities of enhancers for the composite BATF-IRF4 transcription factor complex. *Nat Immunol,* 18**,** 563-572.

JACOB, E., HOD-DVORAI, R., SCHIF-ZUCK, S. & AVNI, O. 2008. Unconventional association of the polycomb group proteins with cytokine genes in differentiated T helper cells. *J Biol Chem,* 283**,** 13471-81.

JACOBS, J. J., KIEBOOM, K., MARINO, S., DEPINHO, R. A. & VAN LOHUIZEN, M. 1999. The oncogene and Polycomb-group gene bmi-1 regulates cell proliferation and senescence through the ink4a locus. *Nature,* 397**,** 164-8.

JACOBS, S. A. & KHORASANIZADEH, S. 2002. Structure of HP1 chromodomain bound to a lysine 9-methylated histone H3 tail. *Science,* 295**,** 2080-3.

JACOBSEN, J. A., WOODARD, J., MANDAL, M., CLARK, M. R., BARTOM, E. T., SIGVARDSSON, M. & KEE, B. L. 2017. EZH2 Regulates the Developmental Timing of Effectors of the Pre-Antigen Receptor Checkpoints. *J Immunol,* 198**,** 4682-4691.

JAMESON, S. C., CARBONE, F. R. & BEVAN, M. J. 1993. Clone-specific T cell receptor antagonists of major histocompatibility complex class I-restricted cytotoxic T cells. *J Exp Med,* 177**,** 1541-50.

JANEWAY, C. A., JR. & MEDZHITOV, R. 2002. Innate immune recognition. *Annu Rev Immunol,* 20**,** 197-216.

JEANNET, G., BOUDOUSQUIE, C., GARDIOL, N., KANG, J., HUELSKEN, J. & HELD, W. 2010. Essential role of the Wnt pathway effector Tcf-1 for the establishment of functional CD8 T cell memory. *Proc Natl Acad Sci U S A,* 107**,** 9777-82.

JENKINS, M. R., KEDZIERSKA, K., DOHERTY, P. C. & TURNER, S. J. 2007. Heterogeneity of effector phenotype for acute phase and memory influenza A virus-specific CTL. *J Immunol,* 179**,** 64-70.

JENKINS, M. R., MINTERN, J., LA GRUTA, N. L., KEDZIERSKA, K., DOHERTY, P. C. & TURNER, S. J. 2008. Cell cycle-related acquisition of cytotoxic mediators defines the progressive differentiation to effector status for virus-specific CD8+ T cells. *J Immunol,* 181**,** 3818-22.

JENKINS, M. R., WEBBY, R., DOHERTY, P. C. & TURNER, S. J. 2006. Addition of a prominent epitope affects influenza A virus-specific CD8+ T cell immunodominance hierarchies when antigen is limiting. *J Immunol,* 177**,** 2917-25.

JOSHI, N. S., CUI, W., CHANDELE, A., LEE, H. K., URSO, D. R., HAGMAN, J., GAPIN, L. & KAECH, S. M. 2007. Inflammation directs memory precursor and short-lived effector CD8(+) T cell fates via the graded expression of T-bet transcription factor. *Immunity,* 27**,** 281-95.

KAECH, S. M. & CUI, W. 2012. Transcriptional control of effector and memory CD8+ T cell differentiation. *Nat Rev Immunol,* 12**,** 749-61.

KAECH, S. M., HEMBY, S., KERSH, E. & AHMED, R. 2002a. Molecular and functional profiling of memory CD8 T cell differentiation. *Cell,* 111**,** 837-51.

KAECH, S. M. & WHERRY, E. J. 2007. Heterogeneity and cell-fate decisions in effector and memory CD8+ T cell differentiation during viral infection. *Immunity,* 27**,** 393-405.

KAECH, S. M., WHERRY, E. J. & AHMED, R. 2002b. Effector and memory T-cell differentiation: implications for vaccine development. *Nat Rev Immunol,* 2**,** 251-62.

KAKARADOV, B., ARSENIO, J., WIDJAJA, C. E., HE, Z., AIGNER, S., METZ, P. J., YU, B., WEHRENS, E. J., LOPEZ, J., KIM, S. H., ZUNIGA, E. I., GOLDRATH, A. W., CHANG, J. T. & YEO, G. W. 2017. Early transcriptional and epigenetic regulation of CD8(+) T cell differentiation revealed by single-cell RNA sequencing. *Nat Immunol,* 18**,** 422-432.

KALB, R., LATWIEL, S., BAYMAZ, H. I., JANSEN, P. W., MULLER, C. W., VERMEULEN, M. & MULLER, J. 2014. Histone H2A monoubiquitination promotes histone H3 methylation in Polycomb repression. *Nat Struct Mol Biol,* 21**,** 569-71.

KALLIES, A., XIN, A., BELZ, G. T. & NUTT, S. L. 2009. Blimp-1 transcription factor is required for the differentiation of effector CD8(+) T cells and memory responses. *Immunity,* 31**,** 283-95.

KHAN, O., GILES, J. R., MCDONALD, S., MANNE, S., NGIOW, S. F., PATEL, K. P., WERNER, M. T., HUANG, A. C., ALEXANDER, K. A., WU, J. E., ATTANASIO, J., YAN, P., GEORGE, S. M., BENGSCH, B., STAUPE, R. P., DONAHUE, G., XU, W., AMARAVADI, R. K., XU, X., KARAKOUSIS, G. C., MITCHELL, T. C., SCHUCHTER, L. M., KAYE, J., BERGER, S. L. & WHERRY, E. J. 2019. TOX transcriptionally and epigenetically programs CD8(+) T cell exhaustion. *Nature,* 571**,** 211-218.

KILBOURNE, E. D. 1969. Future influenza vaccines and the use of genetic recombinants. *Bull World Health Organ,* 41**,** 643-5.

KIM, C., JIN, J., WEYAND, C. M. & GORONZY, J. J. 2020. The Transcription Factor TCF1 in T Cell Differentiation and Aging. *Int J Mol Sci,* 21.

KIMURA, M., KOSEKI, Y., YAMASHITA, M., WATANABE, N., SHIMIZU, C., KATSUMOTO, T., KITAMURA, T., TANIGUCHI, M., KOSEKI, H. & NAKAYAMA, T. 2001. Regulation of Th2 cell differentiation by mel-18, a mammalian polycomb group gene. *Immunity,* 15**,** 275-87.

KING, C. G., KOEHLI, S., HAUSMANN, B., SCHMALER, M., ZEHN, D. & PALMER, E. 2012. T cell affinity regulates asymmetric division, effector cell differentiation, and tissue pathology. *Immunity,* 37**,** 709-20.

KLAUKE, K., RADULOVIC, V., BROEKHUIS, M., WEERSING, E., ZWART, E., OLTHOF, S., RITSEMA, M., BRUGGEMAN, S., WU, X., HELIN, K., BYSTRYKH, L. & DE HAAN, G. 2013. Polycomb Cbx family members mediate the balance between haematopoietic stem cell self-renewal and differentiation. *Nat Cell Biol,* 15**,** 353-62.

KNEZETIC, J. A. & LUSE, D. S. 1986. The presence of nucleosomes on a DNA template prevents initiation by RNA polymerase II in vitro. *Cell,* 45**,** 95-104.

KOLUMAM, G. A., THOMAS, S., THOMPSON, L. J., SPRENT, J. & MURALI-KRISHNA, K. 2005. Type I interferons act directly on CD8 T cells to allow clonal expansion and memory formation in response to viral infection. *J Exp Med,* 202**,** 637-50.

KOMANDER, D. 2010. Mechanism, specificity and structure of the deubiquitinases. *Subcell Biochem,* 54**,** 69-87.

KOSS, B., SHIELDS, B. D., TAYLOR, E. M., STOREY, A. J., BYRUM, S. D., GIES, A. J., WASHAM, C. L., CHOUDHURY, S. R., HYUN AHN, J., URYU, H., WILLIAMS, J. B., KRAGER, K. J., CHIANG, T. C., MACKINTOSH, S. G., EDMONDSON, R. D., AYKIN-BURNS, N., GAJEWSKI, T. F., WANG, G. G. & TACKETT, A. J. 2020. Epigenetic Control of Cdkn2a.Arf Protects Tumor-Infiltrating Lymphocytes from Metabolic Exhaustion. *Cancer Res,* 80**,** 4707-4719.

KOUZARIDES, T. 2007. Chromatin modifications and their function. *Cell,* 128**,** 693-705.

KRUIDENIER, L., CHUNG, C. W., CHENG, Z., LIDDLE, J., CHE, K., JOBERTY, G., BANTSCHEFF, M., BOUNTRA, C., BRIDGES, A., DIALLO, H., EBERHARD, D., HUTCHINSON, S., JONES, E., KATSO, R., LEVERIDGE, M., MANDER, P. K., MOSLEY, J., RAMIREZ-MOLINA, C., ROWLAND, P., SCHOFIELD, C. J., SHEPPARD, R. J., SMITH, J. E., SWALES, C., TANNER, R., THOMAS, P., TUMBER, A., DREWES, G., OPPERMANN, U., PATEL, D. J., LEE, K. & WILSON, D. M. 2012. A selective jumonji H3K27 demethylase inhibitor modulates the proinflammatory macrophage response. *Nature,* 488**,** 404-8.

KUNDIG, T. M., SHAHINIAN, A., KAWAI, K., MITTRUCKER, H. W., SEBZDA, E., BACHMANN, M. F., MAK, T. W. & OHASHI, P. S. 1996. Duration of TCR stimulation determines costimulatory requirement of T cells. *Immunity,* 5**,** 41-52.

KUNDU, S., JI, F., SUNWOO, H., JAIN, G., LEE, J. T., SADREYEV, R. I., DEKKER, J. & KINGSTON, R. E. 2018. Polycomb Repressive Complex 1 Generates Discrete Compacted Domains that Change during Differentiation. *Mol Cell,* 71**,** 191.

KURACHI, M., BARNITZ, R. A., YOSEF, N., ODORIZZI, P. M., DIIORIO, M. A., LEMIEUX, M. E., YATES, K., GODEC, J., KLATT, M. G., REGEV, A., WHERRY, E. J. & HAINING, W. N. 2014. The transcription factor BATF operates as an essential differentiation checkpoint in early effector CD8+ T cells. *Nat Immunol,* 15**,** 373-83.

LA GRUTA, N. L., KEDZIERSKA, K., PANG, K., WEBBY, R., DAVENPORT, M., CHEN, W., TURNER, S. J. & DOHERTY, P. C. 2006. A virus-specific CD8+ T cell immunodominance hierarchy determined by antigen dose and precursor frequencies. *Proc Natl Acad Sci U S A,* 103**,** 994-9.

LA GRUTA, N. L., ROTHWELL, W. T., CUKALAC, T., SWAN, N. G., VALKENBURG, S. A., KEDZIERSKA, K., THOMAS, P. G., DOHERTY, P. C. & TURNER, S. J. 2010. Primary CTL response magnitude in mice is determined by the extent of naive T cell recruitment and subsequent clonal expansion. *J Clin Invest,* 120**,** 1885-94.

LA GRUTA, N. L., TURNER, S. J. & DOHERTY, P. C. 2004. Hierarchies in cytokine expression profiles for acute and resolving influenza virus-specific CD8+ T cell responses: correlation of cytokine profile and TCR avidity. *J Immunol,* 172**,** 5553-60.

LACHNER, M., O'CARROLL, D., REA, S., MECHTLER, K. & JENUWEIN, T. 2001. Methylation of histone H3 lysine 9 creates a binding site for HP1 proteins. *Nature,* 410**,** 116-20.

LADLE, B. H., LI, K. P., PHILLIPS, M. J., PUCSEK, A. B., HAILE, A., POWELL, J. D., JAFFEE, E. M., HILDEMAN, D. A. & GAMPER, C. J. 2016. De novo DNA methylation by DNA

methyltransferase 3a controls early effector CD8+ T-cell fate decisions following activation. *Proc Natl Acad Sci U S A,* 113**,** 10631-6.

LAU, C. M., ADAMS, N. M., GEARY, C. D., WEIZMAN, O. E., RAPP, M., PRITYKIN, Y., LESLIE, C. S. & SUN, J. C. 2018. Epigenetic control of innate and adaptive immune memory. *Nat Immunol,* 19**,** 963-972.

LEE, S. C., MILLER, S., HYLAND, C., KAUPPI, M., LEBOIS, M., DI RAGO, L., METCALF, D., KINKEL, S. A., JOSEFSSON, E. C., BLEWITT, M. E., MAJEWSKI, I. J. & ALEXANDER, W. S. 2015. Polycomb repressive complex 2 component Suz12 is required for hematopoietic stem cell function and lymphopoiesis. *Blood,* 126**,** 167-75.

LESSARD, J., BABAN, S. & SAUVAGEAU, G. 1998. Stage-specific expression of polycomb group genes in human bone marrow cells. *Blood,* 91**,** 1216-24.

LESSARD, J. & SAUVAGEAU, G. 2003. Bmi-1 determines the proliferative capacity of normal and leukaemic stem cells. *Nature,* 423**,** 255-60.

LEWIS, E. B. 1978. A gene complex controlling segmentation in Drosophila. *Nature,* 276**,** 565-70.

LI, J., HARDY, K., OLSHANSKY, M., BARUGAHARE, A., GEARING, L. J., PRIER, J. E., SNG, X. Y. X., NGUYEN, M. L. T., PIOVESAN, D., RUSS, B. E., LA GRUTA, N. L., HERTZOG, P. J., RAO, S. & TURNER, S. J. 2021. KDM6B-dependent chromatin remodeling underpins effective virus-specific CD8(+) T cell differentiation. *Cell Rep,* 34**,** 108839.

LI, J., LI, Y., CAO, Y., YUAN, M., GAO, Z., GUO, X., ZHU, F., WANG, Y. & XU, J. 2014. Polycomb chromobox (Cbx) 7 modulates activation-induced CD4+ T cell apoptosis. *Arch Biochem Biophys,* 564**,** 184-8.

LIU, J., CAO, L., CHEN, J., SONG, S., LEE, I. H., QUIJANO, C., LIU, H., KEYVANFAR, K., CHEN, H., CAO, L. Y., AHN, B. H., KUMAR, N. G., ROVIRA, II, XU, X. L., VAN LOHUIZEN, M., MOTOYAMA, N., DENG, C. X. & FINKEL, T. 2009. Bmi1 regulates mitochondrial function and the DNA damage response pathway. *Nature,* 459**,** 387-392.

LIVAK, K. J. & SCHMITTGEN, T. D. 2001. Analysis of relative gene expression data using real-time quantitative PCR and the 2(-Delta Delta C(T)) Method. *Methods,* 25**,** 402-8.

LU, P., YOUNGBLOOD, B. A., AUSTIN, J. W., MOHAMMED, A. U., BUTLER, R., AHMED, R. & BOSS, J. M. 2014. Blimp-1 represses CD8 T cell expression of PD-1 using a feed-forward transcriptional circuit during acute viral infection. *J Exp Med,* 211**,** 515-27.

LUCKHEERAM, R. V., ZHOU, R., VERMA, A. D. & XIA, B. 2012. CD4(+)T cells: differentiation and functions. *Clin Dev Immunol,* 2012**,** 925135.

MAN, K., GABRIEL, S. S., LIAO, Y., GLOURY, R., PRESTON, S., HENSTRIDGE, D. C., PELLEGRINI, M., ZEHN, D., BERBERICH-SIEBELT, F., FEBBRAIO, M. A., SHI, W. & KALLIES, A. 2017. Transcription Factor IRF4 Promotes CD8(+) T Cell Exhaustion and Limits the Development of Memory-like T Cells during Chronic Infection. *Immunity,* 47**,** 1129-1141 e5.

MAN, K., MIASARI, M., SHI, W., XIN, A., HENSTRIDGE, D. C., PRESTON, S., PELLEGRINI, M., BELZ, G. T., SMYTH, G. K., FEBBRAIO, M. A., NUTT, S. L. & KALLIES, A. 2013.

The transcription factor IRF4 is essential for TCR affinity-mediated metabolic programming and clonal expansion of T cells. *Nat Immunol,* 14**,** 1155-65.

MARGUERON, R., LI, G., SARMA, K., BLAIS, A., ZAVADIL, J., WOODCOCK, C. L., DYNLACHT, B. D. & REINBERG, D. 2008. Ezh1 and Ezh2 maintain repressive chromatin through different mechanisms. *Mol Cell,* 32**,** 503-18.

MCLEAN, C. Y., BRISTOR, D., HILLER, M., CLARKE, S. L., SCHAAR, B. T., LOWE, C. B., WENGER, A. M. & BEJERANO, G. 2010. GREAT improves functional interpretation of cis-regulatory regions. *Nat Biotechnol,* 28**,** 495-501.

MICH, J. K., SIGNER, R. A., NAKADA, D., PINEDA, A., BURGESS, R. J., VUE, T. Y., JOHNSON, J. E. & MORRISON, S. J. 2014. Prospective identification of functionally distinct stem cells and neurosphere-initiating cells in adult mouse forebrain. *Elife,* 3**,** e02669.

MIN, J., ZHANG, Y. & XU, R. M. 2003. Structural basis for specific binding of Polycomb chromodomain to histone H3 methylated at Lys 27. *Genes Dev,* 17**,** 1823-8.

MIYAZAKI, M., MIYAZAKI, K., ITOI, M., KATOH, Y., GUO, Y., KANNO, R., KATOH-FUKUI, Y., HONDA, H., AMAGAI, T., VAN LOHUIZEN, M., KAWAMOTO, H. & KANNO, M. 2008. Thymocyte proliferation induced by pre-T cell receptor signaling is maintained through polycomb gene product Bmi-1-mediated Cdkn2a repression. *Immunity,* 28**,** 231-45.

MOFFAT, J. M., GEBHARDT, T., DOHERTY, P. C., TURNER, S. J. & MINTERN, J. D. 2009. Granzyme A expression reveals distinct cytolytic CTL subsets following influenza A virus infection. *Eur J Immunol,* 39**,** 1203-10.

MOGNOL, G. P., SPREAFICO, R., WONG, V., SCOTT-BROWNE, J. P., TOGHER, S., HOFFMANN, A., HOGAN, P. G., RAO, A. & TRIFARI, S. 2017. Exhaustion-associated regulatory regions in CD8(+) tumor-infiltrating T cells. *Proc Natl Acad Sci U S A,* 114**,** E2776-E2785.

MOOTHA, V. K., LINDGREN, C. M., ERIKSSON, K. F., SUBRAMANIAN, A., SIHAG, S., LEHAR, J., PUIGSERVER, P., CARLSSON, E., RIDDERSTRALE, M., LAURILA, E., HOUSTIS, N., DALY, M. J., PATTERSON, N., MESIROV, J. P., GOLUB, T. R., TAMAYO, P., SPIEGELMAN, B., LANDER, E. S., HIRSCHHORN, J. N., ALTSHULER, D. & GROOP, L. C. 2003. PGC-1alpha-responsive genes involved in oxidative phosphorylation are coordinately downregulated in human diabetes. *Nat Genet,* 34**,** 267-73.

MOREY, L., ALOIA, L., COZZUTO, L., BENITAH, S. A. & DI CROCE, L. 2013. RYBP and Cbx7 define specific biological functions of polycomb complexes in mouse embryonic stem cells. *Cell Rep,* 3**,** 60-9.

MOREY, L. & HELIN, K. 2010. Polycomb group protein-mediated repression of transcription. *Trends Biochem Sci,* 35**,** 323-32.

MOREY, L., PASCUAL, G., COZZUTO, L., ROMA, G., WUTZ, A., BENITAH, S. A. & DI CROCE, L. 2012. Nonoverlapping functions of the Polycomb group Cbx family of proteins in embryonic stem cells. *Cell Stem Cell,* 10**,** 47-62.

MORRIS, A. G., LIN, Y. L. & ASKONAS, B. A. 1982. Immune interferon release when a cloned cytotoxic T-cell line meets its correct influenza-infected target cell. *Nature,* 295**,** 150-2.

MORRIS, R., KERSHAW, N. J. & BABON, J. J. 2018. The molecular details of cytokine signaling via the JAK/STAT pathway. *Protein Sci,* 27**,** 1984-2009.

MORSE, R. H. 2003. Getting into chromatin: how do transcription factors get past the histones? *Biochem Cell Biol,* 81**,** 101-12.

MOUSSA, H. F., BSTEH, D., YELAGANDULA, R., PRIBITZER, C., STECHER, K., BARTALSKA, K., MICHETTI, L., WANG, J., ZEPEDA-MARTINEZ, J. A., ELLING, U., STUCKEY, J. I., JAMES, L. I., FRYE, S. V. & BELL, O. 2019. Canonical PRC1 controls sequence-independent propagation of Polycomb-mediated gene silencing. *Nat Commun,* 10**,** 1931.

NG, H. H., ROBERT, F., YOUNG, R. A. & STRUHL, K. 2003. Targeted recruitment of Set1 histone methylase by elongating Pol II provides a localized mark and memory of recent transcriptional activity. *Mol Cell,* 11**,** 709-19.

NUSSING, S., KOAY, H. F., SANT, S., LOUDOVARIS, T., MANNERING, S. I., LAPPAS, M., Y, D. U., KONSTANTINOV, I. E., BERZINS, S. P., RIMMELZWAAN, G. F., TURNER, S. J., CLEMENS, E. B., GODFREY, D. I., NGUYEN, T. H. & KEDZIERSKA, K. 2019. Divergent SATB1 expression across human life span and tissue compartments. *Immunol Cell Biol,* 97**,** 498-511.

NUSSING, S., MIOSGE, L. A., LEE, K., OLSHANSKY, M., BARUGAHARE, A., ROOTS, C. M., SONTANI, Y., DAY, E. B., KOUTSAKOS, M., KEDZIERSKA, K., GOODNOW, C. C., RUSS, B. E., DALEY, S. R. & TURNER, S. J. 2022. SATB1 ensures appropriate transcriptional programs within naive CD8(+) T cells. *Immunol Cell Biol,* 100**,** 636-652.

O'CARROLL, D., ERHARDT, S., PAGANI, M., BARTON, S. C., SURANI, M. A. & JENUWEIN, T. 2001. The polycomb-group gene Ezh2 is required for early mouse development. *Mol Cell Biol,* 21**,** 4330-6.

O'LOGHLEN, A., MUNOZ-CABELLO, A. M., GASPAR-MAIA, A., WU, H. A., BANITO, A., KUNOWSKA, N., RACEK, T., PEMBERTON, H. N., BEOLCHI, P., LAVIAL, F., MASUI, O., VERMEULEN, M., CARROLL, T., GRAUMANN, J., HEARD, E., DILLON, N., AZUARA, V., SNIJDERS, A. P., PETERS, G., BERNSTEIN, E. & GIL, J. 2012. MicroRNA regulation of Cbx7 mediates a switch of Polycomb orthologs during ESC differentiation. *Cell Stem Cell,* 10**,** 33-46.

OGRYZKO, V. V., SCHILTZ, R. L., RUSSANOVA, V., HOWARD, B. H. & NAKATANI, Y. 1996. The transcriptional coactivators p300 and CBP are histone acetyltransferases. *Cell,* 87**,** 953-9.

OGURO, H., IWAMA, A., MORITA, Y., KAMIJO, T., VAN LOHUIZEN, M. & NAKAUCHI, H. 2006. Differential impact of Ink4a and Arf on hematopoietic stem cells and their bone marrow microenvironment in Bmi1-deficient mice. *J Exp Med,* 203**,** 2247-53.

OGURO, H., YUAN, J., ICHIKAWA, H., IKAWA, T., YAMAZAKI, S., KAWAMOTO, H., NAKAUCHI, H. & IWAMA, A. 2010. Poised lineage specification in multipotential hematopoietic stem and progenitor cells by the polycomb protein Bmi1. *Cell Stem Cell,* 6**,** 279-86.

OKANO, M., BELL, D. W., HABER, D. A. & LI, E. 1999. DNA methyltransferases Dnmt3a and Dnmt3b are essential for de novo methylation and mammalian development. *Cell,* 99**,** 247-57.

OUYANG, W., BECKETT, O., FLAVELL, R. A. & LI, M. O. 2009. An essential role of the Forkhead-box transcription factor Foxo1 in control of T cell homeostasis and tolerance. *Immunity,* 30**,** 358-71.

PACE, L., GOUDOT, C., ZUEVA, E., GUEGUEN, P., BURGDORF, N., WATERFALL, J. J., QUIVY, J. P., ALMOUZNI, G. & AMIGORENA, S. 2018. The epigenetic control of stemness in CD8(+) T cell fate commitment. *Science,* 359**,** 177-186.

PALEY, M. A., KROY, D. C., ODORIZZI, P. M., JOHNNIDIS, J. B., DOLFI, D. V., BARNETT, B. E., BIKOFF, E. K., ROBERTSON, E. J., LAUER, G. M., REINER, S. L. & WHERRY, E. J. 2012. Progenitor and terminal subsets of CD8+ T cells cooperate to contain chronic viral infection. *Science,* 338**,** 1220-5.

PARK, I. K., QIAN, D., KIEL, M., BECKER, M. W., PIHALJA, M., WEISSMAN, I. L., MORRISON, S. J. & CLARKE, M. F. 2003. Bmi-1 is required for maintenance of adult self-renewing haematopoietic stem cells. *Nature,* 423**,** 302-5.

PASINI, D., BRACKEN, A. P., JENSEN, M. R., LAZZERINI DENCHI, E. & HELIN, K. 2004. Suz12 is essential for mouse development and for EZH2 histone methyltransferase activity. *EMBO J,* 23**,** 4061-71.

PEARSON, J. C., LEMONS, D. & MCGINNIS, W. 2005. Modulating Hox gene functions during animal body patterning. *Nat Rev Genet,* 6**,** 893-904.

PEREIRA, M. S., ALVES, I., VICENTE, M., CAMPAR, A., SILVA, M. C., PADRAO, N. A., PINTO, V., FERNANDES, A., DIAS, A. M. & PINHO, S. S. 2018. Glycans as Key Checkpoints of T Cell Activity and Function. *Front Immunol,* 9**,** 2754.

PIRITY, M. K., LOCKER, J. & SCHREIBER-AGUS, N. 2005. Rybp/DEDAF is required for early postimplantation and for central nervous system development. *Mol Cell Biol,* 25**,** 7193-202.

PIUNTI, A. & SHILATIFARD, A. 2021. The roles of Polycomb repressive complexes in mammalian development and cancer. *Nat Rev Mol Cell Biol,* 22**,** 326-345.

PIUNTI, A. & SHILATIFARD, A. 2022. Author Correction: The roles of Polycomb repressive complexes in mammalian development and cancer. *Nat Rev Mol Cell Biol,* 23**,** 444.

POKHOLOK, D. K., HARBISON, C. T., LEVINE, S., COLE, M., HANNETT, N. M., LEE, T. I., BELL, G. W., WALKER, K., ROLFE, P. A., HERBOLSHEIMER, E., ZEITLINGER, J., LEWITTER, F., GIFFORD, D. K. & YOUNG, R. A. 2005. Genome-wide map of nucleosome acetylation and methylation in yeast. *Cell,* 122**,** 517-27.

PRIER, J. E., LI, J., GEARING, L. J., OLSHANSKY, M., SNG, X. Y. X., HERTZOG, P. J. & TURNER, S. J. 2019. Early T-BET Expression Ensures an Appropriate CD8(+) Lineage-Specific Transcriptional Landscape after Influenza A Virus Infection. *J Immunol,* 203**,** 1044-1054.

RAAPHORST, F. M., VAN KEMENADE, F. J., FIERET, E., HAMER, K. M., SATIJN, D. P., OTTE, A. P. & MEIJER, C. J. 2000. Cutting edge: polycomb gene expression patterns reflect distinct B cell differentiation stages in human germinal centers. *J Immunol,* 164**,** 1-4.

RAO, R. R., LI, Q., GUBBELS BUPP, M. R. & SHRIKANT, P. A. 2012. Transcription factor Foxo1 represses T-bet-mediated effector functions and promotes memory CD8(+) T cell differentiation. *Immunity,* 36**,** 374-87.

RAUDVERE, U., KOLBERG, L., KUZMIN, I., ARAK, T., ADLER, P., PETERSON, H. & VILO, J. 2019. g:Profiler: a web server for functional enrichment analysis and conversions of gene lists (2019 update). *Nucleic Acids Res,* 47**,** W191-W198.

REA, S., EISENHABER, F., O'CARROLL, D., STRAHL, B. D., SUN, Z. W., SCHMID, M., OPRAVIL, S., MECHTLER, K., PONTING, C. P., ALLIS, C. D. & JENUWEIN, T. 2000. Regulation of chromatin structure by site-specific histone H3 methyltransferases. *Nature,* 406**,** 593-9.

RICHER, M. J., NOLZ, J. C. & HARTY, J. T. 2013. Pathogen-specific inflammatory milieux tune the antigen sensitivity of CD8(+) T cells by enhancing T cell receptor signaling. *Immunity,* 38**,** 140-52.

ROSETTE, C., WERLEN, G., DANIELS, M. A., HOLMAN, P. O., ALAM, S. M., TRAVERS, P. J., GASCOIGNE, N. R., PALMER, E. & JAMESON, S. C. 2001. The impact of duration versus extent of TCR occupancy on T cell activation: a revision of the kinetic proofreading model. *Immunity,* 15**,** 59-70.

ROTHBART, S. B., KRAJEWSKI, K., NADY, N., TEMPEL, W., XUE, S., BADEAUX, A. I., BARSYTE-LOVEJOY, D., MARTINEZ, J. Y., BEDFORD, M. T., FUCHS, S. M., ARROWSMITH, C. H. & STRAHL, B. D. 2012. Association of UHRF1 with methylated H3K9 directs the maintenance of DNA methylation. *Nat Struct Mol Biol,* 19**,** 1155-60.

ROYCHOUDHURI, R., CLEVER, D., LI, P., WAKABAYASHI, Y., QUINN, K. M., KLEBANOFF, C. A., JI, Y., SUKUMAR, M., EIL, R. L., YU, Z., SPOLSKI, R., PALMER, D. C., PAN, J. H., PATEL, S. J., MACALLAN, D. C., FABOZZI, G., SHIH, H. Y., KANNO, Y., MUTO, A., ZHU, J., GATTINONI, L., O'SHEA, J. J., OKKENHAUG, K., IGARASHI, K., LEONARD, W. J. & RESTIFO, N. P. 2016. BACH2 regulates CD8(+) T cell differentiation by controlling access of AP-1 factors to enhancers. *Nat Immunol,* 17**,** 851-860.

RUSS, B. E., DENTON, A. E., HATTON, L., CROOM, H., OLSON, M. R. & TURNER, S. J. 2012. Defining the molecular blueprint that drives CD8(+) T cell differentiation in response to infection. *Front Immunol,* 3**,** 371.

RUSS, B. E., OLSHANKSY, M., SMALLWOOD, H. S., LI, J., DENTON, A. E., PRIER, J. E., STOCK, A. T., CROOM, H. A., CULLEN, J. G., NGUYEN, M. L., ROWE, S., OLSON, M. R., FINKELSTEIN, D. B., KELSO, A., THOMAS, P. G., SPEED, T. P., RAO, S. & TURNER, S. J. 2014. Distinct epigenetic signatures delineate transcriptional programs during virus-specific CD8(+) T cell differentiation. *Immunity,* 41**,** 853-65.

RUSS, B. E., PRIER, J. E., RAO, S. & TURNER, S. J. 2013. T cell immunity as a tool for studying epigenetic regulation of cellular differentiation. *Front Genet,* 4**,** 218.

RUTISHAUSER, R. L., MARTINS, G. A., KALACHIKOV, S., CHANDELE, A., PARISH, I. A., MEFFRE, E., JACOB, J., CALAME, K. & KAECH, S. M. 2009. Transcriptional repressor Blimp-1 promotes CD8(+) T cell terminal differentiation and represses the acquisition of central memory T cell properties. *Immunity,* 31**,** 296-308.

SANTOS-ROSA, H., SCHNEIDER, R., BANNISTER, A. J., SHERRIFF, J., BERNSTEIN, B. E., EMRE, N. C., SCHREIBER, S. L., MELLOR, J. & KOUZARIDES, T. 2002. Active genes are tri-methylated at K4 of histone H3. *Nature,* 419**,** 407-11.

SAWAI, A., PFENNIG, S., BULAJIC, M., MILLER, A., KHODADADI-JAMAYRAN, A., MAZZONI, E. O. & DASEN, J. S. 2022. PRC1 sustains the integrity of neural fate in the absence of PRC2 function. *Elife,* 11.

SCHARER, C. D., BALLY, A. P., GANDHAM, B. & BOSS, J. M. 2017. Cutting Edge: Chromatin Accessibility Programs CD8 T Cell Memory. *J Immunol,* 198**,** 2238-2243.

SCHARER, C. D., BARWICK, B. G., YOUNGBLOOD, B. A., AHMED, R. & BOSS, J. M. 2013. Global DNA methylation remodeling accompanies CD8 T cell effector function. *J Immunol,* 191**,** 3419-29.

SCHULMAN, J. L. & KILBOURNE, E. D. 1969. The antigenic relationship of the neuraminidase of Hong Kong virus to that of other human strains of influenza A virus. *Bull World Health Organ,* 41**,** 425-8.

SCHUMACHER, A., FAUST, C. & MAGNUSON, T. 1996. Positional cloning of a global regulator of anterior-posterior patterning in mice. *Nature,* 384**,** 648.

SEIFERT, A., WERHEID, D. F., KNAPP, S. M. & TOBIASCH, E. 2015. Role of Hox genes in stem cell differentiation. *World J Stem Cells,* 7**,** 583-95.

SEN, D. R., KAMINSKI, J., BARNITZ, R. A., KURACHI, M., GERDEMANN, U., YATES, K. B., TSAO, H. W., GODEC, J., LAFLEUR, M. W., BROWN, F. D., TONNERRE, P., CHUNG, R. T., TULLY, D. C., ALLEN, T. M., FRAHM, N., LAUER, G. M., WHERRY, E. J., YOSEF, N. & HAINING, W. N. 2016. The epigenetic landscape of T cell exhaustion. *Science,* 354**,** 1165-1169.

SHAN, Q., HU, S. S., ZHU, S., CHEN, X., BADOVINAC, V. P., PENG, W., ZANG, C. & XUE, H. H. 2022. Tcf1 preprograms the mobilization of glycolysis in central memory CD8(+) T cells during recall responses. *Nat Immunol,* 23**,** 386-398.

SHAN, Q., LI, X., CHEN, X., ZENG, Z., ZHU, S., GAI, K., PENG, W. & XUE, H. H. 2021. Tcf1 and Lef1 provide constant supervision to mature CD8(+) T cell identity and function by organizing genomic architecture. *Nat Commun,* 12**,** 5863.

SHAN, Q., ZENG, Z., XING, S., LI, F., HARTWIG, S. M., GULLICKSRUD, J. A., KURUP, S. P., VAN BRAECKEL-BUDIMIR, N., SU, Y., MARTIN, M. D., VARGA, S. M., TANIUCHI, I., HARTY, J. T., PENG, W., BADOVINAC, V. P. & XUE, H. H. 2017. The transcription factor Runx3 guards cytotoxic CD8(+) effector T cells against deviation towards follicular helper T cell lineage. *Nat Immunol,* 18**,** 931-939.

SHAO, Z., RAIBLE, F., MOLLAAGHABABA, R., GUYON, J. R., WU, C. T., BENDER, W. & KINGSTON, R. E. 1999. Stabilization of chromatin structure by PRC1, a Polycomb complex. *Cell,* 98**,** 37-46.

SHEN, X., LIU, Y., HSU, Y. J., FUJIWARA, Y., KIM, J., MAO, X., YUAN, G. C. & ORKIN, S. H. 2008. EZH1 mediates methylation on histone H3 lysine 27 and complements EZH2 in maintaining stem cell identity and executing pluripotency. *Mol Cell,* 32**,** 491-502.

SOARES, A., GOVENDER, L., HUGHES, J., MAVAKLA, W., DE KOCK, M., BARNARD, C., PIENAAR, B., JANSE VAN RENSBURG, E., JACOBS, G., KHOMBA, G., STONE, L., ABEL, B., SCRIBA, T. J. & HANEKOM, W. A. 2010. Novel application of Ki67 to quantify antigen-specific in vitro lymphoproliferation. *J Immunol Methods,* 362**,** 43-50.

SOLOUKI, S., HUANG, W., ELMORE, J., LIMPER, C., HUANG, F. & AUGUST, A. 2020. TCR Signal Strength and Antigen Affinity Regulate CD8(+) Memory T Cells. *J Immunol,* 205**,** 1217-1227.

SPERLING, A. I., AUGER, J. A., EHST, B. D., RULIFSON, I. C., THOMPSON, C. B. & BLUESTONE, J. A. 1996. CD28/B7 interactions deliver a unique signal to naive T cells that regulates cell survival but not early proliferation. *J Immunol,* 157**,** 3909-17.

STEPHEN, T. L., PAYNE, K. K., CHAURIO, R. A., ALLEGREZZA, M. J., ZHU, H., PEREZ-SANZ, J., PERALES-PUCHALT, A., NGUYEN, J. M., VARA-AILOR, A. E., ERUSLANOV, E. B., BOROWSKY, M. E., ZHANG, R., LAUFER, T. M. & CONEJO-GARCIA, J. R. 2017. SATB1 Expression Governs Epigenetic Repression of PD-1 in Tumor-Reactive T Cells. *Immunity,* 46**,** 51-64.

SUBRAMANIAN, A., TAMAYO, P., MOOTHA, V. K., MUKHERJEE, S., EBERT, B. L., GILLETTE, M. A., PAULOVICH, A., POMEROY, S. L., GOLUB, T. R., LANDER, E. S. & MESIROV, J. P. 2005. Gene set enrichment analysis: a knowledge-based approach for interpreting genome-wide expression profiles. *Proc Natl Acad Sci U S A,* 102**,** 15545-50.

SULLIVAN, B. M., JUEDES, A., SZABO, S. J., VON HERRATH, M. & GLIMCHER, L. H. 2003. Antigen-driven effector CD8 T cell function regulated by T-bet. *Proc Natl Acad Sci U S A,* 100**,** 15818-23.

SURH, C. D., BOYMAN, O., PURTON, J. F. & SPRENT, J. 2006. Homeostasis of memory T cells. *Immunol Rev,* 211**,** 154-63.

SUZUKI, A., IWAMURA, C., SHINODA, K., TUMES, D. J., KIMURA, M. Y., HOSOKAWA, H., ENDO, Y., HORIUCHI, S., TOKOYODA, K., KOSEKI, H., YAMASHITA, M. & NAKAYAMA, T. 2010. Polycomb group gene product Ring1B regulates Th2-driven airway inflammation through the inhibition of Bim-mediated apoptosis of effector Th2 cells in the lung. *J Immunol,* 184**,** 4510-20.

TAI, T. S., PAI, S. Y. & HO, I. C. 2013. GATA-3 regulates the homeostasis and activation of CD8+ T cells. *J Immunol,* 190**,** 428-37.

TAMBURRI, S., LAVARONE, E., FERNANDEZ-PEREZ, D., CONWAY, E., ZANOTTI, M., MANGANARO, D. & PASINI, D. 2020. Histone H2AK119 Mono-Ubiquitination Is Essential for Polycomb-Mediated Transcriptional Repression. *Mol Cell,* 77**,** 840-856 e5.

TANIGAWA, Y., DYER, E. S. & BEJERANO, G. 2022. WhichTF is functionally important in your open chromatin data? *PLoS Comput Biol,* 18**,** e1010378.

TAVARES, L., DIMITROVA, E., OXLEY, D., WEBSTER, J., POOT, R., DEMMERS, J., BEZSTAROSTI, K., TAYLOR, S., URA, H., KOIDE, H., WUTZ, A., VIDAL, M., ELDERKIN, S. & BROCKDORFF, N. 2012. RYBP-PRC1 complexes mediate H2A ubiquitylation at polycomb target sites independently of PRC2 and H3K27me3. *Cell,* 148**,** 664-78.

TEIXEIRO, E., DANIELS, M. A., HAMILTON, S. E., SCHRUM, A. G., BRAGADO, R., JAMESON, S. C. & PALMER, E. 2009. Different T cell receptor signals determine CD8+ memory versus effector development. *Science,* 323**,** 502-5.

TESSARZ, P. & KOUZARIDES, T. 2014. Histone core modifications regulating nucleosome structure and dynamics. *Nat Rev Mol Cell Biol,* 15**,** 703-8.

TSAI, S., CLEMENTE-CASARES, X., ZHOU, A. C., LEI, H., AHN, J. J., CHAN, Y. T., CHOI, O., LUCK, H., WOO, M., DUNN, S. E., ENGLEMAN, E. G., WATTS, T. H., WINER, S. & WINER, D. A. 2018. Insulin Receptor-Mediated Stimulation Boosts T Cell Immunity during Inflammation and Infection. *Cell Metab,* 28**,** 922-934 e4.

TUOSTO, L. & ACUTO, O. 1998. CD28 affects the earliest signaling events generated by TCR engagement. *Eur J Immunol,* 28**,** 2131-42.

UTZSCHNEIDER, D. T., CHARMOY, M., CHENNUPATI, V., POUSSE, L., FERREIRA, D. P., CALDERON-COPETE, S., DANILO, M., ALFEI, F., HOFMANN, M., WIELAND, D., PRADERVAND, S., THIMME, R., ZEHN, D. & HELD, W. 2016. T Cell Factor 1-Expressing Memory-like CD8(+) T Cells Sustain the Immune Response to Chronic Viral Infections. *Immunity,* 45**,** 415-27.

UTZSCHNEIDER, D. T., GABRIEL, S. S., CHISANGA, D., GLOURY, R., GUBSER, P. M., VASANTHAKUMAR, A., SHI, W. & KALLIES, A. 2020. Early precursor T cells establish and propagate T cell exhaustion in chronic infection. *Nat Immunol,* 21**,** 1256-1266.

VAN DER LUGT, N. M., DOMEN, J., LINDERS, K., VAN ROON, M., ROBANUS-MAANDAG, E., TE RIELE, H., VAN DER VALK, M., DESCHAMPS, J., SOFRONIEW, M., VAN LOHUIZEN, M. & ET AL. 1994. Posterior transformation, neurological abnormalities, and severe hematopoietic defects in mice with a targeted deletion of the bmi-1 proto-oncogene. *Genes Dev,* 8**,** 757-69.

VAN MIERLO, G., VEENSTRA, G. J. C., VERMEULEN, M. & MARKS, H. 2019. The Complexity of PRC2 Subcomplexes. *Trends Cell Biol,* 29**,** 660-671.

VIOLA, A. & LANZAVECCHIA, A. 1996. T cell activation determined by T cell receptor number and tunable thresholds. *Science,* 273**,** 104-6.

VIVIER, E., TOMASELLO, E., BARATIN, M., WALZER, T. & UGOLINI, S. 2008. Functions of natural killer cells. *Nat Immunol,* 9**,** 503-10.

VOEHRINGER, D., BLASER, C., BRAWAND, P., RAULET, D. H., HANKE, T. & PIRCHER, H. 2001. Viral infections induce abundant numbers of senescent CD8 T cells. *J Immunol,* 167**,** 4838-43.

VOEHRINGER, D., KOSCHELLA, M. & PIRCHER, H. 2002. Lack of proliferative capacity of human effector and memory T cells expressing killer cell lectinlike receptor G1 (KLRG1). *Blood,* 100**,** 3698-702.

VONCKEN, J. W., ROELEN, B. A., ROEFS, M., DE VRIES, S., VERHOEVEN, E., MARINO, S., DESCHAMPS, J. & VAN LOHUIZEN, M. 2003. Rnf2 (Ring1b) deficiency causes gastrulation arrest and cell cycle inhibition. *Proc Natl Acad Sci U S A,* 100**,** 2468-73.

WANG, H., WANG, L., ERDJUMENT-BROMAGE, H., VIDAL, M., TEMPST, P., JONES, R. S. & ZHANG, Y. 2004. Role of histone H2A ubiquitination in Polycomb silencing. *Nature,* 431**,** 873-8.

WANG, Z., ZANG, C., ROSENFELD, J. A., SCHONES, D. E., BARSKI, A., CUDDAPAH, S., CUI, K., ROH, T. Y., PENG, W., ZHANG, M. Q. & ZHAO, K. 2008. Combinatorial patterns of histone acetylations and methylations in the human genome. *Nat Genet,* 40**,** 897-903.

WHERRY, E. J., HA, S. J., KAECH, S. M., HAINING, W. N., SARKAR, S., KALIA, V., SUBRAMANIAM, S., BLATTMAN, J. N., BARBER, D. L. & AHMED, R. 2007.

Molecular signature of CD8+ T cell exhaustion during chronic viral infection. *Immunity,* 27**,** 670-84.

WHERRY, E. J. & KURACHI, M. 2015. Molecular and cellular insights into T cell exhaustion. *Nat Rev Immunol,* 15**,** 486-99.

WHERRY, E. J., MCELHAUGH, M. J. & EISENLOHR, L. C. 2002. Generation of CD8(+) T cell memory in response to low, high, and excessive levels of epitope. *J Immunol,* 168**,** 4455-61.

WILLIAMS, M. A. & BEVAN, M. J. 2007. Effector and memory CTL differentiation. *Annu Rev Immunol,* 25**,** 171-92.

WU, K., WOO, S. M., SEO, S. U. & KWON, T. K. 2021. Inhibition of BMI-1 Induces Apoptosis through Downregulation of DUB3-Mediated Mcl-1 Stabilization. *Int J Mol Sci,* 22.

XIAO, Z., CASEY, K. A., JAMESON, S. C., CURTSINGER, J. M. & MESCHER, M. F. 2009. Programming for CD8 T cell memory development requires IL-12 or type I IFN. *J Immunol,* 182**,** 2786-94.

XIE, H., XU, J., HSU, J. H., NGUYEN, M., FUJIWARA, Y., PENG, C. & ORKIN, S. H. 2014. Polycomb repressive complex 2 regulates normal hematopoietic stem cell function in a developmental-stage-specific manner. *Cell Stem Cell,* 14**,** 68-80.

YAMASHITA, M., KUWAHARA, M., SUZUKI, A., HIRAHARA, K., SHINNAKSU, R., HOSOKAWA, H., HASEGAWA, A., MOTOHASHI, S., IWAMA, A. & NAKAYAMA, T. 2008. Bmi1 regulates memory CD4 T cell survival via repression of the Noxa gene. *J Exp Med,* 205**,** 1109-20.

YANG, X. P., JIANG, K., HIRAHARA, K., VAHEDI, G., AFZALI, B., SCIUME, G., BONELLI, M., SUN, H. W., JANKOVIC, D., KANNO, Y., SARTORELLI, V., O'SHEA, J. J. & LAURENCE, A. 2015. EZH2 is crucial for both differentiation of regulatory T cells and T effector cell expansion. *Sci Rep,* 5**,** 10643.

YASUI, D., MIYANO, M., CAI, S., VARGA-WEISZ, P. & KOHWI-SHIGEMATSU, T. 2002. SATB1 targets chromatin remodelling to regulate genes over long distances. *Nature,* 419**,** 641-5.

YIN, X., ROMERO-CAMPERO, F. J., DE LOS REYES, P., YAN, P., YANG, J., TIAN, G., YANG, X., MO, X., ZHAO, S., CALONJE, M. & ZHOU, Y. 2021. H2AK121ub in Arabidopsis associates with a less accessible chromatin state at transcriptional regulation hotspots. *Nat Commun,* 12**,** 315.

YOUNGBLOOD, B., HALE, J. S., KISSICK, H. T., AHN, E., XU, X., WIELAND, A., ARAKI, K., WEST, E. E., GHONEIM, H. E., FAN, Y., DOGRA, P., DAVIS, C. W., KONIECZNY, B. T., ANTIA, R., CHENG, X. & AHMED, R. 2017. Effector CD8 T cells dedifferentiate into long-lived memory cells. *Nature,* 552**,** 404-409.

YU, M., SU, Z., HUANG, X. & WANG, X. 2021. Single-Cell Sequencing Reveals the Novel Role of Ezh2 in NK Cell Maturation and Function. *Front Immunol,* 12**,** 724276.

ZEHN, D., LEE, S. Y. & BEVAN, M. J. 2009. Complete but curtailed T-cell response to very low-affinity antigen. *Nature,* 458**,** 211-4.

ZHANG, Y. 2003. Transcriptional regulation by histone ubiquitination and deubiquitination. *Genes Dev,* 17**,** 2733-40.

ZHANG, Y., KINKEL, S., MAKSIMOVIC, J., BANDALA-SANCHEZ, E., TANZER, M. C., NASELLI, G., ZHANG, J. G., ZHAN, Y., LEW, A. M., SILKE, J., OSHLACK, A.,

BLEWITT, M. E. & HARRISON, L. C. 2014. The polycomb repressive complex 2 governs life and death of peripheral T cells. *Blood,* 124**,** 737-49.

ZHENG, R., WAN, C., MEI, S., QIN, Q., WU, Q., SUN, H., CHEN, C. H., BROWN, M., ZHANG, X., MEYER, C. A. & LIU, X. S. 2019. Cistrome Data Browser: expanded datasets and new tools for gene regulatory analysis. *Nucleic Acids Res,* 47**,** D729-D735.

ZHOU, X., YU, S., ZHAO, D. M., HARTY, J. T., BADOVINAC, V. P. & XUE, H. H. 2010. Differentiation and persistence of memory CD8(+) T cells depend on T cell factor 1. *Immunity,* 33**,** 229-40.

ZHOU, Y., ZHOU, B., PACHE, L., CHANG, M., KHODABAKHSHI, A. H., TANASEICHUK, O., BENNER, C. & CHANDA, S. K. 2019. Metascape provides a biologist-oriented resource for the analysis of systems-level datasets. *Nat Commun,* 10**,** 1523.

ZINKERNAGEL, R. M. & DOHERTY, P. C. 1974. Restriction of in vitro T cell-mediated cytotoxicity in lymphocytic choriomeningitis within a syngeneic or semiallogeneic system. *Nature,* 248**,** 701-2.